Acta Numerica (2022), pp. 1–82
DOI: 10.1017/S0962492902

Asymptotic-Preserving Schemes for Multiscale Physical Problems

Shi Jin
School of Mathematical Sciences, Institute of Natural Sciences, and MOE-LSC
Shanghai Jiao Tong University, Shanghai 200240, China.
Email: shijin-m@sjtu.edu.cn

We present the asymptotic transitions from microscopic to macroscopic physics, their computational challenges and the Asymptotic-Preserving (AP) strategies to efficiently compute multiscale physical problems. Specifically, we will first study the asymptotic transition from quantum to classical mechanics, from classical mechanics to kinetic theory, and then from kinetic theory to hydrodynamics. We then review some representative AP schemes that mimic, at the discrete level, these asymptotic transitions, hence can be used crossing scales and, in particular, capture the macroscopic behavior without resolving numerically the microscopic physical scale.

1

CONTENTS

[1] S. Jin was partially supported by National Key R&D Program of China Project No. 2020YFA0712000, NSFC grant No. 12031013, and Shanghai Municipal Science and Technology Major Project 2021SHZDZX0102.

1. Introduction

Ignoring relativistic effects, quantum mechanics is considered to be enough for one to understand the physical properties of matters. Since solving the Schrödinger equation analytically is impossible, one relies upon computer simulations to solve the equation. However, there are essential computational bottlenecks in simulation at the quantum level. First is the curse of dimensionality. For common molecules like carbon dioxide CO_2, which consists of 3 nuclei and 22 electrons, the full time-dependent Schrödinger equation is defined in 75 space dimensions! The benzene molecule consists of 12 nuclei and 42 electrons, hence one needs to solve the Schrödinger equation in 162 dimensions. Another challenge is that quantum mechanics is valid at spatial scales of Angstrom, which is 10^{-10} meter, and time scale of femtoseconds, or 10^{-15} second. To simulate such a small scale system to any physical scales of interest, for example, micrometers to millimeters, or microseconds to milliseconds, is computationally formidable by today's computer.

Physical models at larger scales, such as classical mechanics, statistical mechanics, and hydrodynamics, are computationally much less expensive compared to a quantum simulation, but they are valid in certain time and spatial scales, see Fig. 1.1. When one deals with problems that go across different scales, either due to the nature of the problems or computational needs, multiscale computation becomes a viable tool when one cannot afford to resolve the smallest scales.

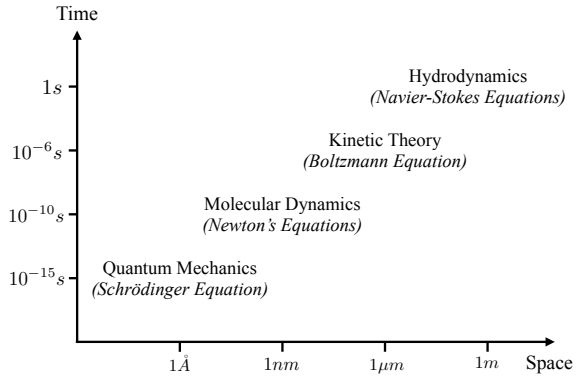

Figure 1.1. Multiscale diagram.

Understanding the transition from one scale to another is a central topic in mathematical physics and partial differential equations. They are related to Hilbert's sixth problem (Corry 2004). These asymptotic transitions are not

only of great mathematical interest, they also guide the design of multiscale computational methods, as will be reflected in this survey.

If the asymptotic or macroscopic equations are uniformly valid in the entire domain of interest, it is much more efficient just to solve the problem at the macroscopic level, which are computationally more economical. However, there are many problems where the macroscopic models break down in part of the domain, or one lacks information or data on the macro models, thus the microscopic models are needed, at least locally. Therefore a multiscale and multiphysics approach, that hybridizes the microscopic and the macroscopic models in a domain-decomposition or heterogeneous multiscale framework, becomes necessary, see for examples (Bourgat, Le Tallec, Perthame and Qiu 1994) (Klar, Neunzert and Struckmeier 2000) (Degond, Jin and Mieussens 2005) for multiscale kinetic problems, and (E and Engquist 2003) (Abdulle, Weinan, Engquist and Vanden-Eijnden 2012) (Kevrekidis, Gear and Hummer 2004) for broader areas of multiscale modeling and simulation.

Central to the design of multiscale computational methods is to identify the critical physical scales in the system and the connections between microscopic and macroscopic models. The Schrödinger equation is valid at the scale of Angstrom, which is exceedingly small compared to the scale of interest. The Newton equations in classical mechanics often involve the number of particles simply formidably too large. Kinetic equations often contain small mean free path or time, or Knudsen number, the average distance or time between two collisions of particles. When the characteristic scales become small, tremendous computational challenges arise since one needs to numerically resolve these small scales which can be prohibitively expensive. A main difficulty in most multiscale and multi-physics type methods is that one has to couple models at different scales through an interface or buffer zone where one has to match two different models. While it is often easy to generate macroscopic data from the micro ones through, for examples, ensemble averages or taking moments, it is difficult to convert macroscopic data to the microscopic ones, since most of the time this conversion is not unique. The coupling locations may also be difficult to determine in a dynamic problem.

On the other hand, asymptotic expansions on these small parameters for a microscopic model usually give rise to the macroscopic equations. One hopes such a transition can guide the design, and help to analyze, effective and efficient multiscale computational methods.

This paper surveys one multiscale framework–the *asymptotic-preserving (AP) schemes*. This approach has its origin in capturing steady-state solution for neutron transport in the diffusive regime (Larsen, Morel and Miller Jr 1987) (Larsen and Morel 1989). Since the 90s of last century, the AP schemes have been developed for a wide range of time-dependent ki-

netic and hyperbolic equations, and far beyond. The basic idea is to develop numerical methods that *preserve the asymptotic limits from the microscopic to the macroscopic models, in the discrete setting.* Comparing with multiphysics domain decomposition type methods, the AP schemes solve one set of equations–the microscopic ones–thus avoid the coupling of different models. An AP scheme switches from a microscopic solver to the macroscopic solver *automatically.* Specifically, if one numerically resolves the small physical scales then the scheme is a micro solver. Otherwise it effectively becomes a macro solver, when the physically small scales are *not numerically resolved.*

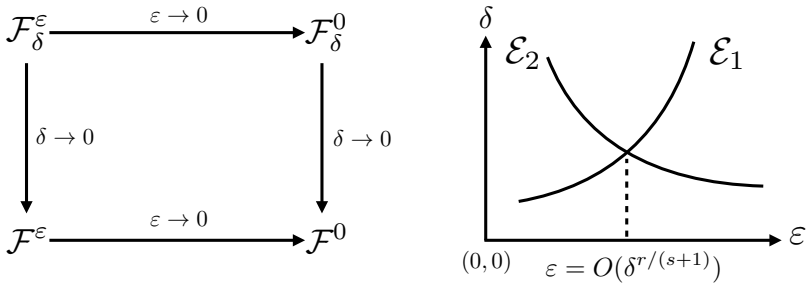

Figure 1.2. Left: Illustration of AP schemes; right: illustration of uniform convergence of AP schemes.

The idea of AP can be illustrated by the left figure in Fig. 1.2. Assume one starts with a microscopic model $\mathcal{F}^\varepsilon$ which depends on the scaling parameter ε. As $\varepsilon \to 0$ the model asymptotically approaches the macroscopic model $\mathcal{F}^0$ which is independent of ε. Denote the numerical discretization of $\mathcal{F}^\varepsilon$ by $\mathcal{F}^\varepsilon_\delta$, where δ is the numerical parameter (such as mesh size and/or time step). The asymptotic limit of $\mathcal{F}^\varepsilon_\delta$, as $\varepsilon \to 0$ (with δ fixed), if exsits, is denoted by $\mathcal{F}^0_\delta$. *Scheme $\mathcal{F}^\varepsilon_\delta$ is called AP if $\mathcal{F}^0_\delta$ is a good (consistent and stable) approximation of $\mathcal{F}^0$,*

Error estimates on an AP scheme can be obtained by the following argument (Golse, Jin and Levermore 1999). Typically,

$$\|\mathcal{F}^\varepsilon - \mathcal{F}^0\| = O(\varepsilon)\,, \tag{1.1}$$

under some suitable, problem dependent, norm. Assume $\mathcal{F}^\varepsilon_\delta$ is an r-th order approximation to $\mathcal{F}^\varepsilon$ for fixed ε. Due to the presence of the small parameter ε, a classical numerical analysis typically gives the following error estimate

$$\mathcal{E}_1 = \|\mathcal{F}^\varepsilon_\delta - \mathcal{F}^\varepsilon\| = O(\delta^r/\varepsilon^s)\,, \quad 1 \le s \le r\,. \tag{1.2}$$

The error is large when $\delta^r \gg \varepsilon^s$, namely, when the small physical scales are not numerically resolved (if one uses coarse meshes or large time steps

relative to ε). An AP scheme usually requires

$$\|\mathcal{F}_\delta^\varepsilon - \mathcal{F}_\delta^0\| = O(\varepsilon) \qquad \text{uniformly in} \quad \delta\,, \tag{1.3}$$

and

$$\|\mathcal{F}_\delta^0 - \mathcal{F}^0\| = O(\delta^r)\,. \tag{1.4}$$

Clearly, if one adds up the errors in (1.1), (1.3) and (1.4), by the triangle inequality, the following error estimate can be obtained

$$\mathcal{E}_2 = \|\mathcal{F}_\delta^\varepsilon - \mathcal{F}^\varepsilon\| \le \|\mathcal{F}_\delta^\varepsilon - \mathcal{F}_\delta^0\| + \|\mathcal{F}_\delta^0 - \mathcal{F}^0\| + \|\mathcal{F}^0 - \mathcal{F}^\varepsilon\| = O(\varepsilon + \delta^r)\,. \tag{1.5}$$

This error is small for $\varepsilon \ll 1$. Clearly both estimates on $\mathcal{E}_1$ (1.2) and $\mathcal{E}_2$ (1.5) are mathematically valid and can hold simultaneously. By comparing the two estimates,

$$\|\mathcal{F}_\delta^\varepsilon - \mathcal{F}^\varepsilon\| = \min(\mathcal{E}_1, \mathcal{E}_2)\,,$$

which has an upper bound around $\varepsilon = O(\delta^{r/(s+1)})$, as shown by the right figure in Fig.1.2. This gives

$$\|\mathcal{F}_\delta^\varepsilon - \mathcal{F}^\varepsilon\| = O(\delta^{r/(s+1)})\,, \qquad \text{uniformly in} \quad \varepsilon\,. \tag{1.6}$$

This argument shows that an AP scheme is *convergent uniformly in* ε. Indeed, if one resolves ε by δ (with $\delta = o(\varepsilon^{s/r})$) one gets a good approximation to the microscopic model $\mathcal{F}^\varepsilon$, as shown by (1.2). If ε is not resolved by δ then one obtains a good approximation to the macroscopic model $\mathcal{F}^0$. This transition is done *automatically* by the code.

There have been a few earlier reviews on AP schemes, for examples for multiscale kinetic equations (Jin 2010)(Dimarco and Pareschi 2014)(Degond and Deluzet 2017*a*)(Hu, Jin and Li 2017), and for semiclassical computation of the Schrödinger equation (Jin, Markowich and Sparber 2011)(Lasser and Lubich 2020). This survey, however, is unique in that it covers in a more comprehensive way the topics in essentially *all* important physical regimes, from quantum to classical mechanics, from classical mechanics to kinetic theory, and then from kinetic theory to hydrodynamics. It has also included the most recent advances, including new directions, in this topic.

Since the design of AP schemes relies upon a good understanding of the asymptotic transitions from the microscopic to the macroscopic models, in the next section we first review such transitions for some of the most fundamental physical equations and scalings shown in Fig. 1.1. They are summarized in Fig. 1.3.

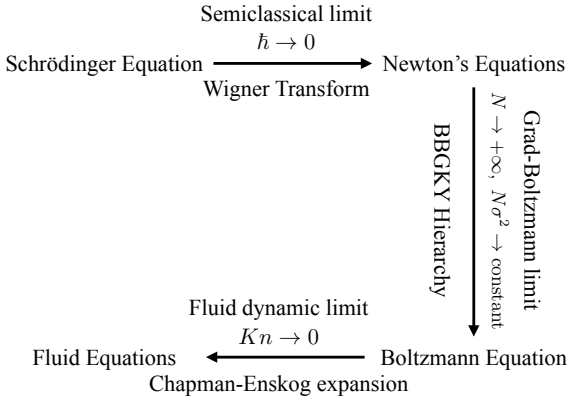

Figure 1.3. Scaling limits from microscopic to macroscopic models.

2. Asymptotic transitions from microscopic to macroscopic physics

2.1. From quantum mechanics to classical mechanics

Consider the dimensionless Schrödinger equation from quantum mechanics:

$$\mathrm{i}\varepsilon\partial_t u^\varepsilon = -\frac{\varepsilon^2}{2}\Delta u^\varepsilon + V(x)u^\varepsilon; \quad u^\varepsilon(0,x) = u_{\mathrm{in}}^\varepsilon(x)\,. \tag{2.2}$$

Here $u^\varepsilon = u^\varepsilon(t,x) \in \mathbb{C}$ is complex-valued quantum mechanical wave function, $(t,x) \in \mathbb{R}\times\mathbb{R}^d$, with $d \in \mathbb{N}$ denoting the spatial dimension. In addition, $\varepsilon > 0$ denotes the small *semiclassical parameter* (the scaled Planck's constant $\hbar$), describing the microscopic/macroscopic scale ratio. In quantum mechanics for N particles, $V(x)$ is the Coulomb potential, but here it is left as a general function of x.

The physical observables are real-valued quadratic quantities of u^ε. They include the *position density*

$$\rho^\varepsilon(t,x) := |u^\varepsilon(t,x)|^2, \tag{2.3}$$

the *current density*

$$j^\varepsilon(t,x) := \varepsilon\,\mathrm{Im}\left(\overline{u^\varepsilon}(t,x)\nabla u^\varepsilon(t,x)\right), \tag{2.4}$$

and the *energy density*

$$e^\varepsilon(t,x) := \frac{1}{2}|\varepsilon\nabla u^\varepsilon(t,x)|^2 + V(x)\rho^\varepsilon(t,x). \tag{2.5}$$

Simple analysis shows these observables are governed by the following dy-

namics:

$$\begin{aligned}
&\partial_t \rho^\varepsilon + \nabla \cdot j^\varepsilon = 0,\\
&\partial_t j^\varepsilon + \nabla \cdot \left[\frac{j^\varepsilon \otimes j^\varepsilon}{\rho^\varepsilon}\right] + \rho \nabla V = \frac{\varepsilon^2}{2}\rho^\varepsilon \nabla\left(\frac{1}{\sqrt{\rho^e}}\Delta\sqrt{\rho^\varepsilon}\right),\\
&\partial_t e^\varepsilon + \nabla \cdot \left(\frac{j^\varepsilon}{\rho^\varepsilon}(e^\varepsilon + \rho^\varepsilon V - V\rho^\varepsilon)\right) = \frac{\varepsilon^2}{4}\nabla \cdot \left[\frac{j^\varepsilon \Delta \rho^\varepsilon}{\rho^\varepsilon} - \frac{\nabla \cdot j^\varepsilon \nabla \rho^\varepsilon}{\rho^\varepsilon}\right].
\end{aligned} \tag{2.6}$$

From here one can easily deduce the conservation in time of total mass and energy:

$$\partial_t \int_{\mathbb{R}} \rho^\varepsilon \, dx = 0, \qquad \partial_t \int_{\mathbb{R}} e^\varepsilon \, dx = 0. \tag{2.7}$$

The two main computational challenges to the Schrödinger equation are:

(i) *small* ε. u^ε oscillates with frequency $1/\varepsilon$ in *both* space *and* time, hence one needs to numerically resolve these oscillations, both spatially and temporally.

(ii) *Large* d. For a system consisting of N particles, $d = 3N$. Typically N is large. For example for the carbon dioxide molecule $d = 75$. For benzene molecule $N = 162$. This causes the curse-of-dimensionality. Totally different techniques need to be used for such high dimensional problems and we shall not elaborate on these issues in this paper.

In this survey we focus on the first challenge, namely how one numerically deals with the small ε problem efficiently. To this aim, we first review the so-called "*semi-classical*" approximation.

The WKB analysis

Consider the initial data of the following form (the so-called WKB initial data)

$$u^\varepsilon(0, x) = A_0(x) e^{iS_0(x)/\varepsilon}. \tag{2.8}$$

The WKB analysis assumes that the solution remains the same form at later time:

$$u^\varepsilon(t, x) = A(t, x) e^{iS(t,x)/\varepsilon}. \tag{2.9}$$

Here A is the amplitude, and S is the phase. Applying this *ansatz*, which is also called the Madelung transform, to the Schrödinger equation (2.2), and separating the real part from the imaginary part, one gets

$$\begin{aligned}
&A\partial_t S = \frac{\varepsilon^2}{2}\Delta A - \frac{1}{2}A|\nabla S|^2 - AV\,,\\
&\partial_t A = -\nabla A \cdot \nabla S - \frac{1}{2}A\Delta S\,.
\end{aligned} \tag{2.10}$$

Ignoring the $O(\varepsilon^2)$ terms, one gets

$$\begin{aligned} &\partial_t |A|^2 + \nabla(|A|^2 \nabla S) = 0\,, \\ &\partial_t S + \frac{1}{2}|\nabla S|^2 + V = 0\,. \end{aligned} \tag{2.11}$$

The first equation above is called the *transport equation*, while the second is the *eiconal equation*. The eiconal equation is a Hamilton-Jacobi equation which admits solutions S with discontinuous derivatives. This can be easily seen once one takes a gradient on the equation to get (by letting $u = \nabla S$)

$$\partial_t u + u \cdot \nabla u + \nabla V = 0\,. \tag{2.12}$$

This is the inviscid Burgers' equation (with forcing term $-\nabla V$) that admits discontinuous solution (shocks) to u even if the initial data of u is smooth. Consequently the gradient of S becomes discontinuous, a point usually refereed to as the *caustic*.

By defining $\rho = |A|^2$, system (2.11) can be written as

$$\begin{aligned} &\partial_t \rho + \nabla \cdot (\rho u) = 0 \\ &\partial_t (\rho u) + \nabla \cdot (\rho u \otimes u) + \rho V = 0. \end{aligned} \tag{2.13}$$

This is the presureless gas system. Clearly the system is decoupled. One can solve the second equation (which is actually (2.12)) for u and then obtain ρ from the first equation. When u becomes discontinuous, ρ becomes a Dirac Delta function, usually called a *delta shock* (Tan, Zhang, Chang and Zheng 1994). Thus at a caustic, the amplitude A blows up (becomes infinity).

Beyond the caustic, one notion of mathematical solution to the Hamilton-Jacobi equation is the *viscosity solution*, introduced by Crandall and Lions (Crandall and Lions 1983). This notion, however, cannot be used here since system (2.13) is in fact the $\varepsilon \to 0$ limit of system (2.6), which is a *zero dispersion limit*. Zero dispersion limit is drastically different from the zero dissipation limit, as studied for the Korteweg–de Vries (KdV) Equation (Lax and Levermore 1983). For semiclasical limit of the defocusing nonlinear Schrödinger equation see (Jin, Levermore and McLaughlin 1999)). Thus the WKB analysis is only valid up to the time when the first caustic forms. Beyond caustics, the solution becomes *multi-valued* (Sparber, Markowich and Mauser 2003).

In contrast to that, the Wigner tranform technique, which we study next, yields the Liouville equation on *phase space*, in the semiclassical limit $\varepsilon \to 0$, whose solution does not exhibit caustics, hence is valid globally in time.

Classical limit via the Wigner transform

The *Wigner transform* of u^ε is defined as (Wigner 1932)

$$w^\varepsilon[u^\varepsilon](x,\xi) := \frac{1}{(2\pi)^d}\int_{\mathbb{R}^d} u^\varepsilon\left(x+\frac{\varepsilon}{2}\eta\right)\overline{u^\varepsilon}\left(x-\frac{\varepsilon}{2}\eta\right)\mathrm{e}^{i\xi\cdot\eta}\,\mathrm{d}\eta \tag{2.14}$$

which is the Fourier transform of the density matrix.

It is easy to see that the Wigner transform w^ε is real-valued, but in general not necessarily positive. The moments of w^ε give the quantum mechanical physical observables. For examples, the particle density (2.3) can be computed via

$$\rho^\varepsilon(t,x) = \int_{\mathbb{R}^d} w^\varepsilon(t,x,\xi)\,\mathrm{d}\xi,$$

the current density (2.4) can be obtained by

$$j^\varepsilon(t,x) = \int_{\mathbb{R}^d} \xi w^\varepsilon(t,x,\xi)\,\mathrm{d}\xi,$$

while the energy density (2.5) is just

$$e^\varepsilon(t,x) = \int_{\mathbb{R}^d}\left(\frac{1}{2}|\xi|^2+V(x)\right)w^\varepsilon(t,x,\xi)\,\mathrm{d}\xi.$$

Applying the Wigner transformation to the Schrödinger equation (2.2), one obtains the Wigner equation (also called the quantum Liouville equation):

$$\partial_t w^\varepsilon + \xi\cdot\nabla_x w^\varepsilon - \Theta^\varepsilon[V]w^\varepsilon = 0, \quad w^\varepsilon(0,x,\xi) = w^\varepsilon_{\mathrm{in}}(x,\xi), \tag{2.15}$$

where $\Theta^\varepsilon[V]$ is given by

$$\Theta^\varepsilon[V]f(x,\xi) := \frac{i}{(2\pi)^d}\iint_{\mathbb{R}^d\times\mathbb{R}^d}\delta V^\varepsilon(x,y)f(x,\xi')\mathrm{e}^{i\eta(\xi-\xi')}\,\mathrm{d}\eta\,\mathrm{d}\xi', \tag{2.16}$$

with

$$\delta V^\varepsilon := \frac{1}{\varepsilon}\left(V\left(x-\frac{\varepsilon}{2}y\right)-V\left(x+\frac{\varepsilon}{2}y\right)\right).$$

When $\varepsilon\to 0$

$$\delta V^\varepsilon \overset{\varepsilon\to 0}{\longrightarrow} y\cdot\nabla_x V,$$

then (2.15) formally becomes the classical *Liouville equation* on phase space:

$$\partial_t w + \xi\cdot\nabla_\xi w - \nabla_x V(x)\cdot\nabla_\xi w = 0\,. \tag{2.17}$$

This is the classical limit of the Schrödinger equation as $\varepsilon\to 0$, valid *globally* in time, even beyond the caustic (Lions and Paul 1993, Gérard, Markowich, Mauser and Poupaud 1997), in contract to the WKB analysis. Note that the Liouville equation (2.17) is linear, which unfolds the singularity, and the

linear superposition and time reversibility of the Schrödinger equation are also preserved.

The (bi)characteristic equations for (2.17) is given by

$$\dot{x} = \xi, \quad \dot{\xi} = -\nabla_x V(x),$$

which is exactly Newton's equation. This system can be written as a Hamiltonian system:

$$\begin{cases} \dot{x} = \nabla_\xi H(x,\xi), \\ \dot{\xi} = -\nabla_x H(x,\xi), \end{cases} \tag{2.18}$$

with the Hamiltonian H (in classical mechanics) given by

$$H(x,\xi) = \frac{1}{2}|\xi|^2 + V(x). \tag{2.19}$$

For $x, \xi \in \mathbb{R}^{dN}$, and V the potential for N-particles, (2.18) is the particle system to be studied in the next subsection.

2.2. From classical mechanics to kinetic equations

From hard sphere particles to the Boltzmann equation

Consider N particles of hard sphere,

$$\dot{x}_i = v_i,$$
$$\dot{v}_i = 0,$$

where $(x_i, v_i) \in \mathbb{R}^d \times \mathbb{R}^d$, $(1 \le i \le N)$ denote the position and velocity of particle i. Assume each particle has the same diameter σ, then they satisfy the exclusion condition

$$|x_i(t) - x_j(t)| > \sigma. \tag{2.20}$$

Assume particles i and j collide elastically when $|x_i - x_j| = \sigma$, then the post-collisional velocities, denoted by v_i' and v_j' respectively, are given by

$$v_i' = v_i - [(v_i - v_j)\cdot\omega]\omega\,, \quad v_j' = v_j + [(v_i - v_j)\cdot\omega]\omega\,, \tag{2.21}$$

where $\omega = (x_j - x_i)/|x_j - x_i|$.

Define

$$Z_N = (z_1, \cdots, z_N) = (x_1, v_1, \cdots, x_N, v_N). \tag{2.22}$$

Let $W^N(t, Z_N)$ be the probability distribution of the particle system. Then it solves the N-body Liouville equation

$$\partial_t W^N(t) = \mathcal{L}_N W^N(t), \quad \mathcal{L}_N = -\sum_{i=1}^{N} (v_i \cdot \nabla_{x_i}), \tag{2.23}$$

which is defined on the domain

$$\mathcal{D}_N = \left\{ Z_N \in \mathbb{R}^{2dN} \middle| \, |x_i - x_j| > \sigma, \quad \text{for } i \neq j \right\}.$$

At the boundary, where $|x_i - x_j| = \sigma$, one has $W^N(t, Z_N') = W^N(t, Z_N)$.

Assume all particles are *identical and indistinguishable*, namely

$$W^N(z_1, \cdots, z_N) = W^N(z_{\sigma_1}, \cdots, z_{\sigma_N})$$

for any $\{\sigma_1, \cdots, \sigma_N\}$, a random permulation of set $\{1, \cdots, N\}$. Furthermore, assume the so-called *molecular chaos* condition:

$$W^N(z_1, \cdots z_N) = W_1^N(x_1, v_1) \cdots W_N^N(x_n, v_N).$$

Under the above assumptions, the Grad-Boltzmann limit of classical particles can be derived by letting $\sigma \to 0$, and $N \to \infty$, and under the assumption

$$N\sigma^2 \to \text{constant}\,,$$

then the one-particle distribution $W_1^N(x_1, v_1)$ approaches formally to the Boltzmann equation for hard spheres (Bouchut, Golse and Pulvirenti 2000*a*):

$$\partial_t f + v \cdot \nabla_x f = \int |(v - v_*) \cdot \omega| \{ f(v') f(v_*') - (f(v) f(v_*) \} d\omega dv_*\,, \quad (2.24)$$

where v and v_* are pre-collisional velocites with corresponding post-collisional velocities v' and v_*' determined by (2.21) (with $v_i = v, v_j = v_*$).

The proof of the Grad-Boltzmann limit is extremely challenging. So far the only rigorous results are available for a very short duration of time–a fraction of a mean free time, see (Lanford 1975) (Gallagher, Saint-Raymond and Texier 2013).

Mean-field limit of particle systems

The Newton type equations also arise in microscopic modeling of a vast number of important phenomena in physical, social, and biological sciences, (Vicsek, Czirók, Ben-Jacob, Cohen and Shochet 1995) (Cucker and Smale 2007) (Motsch and Tadmor 2014)(Albi, Bellomo, Fermo, Ha, Kim, Pareschi, Poyato and Soler 2019) . These problems can all be modelled by interacting particle systems of first order

$$dX^i = b(X^i)\, dt + \alpha_N \sum_{j:j\neq i} K_1(X^i - X^j)\, dt + \eta\, dW^i,\ i = 1, 2, \cdots, N, \quad (2.25)$$

or second order

$$\begin{aligned} dX^i &= V^i\, dt, \\ dV^i &= \left[b(X^i) + \alpha_N \sum_{j:j\neq i} K(X^i - X^j) - \gamma V^i \right] dt + \eta\, dW^i. \end{aligned} \quad (2.26)$$

Here, $(X^i, V^i) \in \mathbb{R}^d \times \mathbb{R}^d$, loosely speaking, represent the position and velocity of the i-th particle, and $b(\cdot)$ is the external field. The stochastic processes $\{W^i\}_{i=1}^N$ are i.i.d. Wiener processes, or the standard Brownian motions. The function $K(\cdot) : \mathbb{R}^d \to \mathbb{R}^d$ is the interaction kernel. For the molecules in the heat bath, η and γ satisfy the so-called "fluctuation-dissipation relation"

$$\eta = \sqrt{2\gamma/\beta}, \tag{2.27}$$

where β is the inverse of the temperature (we assume all the quantities are scaled and hence dimensionless so that the Boltzmann constant is absent). The first order system (2.25) can be viewed as the over-damped limit, namely rescale t to γt and let $\gamma \to \infty$, of the second order system (2.26) (Stanley 1971)(Georges, Kotliar, Krauth and Rozenberg 1996)(Lelievre and Stoltz 2016).

The mean field limit is usually taken by choosing

$$\alpha_N = \frac{1}{N-1}. \tag{2.28}$$

Define the empirical distribution

$$\mu^{(N)} := \frac{1}{N}\sum_{i=1}^{N} \delta(x - X^i) \otimes \delta(v - V^i). \tag{2.29}$$

For the second order system (2.26), as $N \to \infty$, $\mu^{(N)}$ converges almost surely in the weak topology to the solutions of the (mean-field) Fokker-Planck equation

$$\partial_t f = -\nabla_x \cdot (vf) - \nabla_v \cdot \Big((b(x) + K *_x f - \gamma v) f \Big) + \frac{1}{2}\eta^2 \Delta_v f. \tag{2.30}$$

The mean field limit corresponding to the first order system (2.25) is ((McKean 1967) (Golse 2003) (Jabin and Wang 2017))

$$\partial_t f = -\nabla \cdot \Big((b(x) + K_1 * f) f \Big) + \frac{1}{2}\eta^2 \Delta f. \tag{2.31}$$

These mean field limits can also be derived from taking the limit $N \to \infty$ of the N-body distribution with molecular chaos assumptions, like in the derivation of the Boltzmann equation from the N-body Newton's equations described above.

2.3. From kinetic equations to hydrodynamics

Hydrodynamic limit of the Boltzmann equation

The Boltzmann equation describes the probability density function $f(t, x, v)$ of particles that undergo transport and binary collisions (Cercignani 1988):

$$\partial_t f + v \cdot \nabla_x f = \frac{1}{\varepsilon}\mathcal{Q}(f), \quad x, v \in \mathbb{R}^n, \tag{2.32}$$

where the collision term $\mathcal{Q}(f)$ is a nonlinear integral operator:

$$\mathcal{Q}(f)(v) = \frac{1}{\varepsilon}\int_{\mathbb{R}^d}\int_{S^{d-1}} B(v-v_*,\omega)\left[f(v')f(v'_*) - f(v)f(v_*)\right]\,\mathrm{d}\omega\,\mathrm{d}v_*. \quad (2.33)$$

Here (v, v_*) and (v', v'_*) are the velocity pairs before and after an elastic collision, which conserve the momentum and energy. They are related by

$$v' = v - [(v-v_*)\cdot\omega]\omega\,, \quad v'_* = v_* + [(v-v_*)\cdot\omega]\omega\,,$$

with the parameter $\omega \in S^{d-1}$, the unit sphere on $\mathbb{R}^d$. $B(v-v_*,\omega)$ is the (non-negative) collision kernel depending only on $|v-v_*|$ and cosine of the deviation angle $\frac{\sigma\cdot(v-v_*)}{|v-v_*|}$. ε is the Knudsen number, the dimensionless mean free path.

The hydrodynamic quantities ρ, u and T, the density, marcoscopic velocity and temparature respectively, are defined as the moments of f:

$$\rho = \int_{\mathbb{R}^d} f\,\mathrm{d}v = \int_{\mathbb{R}^d}\mathcal{M}\,\mathrm{d}v, \quad u = \frac{1}{\rho}\int_{\mathbb{R}^d} vf\,\mathrm{d}v = \int_{\mathbb{R}^d} v\mathcal{M}\,\mathrm{d}v, \quad (2.34)$$

$$T = \frac{1}{d\rho}\int_{\mathbb{R}^d}|v-u|^2 f\,\mathrm{d}v = \frac{1}{d\rho}\int_{\mathbb{R}^d}|v-u|^2\mathcal{M}\,\mathrm{d}v, \quad (2.35)$$

where the local Maxwellian

$$\mathcal{M} = \frac{\rho}{(2\pi T)^{d/2}}\exp\left(-\frac{|u-v|^2}{2T}\right). \quad (2.36)$$

The collision operator $\mathcal{Q}(f)$ conserves mass, momentum, and energy:

$$\int_{\mathbb{R}^d}\mathcal{Q}(f)\phi(v)\,\mathrm{d}v = 0, \quad \phi(v) = (1, v, |v|^2/2)^T, \quad (2.37)$$

with the momentum $m = \rho u$, and the total energy $E = \frac{1}{2}\rho u^2 + \rho T$.

One of the most important properties of $\mathcal{Q}$ is the celebrated Boltzmann's H-theorem:

$$\partial_t\int_{\mathbb{R}^d} f\log f\,\mathrm{d}v = \int_{\mathbb{R}^d}\mathcal{Q}(f)\ln f\,\mathrm{d}v \le 0.$$

The functional $f\log f$ is the entropy of the system. Boltzmann's H theorem implies that any equilibrium distribution function, i.e., any function which is a maximum of the entropy, has the form of a local Maxwellian distribution

$$\int_{\mathbb{R}^d}\mathcal{Q}(f)\ln f\,\mathrm{d}v = 0 \Longleftrightarrow \mathcal{Q}(f) = 0 \Longleftrightarrow f = \mathcal{M}. \quad (2.38)$$

When $\varepsilon \to 0$, $\mathcal{Q} \to 0$, (2.38) implies that $f = \mathcal{M}$. Consequently the

moments of f solve the compressible Euler equations:

$$\begin{cases} \partial_t \rho + \nabla_x \cdot (\rho u) = 0, \\ \partial_t (\rho u) + \nabla_x \cdot (\rho u \otimes u + pI) = 0, \\ \partial_t E + \nabla_x \cdot ((E+p)u) = 0. \end{cases} \tag{2.39}$$

Via the Chapman-Enskog expansion, one can derive the Navier-Stokes (NS) equations by retaining $O(\varepsilon)$ terms (Bouchut, Golse and Pulvirenti 2000*b*):

$$\begin{cases} \partial_t \rho + \nabla_x \cdot (\rho u) = 0, \\ \partial_t (\rho u) + \nabla_x \cdot (\rho u \otimes u + pI) = \varepsilon \nabla_x \cdot (\mu \sigma(u)), \\ \partial_t E + \nabla_x \cdot ((E+p)u) = \varepsilon \nabla_x \cdot (\mu \sigma(u) u + \kappa \nabla_x T), \end{cases} \tag{2.40}$$

where $\sigma(u) = \nabla_x u + \nabla_x u^T - \frac{2}{d} \nabla_x \cdot u I$, I is the identity matrix, μ and κ are the viscosity and heat conductivity, determined through the linearized Boltzmann collision operator, and usually depend on T.

Diffusion limit of transport equation

In many applications, such as neutron transport and radiative transfer, the collision operator is linear. The interesting scaling is often the diffusive scaling where the scattering rate is large. A typical such equation has the form of

$$\varepsilon \, \partial_t f + v \cdot \nabla_x f = \frac{1}{\varepsilon} \int b(v,w) \{ M(v) f(w) - M(w) f(v) \} dw \,, \quad x, v \in \mathbb{R}^d \tag{2.41}$$

with the normalized Maxwellian M defined by

$$M(v) = \frac{1}{(2\pi)^{d/2}} \exp(-|v|^2/2) \,.$$

The (anisotropic) scattering kernel b is rotationally invariant, satisfying

$$b(v,w) = b(w,v) > 0 \,.$$

Define the collision frequency λ as

$$\lambda(v) = \int b(v,w) M(w) \, dw \,.$$

As $\varepsilon \to 0$, $f \to \rho(x,t) M(v)$, where $\rho(t,x) = \int f(v) \, dv$ satisfies the diffusion equation (Bardos, Santos and Sentis 1984) (Markowich, Ringhofer and Schmeiser 1990)

$$\partial_t \rho = \nabla_x \cdot (D \nabla_x \rho) \tag{2.42}$$

with the diffusion coefficient matrix

$$D = \int \frac{M(v)}{\lambda(v)} v \otimes v \, dv \,. \tag{2.43}$$

3. Numerical passages from quantum to classical mechanics

The highly oscillatory nature of the solution, in both space and time, to the Schrödinger equation (2.2) poses a huge challenge in numerical computations, especially in high dimensions, since one needs to resolve numerically, in both space and time, the small wave length of $O(\varepsilon)$ which is computationally daunting. If one does not use small enough time step or mesh size, even if the numerical scheme is stable, one may get completely wrong solutions (Markowich, Pietra and Pohl 1999)(Bao, Jin and Markowich 2002). To understand the numerical behavior in the semiclassical regime, in addition to standard consistency and stability–which implies convergence by Lax's equivalence theorem– one needs new semiclassical analysis to understand the correct behavior of the numerical solutions.

Here one is interested in two questions:

- What kind of schemes best suits the highly oscillatory problems?
- How to analyze the numerical performance when ε is small?

For the first question, when the solution is smooth but highly oscillatory, the spectral or pseudo-spectral methods give the best performance in terms of numerical accuracy and resolution. It is worthy to point out that taking care of spatial discretization alone is not enough to achieve the best performance for the Schrödinger equation (2.2). It takes a good combination of *both* spatial *and* temporal discretizations to achieve the most favorable mesh strategies (the largest possible ratio between the mesh size and time steps over ε). In this regard the time-splitting spectral methods, as studied in (Bao et al. 2002), offers the best mesh strategy, while finite-difference type schemes require very fine numerical resolution of the oscillations (Markowich et al. 1999).

3.1. Time-splitting spectral methods for the semiclassical Schrödinger equations

For the sake of notation clarity, we shall discuss the method only in one space dimension ($d = 1$). Generalizations to $d > 1$ are straightforward for tensor product grids and the same conclusions hold.

Consider the one-dimensional version of equation (2.2),

$$\mathrm{i}\varepsilon \partial_t u^\varepsilon = -\frac{\varepsilon^2}{2} \partial_{xx} u^\varepsilon + V(x) u^\varepsilon, \quad u^\varepsilon(0,x) = u^\varepsilon_{\mathrm{in}}(x), \tag{3.2}$$

for $x \in [0,1]$, with periodic boundary conditions

$$u^\varepsilon(t,0) = u^\varepsilon(t,1), \quad \partial_x u^\varepsilon(t,0) = \partial_x u^\varepsilon(t,1), \quad \forall\, t \in \mathbb{R}.$$

We choose the spatial mesh size $\Delta x = 1/M$ for some large positive integer M, and time-step $\Delta t > 0$. The spatio-temporal grid-points are then given by

$$x_j := j\Delta x,\ j = 1, \dots, M, \qquad t_n := n\Delta t,\ n \in \mathbb{N}.$$

Let $u_j^{\varepsilon,n}$ be the numerical approximation of $u^\varepsilon(x_j, t_n)$, for $j = 1, \dots, M$.

The Schrödinger equation (3.2) is solved by a time splitting method:

Step 1. From time $t = t_n$ to time $t = t_{n+1}$ first solve the free Schrödinger equation

$$\mathrm{i}\varepsilon \partial_t u^\varepsilon + \frac{\varepsilon^2}{2} \partial_{xx} u^\varepsilon = 0. \tag{3.3}$$

Step 2. Also on $t \in [t_n, t_{n+1}]$, solve the ordinary differential equation

$$\mathrm{i}\varepsilon \partial_t u^\varepsilon - V(x) u^\varepsilon = 0, \tag{3.4}$$

with the solution $u^{\varepsilon,*}$ obtained from Step 1 as initial data.

Note (3.4) can be solved *exactly*,

$$u(t_{n+1}, x) = u(t_n, x) \mathrm{e}^{-\mathrm{i}V(x)\Delta t/\varepsilon}.$$

In Step 1, equation (3.3) will be discretized by a (pseudo-)spectral method in space and consequently integrated in time *exactly* in the Fourier space. More precisely,

$$u_j^{\varepsilon,*} = \frac{1}{M} \sum_{\ell=-M/2}^{M/2-1} \mathrm{e}^{\mathrm{i}\varepsilon\Delta t \gamma_\ell^2/2}\, \widehat{u}_\ell^{\varepsilon,n}\, \mathrm{e}^{\mathrm{i}\gamma_\ell(x_j - a)},$$

where $\gamma_\ell = 2\pi l$ and $\widehat{u}_\ell^{\varepsilon,n}$ is the Fourier coefficients of $u^{\varepsilon,n}$, i.e.

$$\widehat{u}_\ell^{\varepsilon,n} = \sum_{j=1}^{M} u_j^{\varepsilon,n}\, \mathrm{e}^{-i\gamma_\ell x_j}, \quad \ell = -\frac{M}{2}, \dots, \frac{M}{2} - 1\,.$$

Note that in both steps the time integration is *exact*. The only time discretization error of this method is the splitting error, which is *first order* in k, for any *fixed* $\varepsilon > 0$. We will refer this method as TSSP.

The second order in time (for fixed $\varepsilon > 0$) can be obtained via the Strang splitting method. Extensions to higher order (in time) splitting schemes can also be done, see e.g. (Bao and Shen 2005). See also its extension to the case of vector potential (Jin and Zhou 2013).

3.2. Numerical analysis in the semiclassical regime

Classical numerical analysis, based on consistency and stability, does not provide accurate assessment of the numerical performance when $\varepsilon \ll 1$. Wigner analysis, on the other hand, gives more insight about the behavior of numerical solutions, for *physical observables*, in the semiclassical regime.

Assume that the potential $V(x)$ is periodic in domain $[0,1]$, smooth, and satisfies

$$\left\| \frac{d^m}{dx^m} V \right\|_{L^\infty[a,b]} \leq C_m, \tag{3.5}$$

for some constant $C_m > 0$, and furthermore,

$$\left\| \frac{\partial^{m_1+m_2}}{\partial t^{m_1} \partial x^{m_2}} u^\varepsilon \right\|_{C([0,T];L^2[a,b])} \leq \frac{C_{m_1+m_2}}{\varepsilon^{m_1+m_2}}, \tag{3.6}$$

for all $m, m_1,\ m_2 \in \mathbb{N} \cup \{0\}$, namely the solution oscillates in space and time with wavelength ε. The following estimate was given in (Bao et al. 2002).

Theorem 3.1. Let $V(x)$ satisfy assumption (3.5) and $u^\varepsilon(t,x)$ be a solution of (3.2) satisfying (3.6). Denote by $u^{\varepsilon,n}_{\rm int}$ the interpolation of the discrete approximation obtained via TSSP. Then, for $t_n \in [0,T]$,

$$\left\| u^\varepsilon(t_n) - u^{\varepsilon,n}_{\rm int} \right\|_{L^2(0,1)} \leq G_m \frac{T}{\Delta t} \left(\frac{\Delta x}{\varepsilon} \right)^m + \frac{CT\Delta t}{\varepsilon}, \tag{3.7}$$

where $C > 0$ is independent of ε and m and $G_m > 0$ is independent of ε, Δx, Δt.

Clearly, (3.7) implies that, to get an accurate u^ε one needs the following mesh strategy:

$$\Delta t = o(\varepsilon), \quad \Delta x = o(\varepsilon)\,.$$

Hence the oscillations need to be resolved both spatially and temporally.

3.3. Accurate computation of physical observables

If one is just interested in obtaining accurate physical observables, it was observed in (Bao et al. 2002) that the time step can be much relaxed. This cannot be understood from the above classical numerical analysis, rather the Wigner picture of quantum dynamics will offer the clue.

Let $u^\varepsilon(t,x)$ be the solution of (3.2) and $w^\varepsilon(t,x,\xi)$ the corresponding Wigner transform. It is easy to see that the splitting scheme (3.3)-(3.4) corresponds to the following time-splitting scheme for the Wigner equation (2.15):

Step 1. For $t \in [t_n, t_{n+1}]$, first solve the linear transport equation

$$\partial_t w^\varepsilon + \xi\, \partial_x w^\varepsilon = 0\,. \tag{3.8}$$

Step 2. On the same time-interval, solve the scattering term

$$\partial_t w^\varepsilon - \Theta^\varepsilon[V] w^\varepsilon = 0\,, \tag{3.9}$$

with initial data obtained from Step 1.

Since in each step of the splitting, the time integration is *exact*, without any discretization error, thus one can take $\varepsilon \to 0$ limit in each step, consequently obtain the following limiting scheme:

Step 1. For $t \in [t_n, t_{n+1}]$ solve

$$\partial_t w + \xi\, \partial_x w^0 = 0. \tag{3.10}$$

Step 2. Using the outcome of Step 1 as initial data, solve, on the same time-interval:

$$\partial_t w - \partial_x V\, \partial_\xi w^0 = 0. \tag{3.11}$$

This is *exactly* the time-splitting scheme for the limiting Liouville equation (2.17)! Since in the limiting process Δt was held fixed, hence independent of ε, thus when $\Delta t = O(1)$, and as $\varepsilon \to 0$, schemes (3.8) and (3.9) collapse to schemes (3.10) and (3.11), therefore the scheme is AP in time! Hence one can take $\Delta t = O(1)$, combined with the spectral mesh-size $\Delta x = o(\varepsilon)$ to get accurate w^ε, and as a consequence, *all physical observables*!

Remark 3.2. While the above Wigner analysis is formal, rigorous uniform in ε error estimate was obtained recently. In (Golse, Jin and Paul 2021), for both first and second order splittings, a uniform in ε error estimates, with explicit constants, were given (for the von Neumann equation–the density operator representation of the Schrödinger quation which are valid even for mixed states). The errors are measured by a pseudo-metric introduced in (Golse and Paul 2017), which is an analogue of the Wasserstain distance of exponent 2 between a quantum density operator and a classical density in phase space. The regularity requirement for V is $V \in C^{1,1}$. Sharper uniform error estimates for physical observables were also obtained for the Strang splitting (Lasser and Lubich 2020), based on Egorov's theorem, with additional regularity requirement on V.

Example 3.3. We take one example from (Bao et al. 2002). The Schrödinger equation (3.2) is solved with initial condition $u_0(x) = n_0(x)\exp(-\mathrm{i}S_0(x)/\varepsilon)$, where

$$n_0(x) = \left(e^{-25(x-0.5)^2}\right)^2, \quad S_0(x) = -\frac{1}{5}\ln\left(e^{5(x-0.5)} + e^{-5(x-0.5)}\right), \tag{3.12}$$

and $V(x) = 10$. Due to the compressive initial velocity $\frac{d}{dx}S_0(x)$, caustics will form. The weak limits $n^0(x,t)$, $J^0(x,t)$ of $n^\varepsilon(x,t)$, $J^\varepsilon(x,t)$ respectively as $\varepsilon \to 0$ can be computed by evaluating the zeroth and first order velocity

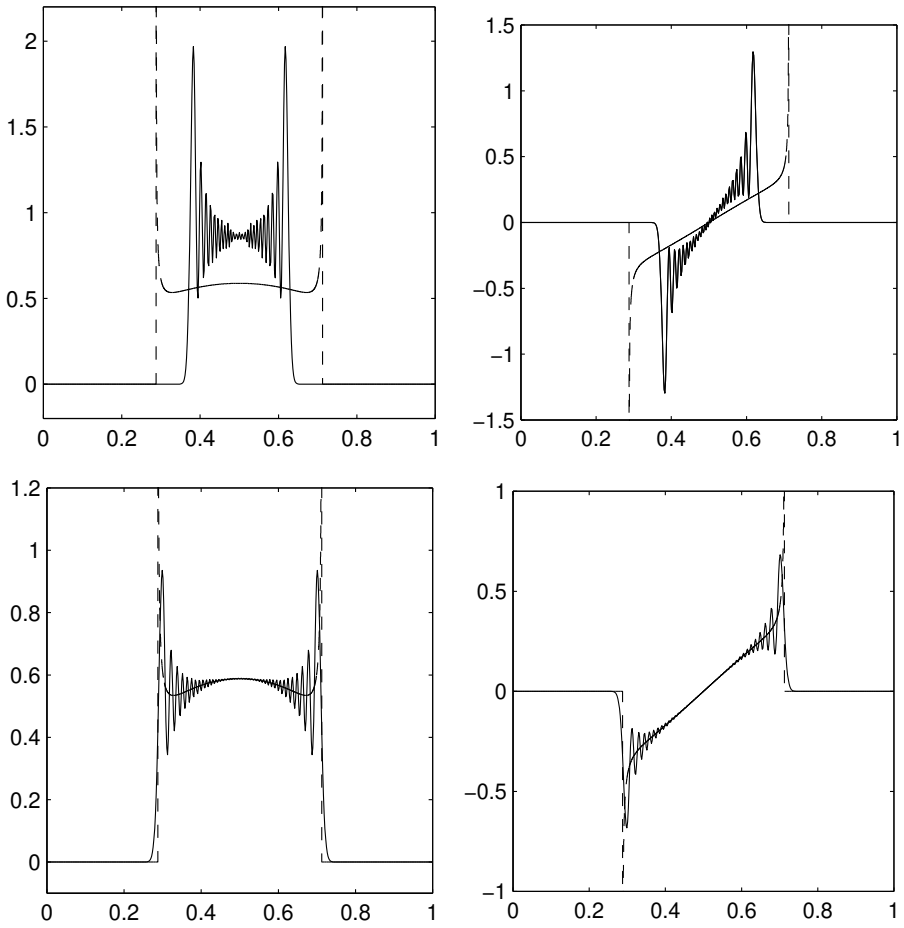

Figure 3.4. Example 3.3. Numerical solutions at $t = 0.54$. Top: CNSP with $k = 0.0001$; Bottom: TSSP2. Left: position density; Right: current density. $\varepsilon = 10^{-3}$, $V(x) = 10$, $h = \frac{1}{512}$.

moments of the solution to the Liouville equation (2.17). As a reference we plot them at $t = 0.54$ (after the caustics formed) in Fig. 3.4. We compare the solutions between CNSP (Crank-Nicolson in time and pseudo-spectral method in space) and TSSP2 (Strang's splitting in time and pseudo-spectral method in space). The mesh size Δx is taken in the same order as $\varepsilon = 10^{-3}$. One can see that for CNSP, even for $\Delta t = 0.0001$, the numerical solution cannot capture the correct weak limit. TSSP2 can capture the physical observations correctly with Δt much larger than ε.

So far no numerical schemes are known to allow $\Delta x = o(1)$ for the

Schrödinger equation (2.2). The best one can do is to allow $\Delta x = o(\sqrt{\varepsilon})$, by using the Guassian beam or Gaussian wave packet methods, see (Heller 2006)(Hill 1990)(Jin, Wu and Yang 2008)(Leung and Qian 2009)(Russo and Smereka 2013). For more recent results about Gaussian type approximations see (Jin et al. 2011)(Lasser and Lubich 2020).

3.4. Ehrenfest dynamics

The *ab initio* methods have played indispensable roles in simulating large systems of quantum molecular dynamics. There the forces acted on the nuclei are computed from electronic structures, a procedure known as the "on-the-fly" calculation in chemistry literature (for detailed reviews, see, e.g., (Tully 1998)(Marx and Hutter 2009). The *Ehrenfest dynamics* is one of popularly used such methods. There one separates the quantum system into two sub-systems: a fast varying, quantum mechanical part for electrons and a slowly varying part for the nuclei. Due to the large mass difference between electrons and nuclei, the nucleonic system can be passed to the (semi-)classical limit, hence the computational cost is significantly reduced.

Take $x \in \mathbb{R}^d$ as the electronic coordinate, $y \in \mathbb{R}^n$ the nucleonic coordinate, with $d, n \in \mathbb{N}$, and denote by $\langle \cdot, \cdot \rangle_{L^2_x}$ and $\langle \cdot, \cdot \rangle_{L^2_y}$ the usual inner product in $L^2(\mathbb{R}^d_x)$ and $L^2(\mathbb{R}^n_y)$, respectively, i.e.

$$\langle f, g \rangle_{L^2_z} \equiv \int_{\mathbb{R}^m} \overline{f}(z) g(z) dz.$$

The total Hamiltonian of the system acting on $L^2(\mathbb{R}^{d+n})$ is assumed to be of the form

$$H = -\frac{\varepsilon^2}{2}\Delta_x - \frac{\delta^2}{2}\Delta_y + V(x, y), \tag{3.13}$$

where $V(x, y) \in \mathbb{R}$ is some real potential.

Consider the following mixed quantum-classical system (corresponding to the limit $\delta \to 0$) (Bisseling, Kosloff, Gerber, Ratner, Gibson and Cerjan 1987)(Makri and Miller 1987) (Jin, Sparber and Zhou 2017*b*):

$$\begin{cases} i\varepsilon \partial_t \psi^\varepsilon = -\dfrac{\varepsilon^2}{2}\Delta_x \psi^\varepsilon + \Upsilon^\varepsilon(x, t)\psi^\varepsilon, \quad \psi^\varepsilon(0, x) = \psi^\varepsilon_{\text{in}}(x) \\ \partial_t \mu^\varepsilon + \eta \cdot \nabla_y \mu^\varepsilon + F^\varepsilon(y, t) \cdot \nabla_\eta \mu^\varepsilon = 0, \quad \mu^\varepsilon(0, x, \eta) = \mu_{\text{in}}(y, \eta). \end{cases} \tag{3.14}$$

Here, $\mu^\varepsilon(\cdot, \cdot, t)$ denotes the phase-space probability density for the slowly varying nuclei at time t, $F^\varepsilon = -\nabla_y V^\varepsilon_{\text{E}}$ is the force obtained from the Ehrenfest potential

$$V^\varepsilon_{\text{E}}(y, t) = \int_{\mathbb{R}^d} V(x, y) \left|\psi^\varepsilon(x, t)\right|^2 dx,$$

and

$$\Upsilon^{\varepsilon}(x,t) \;=\; \iint_{\mathbb{R}^{2n}} V(x,y)\,\mu^{\varepsilon}(y,\eta,t)\,dy\,d\eta. \tag{3.15}$$

This system will be called the *Schrödinger-Liouville-Ehrenfest* (SLE) system. Note that the dependence of μ^{ε} on ε is purely from the forcing through the Ehrenfest potential V_E^{ε} appearing in the Liouville equation. In the case of a single particle distribution concentrated on the classical trajectories $(y(t),\eta(t))$, i.e.,

$$\mu(t,y,\eta) = \delta(y-y(t),\eta-\eta(t)),$$

(3.14) gives (Tully 1998) (Drukker 1999) (Schütte and Bornemann 1999) (Szepessy 2011)

$$\begin{cases} i\varepsilon\partial_t\psi^{\varepsilon} = -\dfrac{\varepsilon^2}{2}\Delta_x\psi^{\varepsilon} + V(x,y(t))\,\psi^{\varepsilon}, \quad \psi^{\varepsilon}(0,x) = \psi_{\text{in}}(x), \\ \quad \dot{y}(t) = \eta(t), \quad y(0) = y_0, \\ \quad \dot{\eta}(t) = -\nabla_y V_{\text{E}}^{\varepsilon}(y(t)), \quad \eta(0) = \eta_0. \end{cases} \tag{3.16}$$

The iterated semiclassical limit ($\delta \to 0$, then $\varepsilon \to 0$) and the full classical limit ($\delta = \varepsilon \to 0$) were rigorously justified in (Jin et al. 2017*b*).

Again, the main numerical difficulty for $\varepsilon \ll 1$ here is that one needs to resolve oscillations of frequency of order $\mathcal{O}(1/\varepsilon)$ in both time and space, as they are present in the solution ψ^{ε}. This requires one to use time-steps of order $\Delta t = o(\varepsilon)$ as well as a spatial grid with $\Delta x = o(\varepsilon)$ to resolve the wave functions. As analyzed in the proceeding subsection, one may ask whether one can design a numerical method which allows the capturing of *physical observables* even for time-steps much larger than $O(\varepsilon)$. For *nonlinear* Schrödinger equations, in general, this is no longer true, as was numerically demonstrated in (Bao, Jin and Markowich 2003). The SLE system (3.14) is a nonlinearly coupled system, and one therefore expects the same type of problem at first glance. Nevertheless, an efficient numerical method for the SLE system was introduced in (Fang, Jin and Sparber 2018) which allows large (compared with ε) computational mesh-sizes in both y and η and a large time step for both the Schrödinger and the Liouville equations, while still *correctly capture the physical observables*. While large meshes in y and η do not seem so surprising, since they are coordinates of the nuclei, the possibility of large time steps for solving the Schrödinger equation for electrons is far from obvious, due to the nonlinear nature of the SLE system.

A time-splitting scheme for the SLE system

Consider the case $d = n = 1$, and the domain $(x, y) \in [0, 1]^2$, with uniform mesh sizes $\Delta y, \Delta\eta$ applied to the classical part of the SLE (3.14). Set

$$J = \frac{1}{\Delta y},\ K = \frac{1}{\Delta\eta},\ M = \frac{1}{\Delta x},\ y_j = j\Delta y,\ \eta_k = k\Delta\eta,\ x_j = j\Delta x.$$

The time-splitting scheme, introduced in (Fang et al. 2018), can then be described as follows: From time $t = t_n = n\Delta t$ to $t = t_{n+1} = (n+1)\,\Delta t$, the SLE system is solved in two steps. First, solve

$$\begin{cases} i\varepsilon\partial_t\psi^\varepsilon = -\dfrac{\varepsilon^2}{2}\Delta_x\psi^\varepsilon, \\ \partial_t\mu^\varepsilon = -\eta\cdot\nabla_y\mu^\varepsilon - F^\varepsilon\,(y,t)\cdot\nabla_\eta\mu^\varepsilon, \end{cases} \tag{3.17}$$

from $t = t_n$ to an intermediate time $t_* = t_n + \Delta t$. Then, solve

$$\begin{cases} ih\partial_t\psi^h = \Upsilon^h\,(x,t)\,\psi^h, \\ \partial_t\mu^h = 0, \end{cases} \tag{3.18}$$

with initial data computed from Step 1, to obtain the solution at time $t = t_{n+1}$.

In (3.17), the Schrödinger equation will be discretized in space by a spectral method using the Fast Fourier Transform, and integrated in the Fourier space in time exactly. The Liouville equation can be solved either by a spectral method, or by a finite difference (e.g., upwind) scheme in space, and then marching the corresponding ODE system forward in time. An advantage of this splitting method is that in the second step, $\Upsilon^h\,(x,t)$ defined in (3.15) is *independent* of time, since obviously μ^h is. Hence, the time integration in (3.18) can also be solved *exactly* as

$$\psi_j^{\varepsilon,n+1} = \exp\left(-\frac{i}{\varepsilon}\Upsilon^\varepsilon\,(x_j,t_*)\,\Delta t\right)\psi_j^{\varepsilon,*}.$$

As an example, consider an upwind spatial discretization of μ. In the first step, solve

$$\begin{cases} i\varepsilon\partial_t\psi^\varepsilon = -\dfrac{\varepsilon^2}{2}\partial_{xx}\psi^\varepsilon, \\ \dfrac{d}{dt}\mu_{jk}^\varepsilon = -\eta_k\,(D_y\mu^\varepsilon)_{jk} - F_j^\varepsilon\,(D_\eta\mu^\varepsilon)_{jk}\,, \end{cases} \tag{3.19}$$

where both $D_y\mu^\varepsilon$ and $D_\eta\mu^\varepsilon$ represent the upwind discretization of the spatial derivatives. To solve the Liouville equation, apply the forward Euler scheme

for the time discretization. Specifically,

$$\begin{cases} \psi_j^{\varepsilon,*} = \dfrac{1}{M} \displaystyle\sum_{\ell=-M/2}^{M/2-1} e^{-i\varepsilon\omega_\ell^2/2} \hat{\psi}_\ell^{\varepsilon,n} e^{i\omega_\ell x_j}, \quad j = 0, \ldots, M-1, \\ \dfrac{\mu_{jk}^{\varepsilon,*} - \mu_{jk}^{\varepsilon,n}}{\Delta t} = -\eta_k \left(D_y \mu^{\varepsilon,n}\right)_{jk} - F_j^{\varepsilon,n} \left(D_\eta \mu^{\varepsilon,n}\right)_{jk}, \end{cases} \tag{3.20}$$

where $w_\ell = 2\pi\ell$.

The second step is then given by

$$\begin{cases} i\varepsilon \partial_t \psi^\varepsilon = \Upsilon_d^\varepsilon (x,t)\, \psi^\varepsilon, \\ \dfrac{d}{dt} \mu_{jk}^\varepsilon = 0, \end{cases} \tag{3.21}$$

where $\Upsilon_d^\varepsilon (x,t)$ is the quadrature approximation of $\Upsilon^\varepsilon (x,t)$. Thus, one explicitly gets

$$\psi_j^{\varepsilon,n+1} = \exp\left(-i\Upsilon_d^{\varepsilon,*}(x_j)\, \Delta t/\varepsilon\right) \psi_j^{\varepsilon,*}, \quad \mu_{jk}^{\varepsilon,n+1} = \mu_{jk}^{\varepsilon,*} \tag{3.22}$$

where

$$\Upsilon_d^{\varepsilon,*}(x) = \sum_{j=0}^{J-1} \sum_{k=0}^{K-1} V(x, y_j)\, \mu_{jk}^{\varepsilon,*} \Delta y \Delta\eta = \sum_{j=0}^{J-1} \sum_{k=0}^{K-1} V(x, y_j)\, \mu_{jk}^{\varepsilon,n+1} \Delta y \Delta\eta,$$

which is the trapezoidal rule for μV with compact support.

The spatial meshing strategy

We first show that one can take the limit $\varepsilon \to 0$, for fixed Δy and $\Delta\eta$. Consider a semi-discretized version of the SLE system (3.14) in one spatial dimension $d = n = 1$ where the Liouville equation is discretized by the upwind scheme:

$$\begin{cases} i\varepsilon \partial_t \psi^\varepsilon = -\dfrac{\varepsilon^2}{2} \partial_{xx} \psi^\varepsilon + \Upsilon_d^\varepsilon (x,t)\, \psi^\varepsilon, \quad \psi^\varepsilon(0,x) = \psi_{\text{in}}^\varepsilon(x), \\ \partial_t \mu^\varepsilon + \eta D_y \mu^\varepsilon + F^\varepsilon (y,t)\, D_\eta \mu^\varepsilon = 0, \quad \mu^\varepsilon(0,y,\eta) = \mu_{\text{in}}^\varepsilon(y,\eta). \end{cases} \tag{3.23}$$

The following theorem is given in (Fang et al. 2018):

Theorem 3.4. Under some suitable conditions for V and initial data, for any $T > 0$, the solution of semi-discretized SLE system (3.23) satisfies, up to extraction of sub-sequences,

$$w^\varepsilon[\psi^\varepsilon] \overset{\varepsilon\to 0_+}{\longrightarrow} \nu, \quad \mu_{jk}^\varepsilon \overset{\varepsilon\to 0_+}{\longrightarrow} \mu_{jk}^0,$$

in w–$*$ topology, where $j = 0, \cdots, J-1$ and $k = 0, \cdots, K-1$. In addition,

ν and μ_{jk} solve the semi-discretized Liouville-system

$$\begin{cases} \partial_t \nu + \xi \partial_x \nu - \partial_x \Upsilon_d^0(x,t)\, \partial_\xi \nu = 0, \\ \dfrac{d}{dt}\mu_{jk}^0 + \eta_k D_y \mu_{jk}^0 + F_j^0 D_\eta \mu_{jk}^0 = 0. \end{cases}$$

The above result shows that the scheme is AP in y, η with respect to ε, namely one can use $\Delta y, \Delta \eta \sim O(1)$. This is the *first* such result for highly oscillatory problem in spatial variables, and more interestingly, the problem under study is *nonlinear*!

Remark 3.5. Numerical experiments show that the same type of behavior is true not only for mixed spectral-finite difference schemes, but also for purely spectral schemes, see (Fang et al. 2018). The proof, however, only works for the former case since it requires positivity of the energy. For spectral method the theory is still lacking.

Time-discretization

The time-discretization of the splitting scheme can also be shown to be AP. Notice the semiclassical limit of SLE (3.14), as $\varepsilon \to 0$, is (Jin et al. 2017*b*):

$$\partial_t \mu + \eta \cdot \nabla_y \mu + F^0(y,t) \cdot \nabla_\eta \mu = 0, \tag{3.24}$$

$$\partial_t \nu + \xi \cdot \nabla_x \nu - \nabla_x \Upsilon^0(x,t) \cdot \nabla_\xi \nu = 0. \tag{3.25}$$

As $\varepsilon \to 0$, the splitting schemes (3.19) and (3.21) approach respectively

$$\begin{cases} \partial_t \nu + \xi \partial_x \nu = 0, \\ \dfrac{d}{dt}\mu_{jk} + \eta_k \left(D_y \mu\right)_{jk} + F_j^0 \left(D_\eta \mu\right)_{jk} = 0, \end{cases} \tag{3.26}$$

and

$$\begin{cases} \partial_t \nu - \partial_x \Upsilon_d^0(x,t)\, \partial_\xi \nu = 0, \\ \dfrac{d}{dt}\mu_{jk} = 0. \end{cases} \tag{3.27}$$

This is the time splitting scheme for (3.24)-(3.25), which ν is the limit of the Wigner transform of ψ^ε on x variable. This shows that $\Delta t \sim O(1)$ can be chosen independent of the small parameter ε. In turn, this yields the convergence of the scheme towards the corresponding scheme of the limiting equation, as stated in (3.26) and (3.27), uniformly in Δt. Hence it is AP in t.

In summary, the scheme (3.19)-(3.21) is AP in t, y, η with respect to ε. One only needs $\Delta x = O(\varepsilon)$.

Numerical experiments

We now present some numerical experiments from (Fang et al. 2018). The interaction potential is given by

$$V(x,y)=\frac{(x+y)^2}{2}.$$

The one-dimensional SLE system is solved on the interval $x\in[-\pi,\pi]$ and $y,\eta\in[-2\pi,2\pi]$ with periodic boundary conditions.

Example 3.6. The initial conditions for the SLE system (3.14) is:

$$\psi_{\text{in}}(x)=\exp\left(-25\,(x+0.2)^2\right)\exp\left(\frac{-i\ln\left(2\cosh\left(5\,(x+0.2)\right)\right)}{5\varepsilon}\right),$$

and

$$\mu_{\text{in}}(y,\eta)=\begin{cases} C_{\text{N}}\exp\left(-\frac{1}{1-y^2}\right)\exp\left(-\frac{1}{1-\eta^2}\right), & \text{for } |y|<1,\ |\eta|<1\\ 0, & \text{otherwise.}\end{cases}$$

Here, $C_{\text{N}}>0$ is the normalization factor such that $\iint_{\mathbb{R}^2}\mu_{in}dy\,d\eta$=1. The time-splitting method with spectral-upwind scheme (i.e., with an upwind scheme for the Liouville's equation) is used. For $\varepsilon=\frac{1}{256},\frac{1}{1024},\frac{1}{4096}$, $T=0.5$, choose $\Delta x=\frac{2\pi\varepsilon}{16}$, $\Delta y=\Delta\eta=\frac{4\pi}{128}$. For each choice of ε, the SLE system is solved first with Δt independent of h and, second, with $\Delta t=o(\varepsilon)$, specifically, we compare the two cases where $\Delta t=0.01$ and $\Delta t=\frac{\varepsilon}{10}$, for numerical values of μ (denoted as μ_1 and μ_2, respectively). As shown in Table 3.1, the error is insensitive in ε, showing a uniform in ε convergence in $\Delta t,\Delta\eta$ and Δy.

ε	1/256	1/1024	1/4096
$\frac{\|\mu_1-\mu_2\|_{\ell^2}}{\|\mu_2\|_{\ell^2}}$	1.65e-03	1.69e-03	1.70e-03

Table 3.1. Example 3.6. The relative ℓ^2-difference (defined as $\frac{\|\mu_1-\mu_2\|_{\ell^2}}{\|\mu_2\|_{\ell^2}}$) for various ε.

Example 3.7. In this example, we choose the same initial data for μ_{in} as in Example 3.6 but

$$\psi_{\text{in}}(x)=\exp\left(-5\,(x+0.1)^2\right)\exp\left(\frac{i\sin x}{h}\right).$$

Now, fix $\Delta t=0.01$, a stopping time $T=0.4$, and $\Delta y=\Delta\eta=\frac{4\pi}{128}$, while

$\Delta x = \frac{2\pi\varepsilon}{16}$, for $\varepsilon = \frac{1}{64}, \frac{1}{128}, \frac{1}{256}, \frac{1}{512}, \frac{1}{1024}, \frac{1}{2048}$, respectively. The reference solution is computed with $\Delta t = \frac{h}{10}$. From the ℓ^2-error plotted in Figure 3.5, one can see that although the error in the wave function increases as ε decreases, the error for the position density $|\psi^\varepsilon|^2$ as well as for the macroscopic quantity μ does not change noticeably. This shows that $\varepsilon-$independent $\Delta t, \Delta y$ and $\Delta\eta$ can be taken to accurately obtain physical observables, but not the wave function ψ^ε itself.

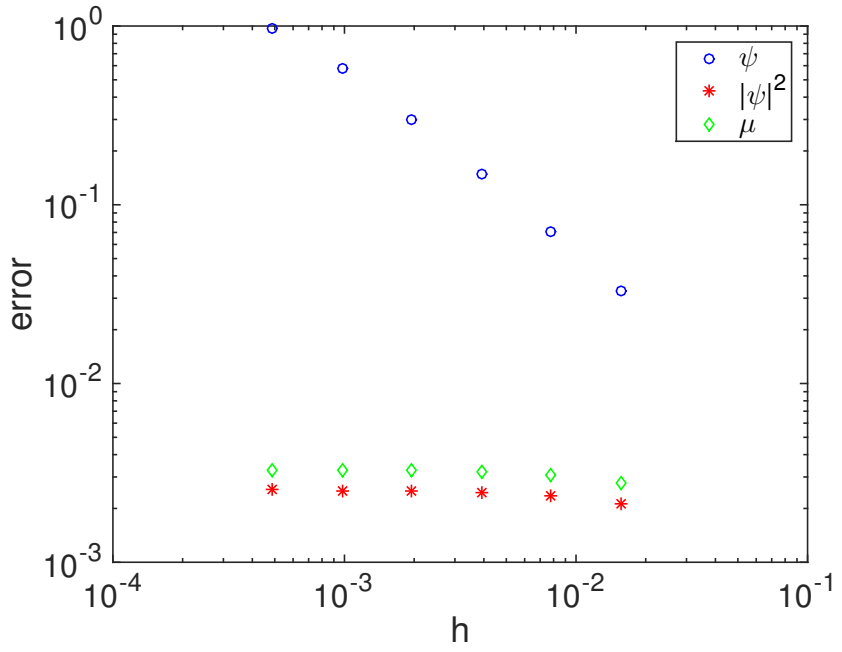

Figure 3.5. Example 3.7: ℓ^2-errors of the wave function ψ^ε, position density $|\psi^\varepsilon|^2$ and μ for various ε. Fix $\Delta t = 0.01$. For $h = \frac{1}{64}, \frac{1}{128}, \frac{1}{256}, \frac{1}{512}, \frac{1}{1024}, \frac{1}{2048}$, choose $\Delta x = \frac{2\pi\varepsilon}{16}$ respectively. The reference solution is computed with $\Delta t = \frac{\varepsilon}{10}$.

4. Numerical passages from classical mechanics to kinetic equations

4.1. The Random Batch Methods

Consider the second order interacting particle systems described by

$$\begin{aligned} dr_i &= v_i\, dt, \\ dv_i &= \Big[b(r_i) + \alpha_N \sum_{j:j\neq i} K(r_i - r_j) - \gamma v_i\Big]\, dt + \sigma\, dW_i, \end{aligned} \tag{4.1}$$

and the first order system,

$$dr_i = b(r_i)\, dt + \alpha_N \sum_{j:j\neq i} K_1(r_i - r_j)\, dt + \sigma\, dW_i,\ \ i = 1, 2, \cdots, N. \tag{4.2}$$

The main difficulty for the numerical simulations of particle system (4.1) or (4.2) is that for lager N, the computational cost per time step is $\mathcal{O}(N^2)$. The Fast Multipole Method (FMM) (Rokhlin 1985) reduces the complexity to $\mathcal{O}(N)$ if the interaction decays sufficiently fast. However, the implementation of FMM is quite delicate. A simple random algorithm, called the Random Batch Method (RBM), has been proposed in (Jin, Li and Liu 2020*a*) to reduce the computation cost per time step from $\mathcal{O}(N^2)$ to $\mathcal{O}(N)$. The key idea of RBM is to use randomly chosen "mini-batch" in the summation term in (4.2) and (4.1). Such an idea has its origin in the stochastic gradient descent (SGD) method. The idea was also used for the computation of the mean-field flocking model (Albi and Pareschi 2013)(Carrillo, Pareschi and Zanella 2019).

Let $T > 0$ be the simulation time, and one chooses a time step $\Delta t > 0$. Pick a batch size $2 \leq p \ll N$ that divides N. Consider the discrete time grids $t_k := k\Delta t$, $k \in \mathbb{N}$. For each sub-interval $[t_{k-1}, t_k)$, the method has two sub-steps: (1) at t_{k-1}, randomly group the N particles into $n := N/p$ subgroups (batches); (2) particles only interact with those in the same batch. This is given in Algorithm 1.

Algorithm 1 (RBM for (4.1))

for m in $1 : [T/\Delta t]$ **do**
  Divide $\{1, 2, \ldots, N = pn\}$ into n batches $\mathcal{C}_q, 1 \le q \le n$ randomly.
  for each batch $\mathcal{C}_q$ **do**
    Update r_i, v_i $(i \in \mathcal{C}_q)$ by solving for $t \in [t_{m-1}, t_m)$ the following

$$\begin{aligned} dr_i &= v_i\, dt, \\ dv_i &= \Big[b(r_i) + \frac{\alpha_N(N-1)}{p-1} \sum_{j \in \mathcal{C}_q, j \neq i} K(r_i - r_j) - \gamma v_i\Big]\, dt + \sigma dW_i. \end{aligned} \tag{4.3}$$

  end for
end for

RBM uses the random permutation, and each particle belongs to one and only one batch. An alternative approach, which allows replacement, is the following algorithm:

Algorithm 2 (RBM-r)

for m in $1 : [T/\Delta t]$ **do**
  for k from 1 to N/p **do**
    Pick a set $\mathcal{C}_k$ of size p randomly with replacement.
    Update r_i's $(i \in \mathcal{C}_k)$ by solving the following SDE for time Δt.

$$\begin{cases} dx_i = u_i\, dt, \\ du_i = \Big[b(x_i) + \dfrac{\alpha_N(N-1)}{p-1} \displaystyle\sum_{j \in \mathcal{C}_k, j \neq i} K(x_i - x_j) - \gamma u_i\Big]\, dt + \sigma\, dW_i. \\ x_i(0) = r_i, \quad u_i(0) = v_i, \end{cases} \tag{4.4}$$

    i.e., solve (4.4) with initial values $x_i(0) = r_i, u_i(0) = v_i$, and set $r_i \leftarrow x_i(\Delta t)$, $v_i \leftarrow u_i(\Delta t)$.
  end for
end for

Different from Algorithm 1, in Algorithm 2, for one iteration of k, some particles may not be updated while some may be drawn more than once.

The random division into n batches of equal size can be implemented using random permutation, which can be realized in $O(N)$ operations by Durstenfeld's modern revision of Fisher-Yates shuffle algorithm (Durstenfeld 1964) (in MATLAB, one can use "randperm(N)"). The ODE solver per particle per time step in (4.3) or (4.4) requires merely $O(p)$ operations, thus

for all particles, each time step costs only $O(pN)$. Since $p \ll N$ the overall cost per time step is significantly reduced from $O(N^2)$ to basically $O(N)$.

For RBM to really gain significant efficiency, one needs Δt to be *independent* of N. We state an error estimate on RBM for the second order systems (4.1) in the mean field regime (i.e., $\alpha_N = 1/(N-1)$) from (Jin, Li and Sun 2020*b*), which was built upon the argument for the first order system in (Jin et al. 2020*a*).

Denote $(\tilde{r}_i, \tilde{v}_i)$ the solutions to the random batch process (4.3) with the Brownian motion used being $\tilde{W}_i$. Consider the synchronization coupling:

$$r_i(0) = \tilde{r}_i(0) \sim \mu_0, \ W_i = \tilde{W}_i. \tag{4.5}$$

Let $\mathbb{E}$ denote the expected value, namely integration on Ω with respect to the probability measure $\mathbb{P}$, and consider the $L^2(\cdot)$ norm of a random variable

$$\|\zeta\| = \sqrt{\mathbb{E}|\zeta|^2}. \tag{4.6}$$

For finite time interval, the error of RBM is given by the following theorem.

Theorem 4.1. Let $b(\cdot)$ be Lipschitz continuous, and assume that $|\nabla^2 b|$ has polynomial growth, and the interaction kernel K is Lipschitz continuous. Then,

$$\sup_{t\in[0,T]} \sqrt{\mathbb{E}|\tilde{r}_i(t) - r_i(t)|^2 + \mathbb{E}|\tilde{v}_i(t) - v_i(t)|^2} \le C(T)\sqrt{\frac{\Delta t}{p-1} + (\Delta t)^2}, \tag{4.7}$$

where $C(T)$ is independent of N.

RBM has also been proposed for interacting particle systems used as a sampling method for the invariant measure of (4.1) (Li, Li, Liu, Liu and Lu 2020*a*)(Li, Xu and Zhao 2020*b*)(Jin and Li 2020). In these applications, the long-time behavior, and in particular the convergence to the invariant measure, is of interest. For such analysis some additional contraction assumptions are needed:

Assumption 1. $b = -\nabla V$ for some $V \in C^2(\mathbb{R}^d)$ that is bounded from below (i.e., $\inf_x V(x) > -\infty$), and there exist $\lambda_M \ge \lambda_m > 0$ such that the eigenvalues of $H := \nabla^2 V$ satisfy

$$\lambda_m \le \lambda_i(x) \le \lambda_M, \ \forall\ 1 \le i \le d, x \in \mathbb{R}^d.$$

The interaction kernel K is bounded and Lipschitz continuous. Moreover, the friction γ and the Lipschitz constant L of $K(\cdot)$ satisfy

$$\gamma > \sqrt{\lambda_M + 2L}, \ \lambda_m > 2L. \tag{4.8}$$

Then the following uniform strong convergence estimate holds (Jin et al. 2020*b*):

Theorem 4.2. Under Assumption 1 and the coupling (4.5), the solutions to (4.1) and (4.3) satisfy

$$\sup_{t\geq 0}\sqrt{\mathbb{E}|\tilde{r}_i(t)-r_i(t)|^2+\mathbb{E}|\tilde{v}_i(t)-v_i(t)|^2}\leq C\sqrt{\frac{\Delta t}{p-1}+(\Delta t)^2}, \tag{4.9}$$

where the constant C does not depend on p and N.

Since the errors in RBM-error and (4.9) are independent of N, in the mean-field regime, thus RBM is AP in particle number N in this regime.

An illustrating example: Dyson Browinan motion
The following example is from (Jin et al. 2020*a*). Consider a typical example in random matrix theory, where one is interested in solving the following system of SDEs ($1\leq j\leq N$), called the Dyson Brownian motion:

$$d\lambda_j(t)=-\beta\lambda_j(t)\,dt+\frac{1}{N}\sum_{k:k\neq j}\frac{1}{\lambda_j-\lambda_k}dt+\frac{1}{\sqrt{N}}dW_j, \tag{4.10}$$

where $\{W_j\}$'s are independent standard Brownian motions. The system can be used to find the eigenvalues of a Hermitian-valued Ornstein-Uhlenbeck process. The Brownian motion effect is small when N is large. The limiting equation for $N\to\infty$ is given by

$$\partial_t\rho(x,t)+\partial_x(\rho(u-\beta x))=0,\ u(x,t)=\pi(H\rho)(x,t), \tag{4.11}$$

where ρ is the density for λ as $N\to\infty$, $H(\cdot)$ is the Hilbert transform on $\mathbb{R}$, and $\pi=3.14\ldots$ is the circumference ratio.

For $\beta=1$, it can be shown that the corresponding limiting equation (4.11) has an invariant measure, given by the semicircle law:

$$\rho(x)=\frac{1}{\pi}\sqrt{2-x^2} \tag{4.12}$$

To numerically test the behavior of RBM, note an analytic solution to the limiting equation (4.11)

$$\rho(x,t)=\frac{\sqrt{2\sigma(t)-x^2}}{\sigma(t)\pi},\ \sigma(t)=1+e^{-2t}. \tag{4.13}$$

For each iteration, the force is singular, a splitting strategy is adopted. Specifically, define

$$X^{ij}:=X^i-X^j. \tag{4.14}$$

The RBM is implemented as follows:

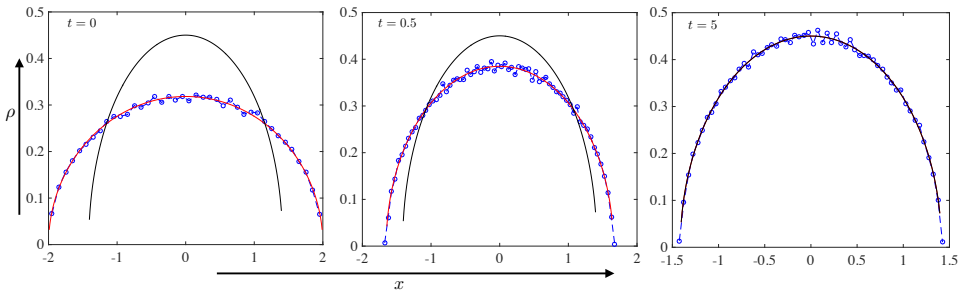

Figure 4.6. The RBM solution (circles) of the Dyson Brownian motion. The empirical densities at various times are plotted. The red curve is the density distribution predicted by the analytic solution (4.13). The black curve is the equilibrium semicircle law (4.12).

- $$Y_m^i = \frac{1}{2}(X_{m-1}^i + X_{m-1}^j) + \mathrm{sgn}(X_{m-1}^{ij})\sqrt{|X_{m-1}^{ij}|^2 + 4\Delta t},$$
$$Y_m^j = \frac{1}{2}(X_{m-1}^i + X_{m-1}^j) - \mathrm{sgn}(X_{m-1}^{ij})\sqrt{|X_{m-1}^{ij}|^2 + 4\Delta t}.$$

- $$X_m^i = Y_m^i - \Delta t Y_m^i + \sqrt{\frac{\Delta t}{N}} z^i, \;\; X_m^j = Y^j(t_m) - \Delta t Y_m^j + \sqrt{\frac{\Delta t}{N}} z^j.$$

Here, $z^i, z^j \sim \mathcal{N}(0,1)$.

Fig. 4.6 shows that RBM captures the evolution of distribution and the equilibrium semicircle law (4.12), as desired. RBM-r also has similar behavior.

The mean-field limit of RBM

To further understanding the behavior of RBM, when N is large, it will be interesting to investigate its mean field limit. To this aim, consider RBM for the first order system (4.2) with $\alpha_N = 1/(N-1)$.

Intuitively, when $N \gg 1$, the probability that two chosen particles are correlated is very small. Hence, in the $N \to \infty$ limit, two chosen particles will be independent with probability 1. Due to the exchangeability, the marginal distributions of the particles will be identical. Based on this observation, the following mean field limit was derived and proved in (Jin and Li 2021*a*):

Algorithm 3 (Mean Field Dynamics of RBM for first order system (4.2)

1: $\tilde{\mu}(\cdot, t_0) = \mu_0$.
2: **for** $k \geq 0$ **do**
3: Let $\rho^{(p)}(\cdots, 0) = \tilde{\mu}(\cdot, t_k)^{\otimes p}$ be a probability measure on $(\mathbb{R}^d)^p \cong \mathbb{R}^{pd}$.
4: Evolve the measure $\rho^{(p)}$ to find $\rho^{(p)}(\cdots, \Delta t)$ by the following Fokker-Planck equation:

$$\partial_t \rho^{(p)} = -\sum_{i=1}^{p} \nabla_{x_i} \cdot \left(\Big[b(x_i) + \frac{1}{p-1} \sum_{j=1, j\neq i}^{p} K_1(x_i - x_j) \Big] \rho^{(p)} \right) + \frac{1}{2}\sigma^2 \sum_{i=1}^{p} \Delta_{x_i} \rho^{(p)}. \tag{4.15}$$

5: Set

$$\tilde{\mu}(\cdot, t_{k+1}) := \int_{(\mathbb{R}^d)^{\otimes(p-1)}} \rho^{(p)}(\cdot, dy_2, \cdots, dy_p, \Delta t). \tag{4.16}$$

6: **end for**

The dynamics in Algorithm 3 naturally gives a nonlinear operator $\mathcal{G}_\infty : \mathbf{P}(\mathbb{R}^d) \to \mathbf{P}(\mathbb{R}^d)$ as

$$\tilde{\mu}(\cdot, t_{k+1}) =: \mathcal{G}_\infty(\tilde{\mu}(\cdot, t_k)). \tag{4.17}$$

Corresponding to this is the following SDE system for $t \in [t_k, t_{k+1})$

$$dmx_i = b(mx_i)\, dt + \frac{1}{p-1} \sum_{j=1, j\neq i}^{p} K_1(mx_i - mx_j)\, dt + \sigma\, dmW_i, \ \ i = 1, \cdots, p, \tag{4.18}$$

with $\{mx_i(t_k)\}$ drawn i.i.d from $\tilde{\mu}(\cdot, t_k)$.

Hence, in the mean field limit of RBM, one starts with a configuration in molecular chaos, then the p particles evolve by interacting with each other. One takes the first marginal of this new p-particle distribution, and at the starting point of the next time interval, one imposes the molecular chaos condition so that the particles are independent again.

Furthermore, in (Jin and Li 2021*a*) it was proven that this mean-field limit is $O(\Delta t)$ distance (in Wasserstein-1 sense) to the mean-field limit of the original particle system (2.31), thus completing the AP diagram in Fig. 1.2.

4.2. Molecular dynamics

One of the most important interacting particle systems is molecular dynamics (MD), which simulates dynamics or equilibrium properties of large system of atoms and molecules using Newton's second law. It has wide range of applications, such as chemical physics, soft materials and biophysics (Ciccotti,

Frenkel and McDonald 1987, Frenkel and Smit 2001). Here we review an interesting application of RBM to MD simulation, called Random Batch Ewald (Jin, Li, Xu and Zhao 2021*a*), which achieves an $O(N)$ complexity with a high parallel efficiency (Liang, Tan, Zhao, Liu, Li, Jin, Hong and Xu In preparation).

The equations of motion governing N "molecules" with masses m_i's are given by

$$\begin{aligned} dr_i &= v_i\, dt, \\ m_i dv_i &= \Big[-\sum_{j:j\neq i} \nabla\phi(r_i - r_j) \Big]\, dt + \sigma_i dW_i. \end{aligned} \tag{4.19}$$

Here, W_i are noise or other external forcing terms, $\phi(\cdot)$ is the Coulomb potential

$$\phi(x) = \frac{q_i q_j}{r},$$

where q_i is the charge for the ith particle and $r = |x|$. Another popular potential often used is the Lennard-Jones potential (Frenkel and Smit 2001):

$$\phi(x) = 4\left(\frac{1}{r^{12}} - \frac{1}{r^6}\right). \tag{4.20}$$

Between ions, both types of potential exist and between charge-neutral molecules, the Lennard-Jones potential might be the main force.

RBM with kernel splitting

Due to the singularity at $x = 0$ of the Lenard-Jones potential (4.20), a direct application of RBM could give poor results. One effective strategy is to decompose the K into two parts (Martin, Chen and Siepmann 1998, Hetenyi, Bernacki and Berne 2002),

$$K(x) = K_1(x) + K_2(x). \tag{4.21}$$

Here, K_1 has short range that decays quickly hence can be ignored for $|x| \geq r_0$, for some r_0 chosen to be comparable to the mean distance of the particles. $K_2(x)$ is a bounded smooth function. One then applies RBM to the K_2 part only (Li et al. 2020*b*).

Random Batch Ewald: importance sampling

The Coulomb interaction is a long range interaction, which decays slowly as $1/r$, and in the mean time contains a singularity at $r = 0$. The bottleneck in MD simulation lies in the expensive simulation of the Coulomb interaction, which has the computational complexity of $O(N^2)$. Some popular methods include the particle-particle particle mesh Ewald (PPPM) (Luty, Davis, Tironi and Van Gunsteren 1994, Deserno and Holm 1998), and multipole type methods such as treecode (Barnes and Hut 1986, Duan and

Krasny 2000) and fast multipole methods (FMM) (Greengard and Rokhlin 1987, Ying, Biros and Zorin 2004). These methods can reduce the complexity per time step from $O(N^2)$ to $O(N \log N)$ or even $O(N)$, and have gained big success in practice. However, some issues still remain to be resolved, e.g., the prefactor in the linear scaling can be large, or the implementation can be nontrivial, or the scalability for parallel computing is not high.

The RBE method is based on the Ewald splitting for the Coulomb kernel with a random "mini-batch" type technique applied in the Fourier series for the long-range part.

The solids or fluids with large volume are usually modeled in a box with length L, with periodic conditions. Consider N particles with net charge q_i $(1 \le i \le N)$ under the electroneutrality condition

$$\sum_{i=1}^{N} q_i = 0. \tag{4.22}$$

The forces are computed using $F_i = -\nabla_{r_i} U$, where U is the Coulomb potential energy, with periodic boundary condition, given by

$$U = \frac{1}{2} {\sum_n}' \sum_{i,j=1}^{N} q_i q_j \frac{1}{|r_{ij} + nL|}, \tag{4.23}$$

where $n \in \mathbb{Z}^3$. $\sum'$ is defined such that $n = 0$ is not included when $i = j$.

The classical Ewald summation decomposes $1/r$ into the long-range smooth parts and short-range singular parts:

$$\frac{1}{r} = \frac{\mathrm{erf}(\sqrt{\alpha} r)}{r} + \frac{\mathrm{erfc}(\sqrt{\alpha} r)}{r}, \tag{4.24}$$

where $\mathrm{erf}(x) := \frac{2}{\sqrt{\pi}} \int_0^x \exp(-u^2) du$ is the error function and $\mathrm{erfc} = 1 - \mathrm{erf}$. Correspondingly, $U = U_1 + U_2$ with

$$U_1 = \frac{1}{2} {\sum_n}' \sum_{i,j} q_i q_j \frac{\mathrm{erf}(\sqrt{\alpha}|r_{ij} + nL|)}{|r_{ij} + nL|}, \tag{4.25}$$

$$U_2 = \frac{1}{2} {\sum_n}' \sum_{i,j} q_i q_j \frac{\mathrm{erfc}(\sqrt{\alpha}|r_{ij} + nL|)}{|r_{ij} + nL|}, \tag{4.26}$$

where U_2 corresponds to the short-range forces which is inexpensive, while U_1 is the long-range part that will be put into the Fourier space

$$U_1 = \frac{2\pi}{V} \sum_{k \neq 0} \frac{1}{k^2} |\rho(k)|^2 e^{-k^2/4\alpha} - \sqrt{\frac{\alpha}{\pi}} \sum_{i=1}^{N} q_i^2, \tag{4.27}$$

where $\rho(k) := \sum_{i=1}^{N} q_i e^{ik\cdot r_i}$. Then

$$F_{i,1} = -\nabla_{r_i} U_1 = -\sum_{k\neq 0} \frac{4\pi q_i k}{Vk^2} e^{-k^2/(4\alpha)} \mathrm{Im}(e^{-ik\cdot r_i}\rho(k)), \tag{4.28}$$

where $r_{ij} = r_j - r_i$, is bounded for small k. The key idea of RBE is to do *importance sampling* according to the discrete Gaussian distribution $e^{-k^2/(4\alpha)}$. Denote

$$S := \sum_{k\neq 0} e^{-k^2/(4\alpha)} = H^3 - 1, \tag{4.29}$$

where

$$H := \sum_{m\in mathbbZ} e^{-\pi^2 m^2/(\alpha L^2)} = \sqrt{\frac{\alpha L^2}{\pi}} \sum_{m=-\infty}^{\infty} e^{-\alpha m^2 L^2} \approx \sqrt{\frac{\alpha L^2}{\pi}}(1 + 2e^{-\alpha L^2}), \tag{4.30}$$

since often $\alpha L^2 \gg 1$. Hence, S is the sum for all three-dimensional vectors k except 0. Then, one can regard the sum as an expectation over the probability distribution

$$\mathscr{P}_k := S^{-1} e^{-k^2/(4\alpha)}, \tag{4.31}$$

which, with $k \neq 0$, is a discrete Gaussian distribution that can be sampled efficiently *offline*. Once the time evolution starts one just needs to randomly draw a few ($O(p)$) samples for each time step from this pre-sampled Guassian sequence.

Ultimately, the force $F_{i,1}$ in (4.28) will be calculated by the following mini-batch random variable:

$$F_{i,1} \approx F^*_{i,1} := -\sum_{\ell=1}^{p} \frac{S}{p} \frac{4\pi k_\ell q_i}{Vk_\ell^2} \mathrm{Im}(e^{-ik_\ell\cdot r_i}\rho(k_\ell)). \tag{4.32}$$

The PPPM uses FFT, while RBE uses random mini-batch to speed up the computation in the Fourier space. The complexity of RBE for the real space part is $\mathcal{O}(N)$. By choosing *the same batch* of frequencies for all forces (4.32) (i.e., using the same k_ℓ, $1 \leq \ell \leq p$ for all $F^*_{i,1}, 1 \leq i \leq N$) in the same time step, the complexity per iteration for the frequency part is reduced to $\mathcal{O}(pN)$. Therefore the RBE method has linear complexity per time step if one chooses $p = \mathcal{O}(1)$.

Another advantage of RBE is that there are few particle interactions at each iteration. This significantly reduces the amount of message passing when many CPUs are used for parallel computing, hence one achieves remarkable scalability (Liang et al. In preparation).

To illustrate the performance of the RBE method, consider an electrolyte with monovalent binary ions (first example in (Jin et al. 2021*a*)). In the

reduced units ((Frenkel and Smit 2001, section 3.2)), the dielectric constant is taken as $\varepsilon = 1/4\pi$ so that the potential of a charge is $\phi(r) = q/r$ and the temperature is $T = \beta^{-1} = 1$. Under the Debye-Hückel (DH) theory (linearized Poisson-Boltzmann equation), the charge potential outside one ion is given by

$$-\varepsilon\Delta\phi = \begin{cases} 0 & r < a \\ q\rho_{\infty,+}e^{-\beta q\phi} - q\rho_{\infty,-}e^{\beta q\phi} \approx \beta q^2\rho_r\phi, & r > a \end{cases}$$

where $\rho_{\infty,+} = \rho_{\infty,-} = N/(2V)$ are the densities of the positive and negative ions at infinity, both being $\rho_r/2$. The parameter a is the effective diameter of the ions, which is related to the setting of the Lennard-Jones potential. In the simulations, $a = 0.2$ and the setting of Lennard-Jones potential can be found in (Jin et al. 2021*a*). This approximation gives the net charge density $\rho = -\varepsilon\Delta\phi$ for $r \gg a$,

$$\ln(r\rho(r)) \approx -1.941r - 1.144.$$

Fig. 4.7 shows the CPU time consumed for different particle numbers inside the box with the same side length $L = 10$. Both the PPPM and RBE methods scale linearly with the particle numbers. However, even for batch size $p = 100$, the RBE method consumes much less time. Clearly, the RBE method has the same level of accuracy compared with the PPPM method for the densities considered.

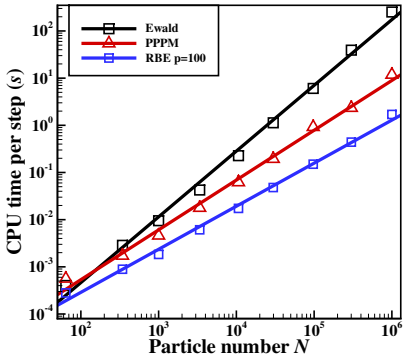

Figure 4.7. Comparision of the Ewald sum, the PPPM and the RBE methods

Next, in Fig. 4.8, the parallel efficiency of the PPPM and RBE methods from (Liang et al. In preparation) for the all-atom simulation of pure water systems is shown. As can be seen, due to the reduction of communications

for the particles, the RBE method gains better parallel efficiency. This parallel efficiency is more obvious when the number of particles is larger. In (Liang et al. In preparation), the simulation results of pure water system also indicate that the RBE type methods can not only sample from the equilibrium distribution, but also compute accurately the dynamical properties of the pure water systems.

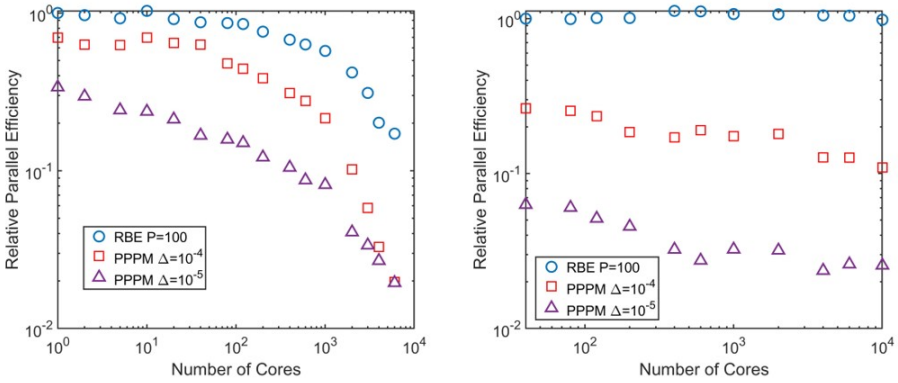

Figure 4.8. The parallel efficiency of the PPPM and the RBE methods for all-atom simulation of pure water system (Left) 3×10^5 atoms; (Right) 3×10^7 atoms

For a comprehensive review of RBM and its extensions and applications, see a recent review (Jin and Li 2021*b*).

5. Numerical passages from kinetic equations to hydrodynamic equations

In nuclear reactor, neutrons may conduct significant amount of scattering, in the diffusive regime. In the space shuttle reentry problem, the mean free path could vary from $O(1)$ meter in the space to $O(10^{-8})$ meter, when the vehicle passes from free streaming, rarefied gas (described by the Boltzmann equation), transition to the hydrodynamic (described by the Euler or Navier-Stokes equations) regimes (Rivell 2006). It is also known that in hypersonic flows (Mach number larger than 1.4), the shock profile of the Navier-Stokes equations do not give accurate shock width, hence one needs to use the Boltzmann equation in the shock region (Foch 1973)(Agarwal, Yun and Balakrishnan 1999). In plasma physics, the Debye length could be small, and one needs to deal with quasi-neutral regime (Fornberg 1996)(Degond and Deluzet 2017*a*). In all these kinetic problems one needs to deal with multiple time and spatial scales.

Kinetic theory is the area in which the concept of AP was first introduced, and also most successfully and extensively used. Earlier effort in this direction concentrates on time-independent transport equations that have diffusive behavior (Larsen et al. 1987)(Larsen and Morel 1989). However for multiscale kinetic equations the main challenges lie in time discretizations, due to the stiffness, non-locality and nonlinearity of the collision operators.

The term "Asymptotic-Preserving" was first coined in (Jin 1999). An AP scheme typically possesses the following key features for multiscale kinetic equations:

- Implicit time discretization that can be either explicitly or easily implemented: for example at least avoids complicated nonlinear algebraic system solvers such as Newton's iteration;
- when the Knudsen number $\varepsilon \to 0$ the scheme for the kinetic equations automatically become a good scheme for the limiting hydrodynamic equations

This program is also related to the development of kinetic schemes for compressible Euler equations, which was based on discretizing a linear kinetic equation thanks to its linear convection, followed by a projection to the local Maxwellian (Deshpande 1986)(Perthame 1990)(Prendergast and Xu 1993). It is also relevant to the lattice Boltzmann approximation to incompressible Navier-Stokes equations (Chen, Chen and Matthaeus 1992)(Chen and Doolen 1998) (Qian, d'Humières and Lallemand 1992)(He and Luo 1997). Relaxation schemes for nonlinear hyperbolic systems also share similar spirit (Jin and Xin 1995). Below we review a few representative AP schemes.

5.1. The BGK-penalization method

We are mainly interested in dealing with the numerical difficulties when the Knudsen number $\varepsilon \ll 1$. The first challenge is numerical stiffness, which puts severe constraint on Δt. In order to allow $\Delta t \gg \varepsilon$, one needs some implicit treatment for the nonlocal, nonlinear collision operator, which is numerically nontrivial.

The *penalization method*, introduced by Filbet and Jin (Filbet and Jin 2010), was the first AP scheme for the nonlinear Boltzmann equation that overcomes the stiffness issue of the collision operator. The idea is to penalize $\mathcal{Q}(f)$ by the BGK operator $\beta(\mathcal{M} - f)$:

$$\partial_t f + v \cdot \nabla_x f = \underbrace{\frac{\mathcal{Q}(f) - \beta(\mathcal{M} - f)}{\varepsilon}}_{\text{less stiff, explicit}} + \underbrace{\frac{\beta(\mathcal{M} - f)}{\varepsilon}}_{\text{stiff, explicit}}, \tag{5.2}$$

where β is some constant chosen properly to approximate the Frechet derivative of $\mathcal{Q}(f)$ around $\mathcal{M}$, such that terms in the first brace become less stiff

or non-stiff and can be treated explicitly. The other part is a BGK operator, which can be inverted *explicitly* (Coron and Perthame 1991), thanks to the conservation properties of the collision terms on the right hand side of (5.2).

A first-order IMEX (Implicit-Explicit) discretization of (5.2) can be written as:

$$\frac{f^{n+1}-f^n}{\Delta t}+v\cdot\nabla_x f^n=\frac{\mathcal{Q}(f^n)-\beta(\mathcal{M}^n-f^n)}{\varepsilon}+\frac{\beta(\mathcal{M}^{n+1}-f^{n+1})}{\varepsilon}. \quad (5.3)$$

Taking the moments $\int_{\mathbb{R}^d}\cdot\,\phi(v)\,\mathrm{d}v$, with $\phi(v)$ defined in (2.37) on both sides of (5.3), and using the properties (2.37), one gets

$$\frac{\langle f\rangle^{n+1}-\langle f\rangle^n}{\Delta t}+\nabla_x\cdot\langle vf\rangle^n=0\,, \quad (5.4)$$

where $\langle\cdot\rangle=\int\phi(v)\cdot dv$ means the moments. From (5.4) one can solve for the moments ρ,u and T at $t=t^{n+1}$, hence $\mathcal{M}^{n+1}$ is obtained. Then f^{n+1} can be obtained from (5.3) explicitly. Notice the entire process is *explicit*!

In practice, β can be roughly estimated as

$$\beta=\sup_v|\mathcal{Q}^-(f)|,$$

where $\mathcal{Q}^-$ is the loss part of the collision operator defined such that $\mathcal{Q}(f)=\mathcal{Q}^+(f)-f\mathcal{Q}^-(f)$. β can also be made time and spatially dependent for better numerical accuracy (Yan and Jin 2013).

To capture the compressible Euler limit, a necessary condition is that, as $\varepsilon\to 0$,

$$f^n=\mathcal{M}^n,\quad \text{for any } n,\quad \text{with}\quad \Delta t,\Delta x\quad \text{fixed}.$$

It was formally shown in (Filbet and Jin 2010) that

$$\text{for } \varepsilon\ll 1,\quad \text{if } f^n=\mathcal{M}^n+O(\varepsilon),\ \text{then } f^{n+1}=\mathcal{M}^{n+1}+O(\varepsilon).$$

Numerical experiments in (Filbet and Jin 2010) shows that regardless of the initial condition f^0, there exists an integer $N>0$ such that

$$f^n=\mathcal{M}^n+O(\varepsilon),\quad \text{for any } n\geq N. \quad (5.5)$$

Substituting (5.5) into (5.3) and taking the moments, one has

$$\frac{\langle f\rangle^{n+1}-\langle f\rangle^n}{\Delta t}+\nabla_x\cdot\int_{\mathbb{R}^d}v\phi(v)\,\mathcal{M}^n\,\mathrm{d}v=O(\varepsilon),\quad \text{for any } n\geq N,$$

which is a consistent discretization to the limiting Euler system (2.39). This means the scheme is AP after an initial transient time.

Remark 5.1. A possible way to remove the initial layer problem and hence achieve AP in one time step was suggested in (Yan and Jin 2013), where the

idea is to perform the penalization in two successive steps:

$$\begin{cases} \dfrac{f^* - f^n}{\Delta t} + v \cdot \nabla_x f^n = \dfrac{\mathcal{Q}(f^n) - \beta(\mathcal{M}^n - f^n)}{\varepsilon} + \dfrac{\beta(\mathcal{M}^* - f^*)}{2\varepsilon}, \\ \dfrac{f^{n+1} - f^*}{\Delta t} = \dfrac{\beta(\mathcal{M}^{n+1} - f^{n+1})}{2\varepsilon}. \end{cases}$$

The idea of using a linear or simpler operator to penalize the nonlinear or complicated operator turns out to be a generic approach. For specific problems, one needs to seek appropriate penalization operator. For example, consider the nonlinear Fokker-Planck-Landau equation, whose collision operator is given by

$$\mathcal{Q}(f)(v) = \nabla_v \cdot \int_{\mathbb{R}^d} A(v - v_*) \left[f(v_*) \nabla_v f(v) - f(v) \nabla_{v_*} f(v_*) \right] \mathrm{d}v_*, \quad (5.6)$$

where A is a semi-positive definite matrix. This equation is relevant in the study of Coulomb interactions. The diffusive nature of the collision operator introduces more stiffness. An explicit scheme would require $\Delta t = O(\varepsilon(\Delta v)^2)$, where Δv is the mesh size in v, which is even more restrictive than the Boltzmann collision operator. In (Jin and Yan 2011) the following Fokker-Planck operator was proposed as a penalization:

$$\mathcal{P}_{FP}(f) = \nabla_v \cdot \left(\mathcal{M} \nabla_v \left(\frac{f}{\mathcal{M}} \right) \right).$$

Similar approaches, with variant penalties, have been proposed for the quantum Boltzmann equation (Filbet, Hu and Jin 2012), the quantum Fokker-Planck-Landau equation (Hu, Jin and Yan 2012), and the multi-species Boltzmann equation (Jin and Li 2013).

Another AP scheme for the Boltzmann equation, developed later in (Liu, Xu, Sun and Cai 2016), relies on the integral representation of the BGK model. The final form of the scheme also ends up with a linear combination of the Boltzmann collision operator and the BGK operator, with a slightly different combination coefficients.

5.2. Exponential integration

Another class of asymptotic preserving method is the *exponential integration method*. This method is based on a reformulation of the equation into an exponential form, with the Maxwellian embedded. This makes it easier to capture the asymptotic limit and other physical properties such as positivity.

For the space homogeneous Boltzmann equation:

$$\partial_t f = \frac{1}{\varepsilon} \mathcal{Q}(f), \quad (5.7)$$

Dimarco and Pareschi in (Dimarco and Pareschi 2011) introduced the fol-

lowing reformulation:

$$\partial_t \left[(f - \mathcal{M}) e^{\beta t/\varepsilon} \right] = \partial_t f e^{\beta t/\varepsilon} + \frac{\beta(f - \mathcal{M})}{\varepsilon} e^{\beta t/\varepsilon} = \frac{\mathcal{Q} - \beta(\mathcal{M} - f)}{\varepsilon} e^{\beta t/\varepsilon} . \tag{5.8}$$

Here β is an auxiliary parameter and as in the penalization method, $\beta(\mathcal{M} - f)$ is used to approximate the Frechet derivative of $\mathcal{Q}$. β is chosen to be the smallest value that preserves the positivity of f.

Equation (5.8) is fully equivalent to the original problem (5.7). However, it updates the difference between f and $\mathcal{M}$, and the exponential term $\exp(-\beta t/\varepsilon)$ removes the stiffness and forces numerically the convergence between f and $\mathcal{M}$, an essential mechanism for the AP property. It can be easily extended to all explicit Runge-Kutta methods which are not only of high order but also holds the AP property automatically.

The need to convect $\mathcal{M}$ makes it difficult to extend the scheme to the nonhomogenous case. In (Li and Pareschi 2014), Li and Pareschi use an evolving Maxwellian function *within* each time step. They reformulate the Boltzmann equation as

$$\partial_t \left[(f - \mathcal{M}) \exp(\beta t/\varepsilon) \right] = \left(\frac{\mathcal{P} - \beta \mathcal{M}}{\varepsilon} - v \cdot \nabla_x f - \partial_t \mathcal{M} \right) \exp(\beta t/\varepsilon) , \tag{5.9}$$

while the moment equations are obtained after taking the moments of the original Boltzmann equation (2.32):

$$\partial_t \langle f \rangle + \nabla_x \cdot \langle \phi v f \rangle = 0 . \tag{5.10}$$

To compute $\partial_t \mathcal{M}$, note that

$$\partial_t \mathcal{M} = \partial_\rho \mathcal{M} \partial_t \rho + \nabla_u \mathcal{M} \cdot \partial_t u + \partial_T \mathcal{M} \partial_t T , \tag{5.11}$$

where $\partial_\rho \mathcal{M}$, $\nabla_u \mathcal{M}$ can be expressed analytically and $\partial_T \mathcal{M}$ are all explicit. The time derivatives of the other three macroscopic quantities ρ, u, T can be obtained from (5.10).

With this formulation, one can just use the Runge-Kutta time discretization.

This method preserves positivity, high order accuracy, and strong AP properties.

5.3. Micro-macro decomposition

The "micro-macro" decomposition decomposes the density distribution function into the local Maxwellian, plus the deviation

$$f = \mathcal{M} + \varepsilon g , \quad \text{with} \quad \int \phi [f - \mathcal{M}] \mathrm{d}v = 0 . \tag{5.12}$$

One early approach of using such a decomposition to design an AP scheme for the radiative heat transfer equations was used by Klar and Schmeiser

in (Klar and Schmeiser 2001), and it was also used by Liu and Yu in (Liu and Yu 2004) for analyzing the shock propagation of the Euler equations in passing the fluid limit of the Boltzmann equation. Its application to the nonlinear Boltzmann equation started with the work of Bennoune-Lemou-Mieussens in (Bennoune, Lemou and Mieussens 2008).

Define the linearized collision operator around $\mathcal{M}$, as:

$$\mathcal{L}_{\mathcal{M}} g = \mathcal{Q}[\mathcal{M}, g] + \mathcal{Q}[g, \mathcal{M}] .$$

With some calculation, one gets

$$\begin{cases} \partial_t g + (\mathrm{I} - \Pi_{\mathcal{M}})(v \cdot \nabla_x g) - \mathcal{Q}[g, g] = \dfrac{1}{\varepsilon} \left[\mathcal{L}_{\mathcal{M}} g - (\mathrm{I} - \Pi_{\mathcal{M}})(v \cdot \nabla_x \mathcal{M}) \right] , \\ \partial_t \displaystyle\int \phi \mathcal{M} \mathrm{d}v + \int \phi v \cdot \nabla_x \mathcal{M} \mathrm{d}v + \varepsilon \nabla_x \cdot \langle v \phi g \rangle = 0 . \end{cases} \tag{5.13}$$

Here $\Pi_{\mathcal{M}}$ is the projection operator that maps arbitrary $\mathcal{M}$-weighted L_2 function into the null space of $\mathcal{L}_{\mathcal{M}}$, namely, for any $\psi \in L_2(\mathcal{M}\mathrm{d}v)$:

$$\Pi_{\mathcal{M}}(\psi) \in \mathrm{Null}\mathcal{L}_{\mathcal{M}} = \mathrm{Span}\{\mathcal{M}, v\mathcal{M}, |v|^2 \mathcal{M}\} . \tag{5.14}$$

For the Boltzmann equation, the projection operator can be written explicitly as:

$$\begin{aligned} \Pi_{\mathcal{M}}(\psi) = \frac{1}{\rho} \Bigg[& \langle \psi \rangle + \frac{(v-u) \cdot \langle (v-u)\psi \rangle}{T} \\ & + \left(\frac{|v-u|^2}{2T} - \frac{d}{2} \right) \frac{2}{d} \langle \left(\frac{|v-u|^2}{2T} - \frac{d}{2} \right) \psi \rangle \Bigg] \mathcal{M} , \end{aligned} \tag{5.15}$$

where $\langle \cdot \rangle$ is the integration over v.

In the original Boltzmann equation, the stiff term $\mathcal{Q}[f, f]$ is quadratic in f, hence difficult to invert. The two stiff terms here are both linear thus their implicit discretization can be inverted more easily. In (Bennoune et al. 2008), the following discretization is taken:

$$\begin{cases} \dfrac{g^{n+1} - g^n}{\Delta t} + (\mathrm{I} - \Pi_{\mathcal{M}^n}) (v \cdot \nabla_x g^n) - \mathcal{Q}[g^n, g^n] = \dfrac{1}{\varepsilon} \left[\mathcal{L}_{\mathcal{M}^n} g^{n+1} \right. \\ \qquad \left. - (\mathrm{I} - \Pi_{\mathcal{M}^n}) (v \cdot \nabla_x \mathcal{M}^n) \right] , \\ \displaystyle\int \phi \mathcal{M}^{n+1} \mathrm{d}v + \Delta t \varepsilon \int \phi v \cdot \nabla_x g^{n+1} \mathrm{d}v = \int \phi \mathcal{M}^n \mathrm{d}v - \Delta t \int \phi v \cdot \nabla_x \mathcal{M}^n \mathrm{d}v \end{cases} \tag{5.16}$$

The only term that needs to be inverted is $\mathrm{I} - \frac{\Delta t}{\varepsilon} \mathcal{L}_{\mathcal{M}}$ in the first equation. It is a linear operator, and the negative spectrum of $\mathcal{L}$ guarantees the invertibility. The quadratic operator $\mathcal{Q}[f, f]$ is no longer stiff thus is treated explicitly.

The following AP property was proved in (Bennoune et al. 2008):

Theorem 5.2. The scheme is AP, more specifically:

(i) The time discretization (5.16) of the Boltzmann equation (5.13) gives in the limit $\varepsilon \to 0$ a scheme consistent to the compressible Euler system (2.39).
(ii) For small ε, scheme (5.16) is asymptotically equivalent, up to $\mathcal{O}(\varepsilon^2)$, to an explicit time discretization of the Navier-Stokes equations (2.40).

In (Gamba, Jin and Liu 2019) the BGK-penalization method was used in the micro-macro decomposition framework to further avoid the inversion of the linearized collision operator $\mathcal{L}$.

5.4. Linear transport equations

Parity equations-based AP schemes
We now consider the linear transport equation in diffusive regime (2.41). Let

$$\mathcal{L}(f) = \int b(v,w)\{M(v)f(w) - M(w)f(v)\}dw\,.$$

Split (2.41) into two equations, one for v and one for $-v$:

$$\begin{aligned} \varepsilon\,\partial_t f(v) + v\cdot\nabla_x f(v) &= \frac{1}{\varepsilon}\mathcal{L}(f)(v), \\ \varepsilon\,\partial_t f(-v) - v\cdot\nabla_x f(-v) &= \frac{1}{\varepsilon}\mathcal{L}(f)(-v). \end{aligned} \tag{5.17}$$

Define the even- and odd-parities as

$$\begin{aligned} r(t,x,v) &= \frac{1}{2}\left[f(t,x,v) + f(t,x,-v)\right], \\ j(t,x,v) &= \frac{1}{2\varepsilon}\left[f(t,x,v) - f(t,x,-v)\right]. \end{aligned} \tag{5.18}$$

Adding and subtracting the two equations in (5.17) lead to

$$\partial_t r + v\cdot\nabla_x j = \frac{1}{\varepsilon^2}\mathcal{L}(r)\,, \tag{5.19}$$

$$\partial_t j + \frac{1}{\varepsilon^2}v\cdot\nabla_x r = -\frac{1}{\varepsilon^2}\,\lambda j\,, \tag{5.20}$$

where we used the property that

$$\int b(v,w)j(w)\,dw = 0$$

since $j(w)$ is an odd-function in w.

Remark 5.3. If $b(v,w) = b(|v|,|w|)$, then it is possible to use the even and odd parities only for the positive components of v and w, hence reduces the computational domain, as is the case for neutron-transport equation (Lewis and Miller 1984).

Since now the convection term is also stiff, the idea of (Jin, Pareschi and Toscani 2000) was to rewrite (5.19) and (5.20) into the following form

$$\partial_t r + v \cdot \nabla_x j = \tfrac{1}{\varepsilon^2}\mathcal{L}(r), \tag{5.21}$$

$$\partial_t j + v \cdot \nabla_x r = -\tfrac{1}{\varepsilon^2}\left[\lambda j + (1-\varepsilon^2\psi) v \cdot \nabla_x r\right], \tag{5.22}$$

where $\psi = \psi(\varepsilon)$ is a free parameter satisfying $0 \le \psi \le 1/\varepsilon^2$. Hence the characteristic speeds on the right hand side are now independent of ε. The simplest choice of ψ is

$$\psi(\varepsilon) = \min\left\{1, \frac{1}{\varepsilon^2}\right\}.$$

(A related approach in (Klar 1998) moves all the stiff terms in (5.20) to the right hand side).

One can easily derive the diffusion equation from (5.21) and (5.22). As $\varepsilon \to 0$, they give

$$\mathcal{L}(r) = 0, \tag{5.23}$$

$$\lambda j = -v \cdot \nabla_x r. \tag{5.24}$$

Solving (5.23) gives

$$r = \rho(x,t) M(v), \tag{5.25}$$

where

$$\rho(x,t) = \langle f(x,\cdot,t)\rangle = \langle r(x,\cdot,t)\rangle.$$

With (5.25), equation (5.24) gives

$$j = \frac{M(v)}{\lambda(v)}[-v \cdot \nabla_x \rho]. \tag{5.26}$$

Applying (5.25) and (5.26) in (5.21), and integrating over v, one gets the diffusion equation (2.42) with (2.43). Thus (5.21) and (5.22) set the foundation for AP schemes. One can split the stiff relaxation step

$$\partial_t r = \frac{1}{\varepsilon^2}\mathcal{L}(r), \tag{5.27}$$

$$\partial_t j = \frac{1}{\varepsilon^2}\left[-\lambda j - (1-\varepsilon^2\phi)(v \cdot \nabla_x r)\right], \tag{5.28}$$

from the non-stiff transport step

$$\begin{aligned} &\partial_t r + v \cdot \nabla_x j = 0, \\ &\partial_t j + v \cdot \nabla_x r = 0. \end{aligned} \tag{5.29}$$

Equations (5.29) can be solved using an explicit scheme, whereas for step (5.27)-(5.28) one uses an implicit scheme.

The key is how to solve the collision step (5.27) implicitly in an efficient

way. In the case of neutron transport, where $L(r) = \rho - r$, the implicit term can be integrated explicitly (Jin et al. 2000). Otherwise, one can use the penalty method of Filbet-Jin (Filbet and Jin 2010), see (Deng 2012).

As far as spatial discretization is concerned, one can use any upwind type scheme for convection terms in (5.29), while on the right hand side of (5.28), it was suggested in (Jin et al. 2000) to use center difference for the gradient of r. When $\varepsilon \to 0$, these spatial discretizations become consistent and stable discretization of (2.42), thus is AP spatially. However, the limiting discrete diffusion equation is not compact. In 1d it is a five-point rather than a three-point discretization of the diffusion equation. This problem can be fixed by using staggered grid for r and j, as pointed out in (Jin and Pareschi 2001) and then extended to two space dimensions in (Kupper, Frank and Jin 2016).

One AP scheme developed in (Sun, Jiang and Xu 2015) allows one to get a compact three point scheme in the limit.

Micro-macro decomposition based AP schemes

The micro-macro decomposition approach, proposed by Lemou and Mieussens (Lemou and Mieussens 2008), begins with the decomposition

$$f = \rho M + \varepsilon g\,. \tag{5.30}$$

Clearly $\langle g \rangle = 0$. Applying (5.30) in (2.41) gives

$$\varepsilon M \partial_t \rho + \varepsilon^2 \partial_t g + v \cdot M \nabla_x \rho + \varepsilon v \cdot \nabla_x g = \mathcal{L} g\,. \tag{5.31}$$

Integrating this equation with respect to v gives the following continuity equation:

$$\partial_t \rho + \nabla_x \cdot \langle v g \rangle = 0\,. \tag{5.32}$$

Define operator $\Pi : \Pi(\cdot)(v) := M\langle \cdot \rangle$, and I the identity operator. Applying the orthogonal projection $I - \Pi$ to (5.31) gives the equation for g:

$$\varepsilon^2 \partial_t g + \varepsilon (I - \Pi)(v \cdot \nabla_x g) + v \cdot M \nabla_x \rho = \mathcal{L} g\,. \tag{5.33}$$

(5.32) and (5.33) constitute the micro-macro formulation of (2.41).

We first consider the time discretization. The following was used in (Lemou and Mieussens 2008):

$$\frac{g^{n+1} - g^n}{\Delta t} + \frac{1}{\varepsilon}(I - \Pi)(v \cdot \nabla_x g^n) = \frac{1}{\varepsilon^2}\mathcal{L} g^{n+1} - \frac{1}{\varepsilon^2} v \cdot M \nabla_x \rho^n\,. \tag{5.34}$$

In the continuity equation (5.32) there is no stiff term, but to recover the correct diffusion limit, the flux of g is taken at t_{n+1}, which gives

$$\frac{\rho^{n+1} - \rho^n}{\Delta t} + \nabla_x \cdot \langle v g^{n+1} \rangle = 0\,. \tag{5.35}$$

As $\varepsilon \to 0$, (5.34) gives

$$\mathcal{L} g^{n+1} = v \cdot M \nabla_x \rho^n\,,$$

which implies

$$g^{n+1}(v) = \mathcal{L}^{-1}(vM)\cdot\nabla_x\rho^n = \frac{M(v)}{\lambda(v)}\left[\int b(v,w)g^{n+1}(w)\,dw - v\cdot\nabla_x\rho^n\right].$$

Applying this to (5.35), and using the rotational invariance of σ, yield the following time explicit discretization of the diffusion equation (2.42)

$$\frac{\rho^{n+1}-\rho^n}{\Delta t} + \nabla_x\cdot\langle D\nabla\rho^n\rangle = 0\,.$$

Thus this time discretization is AP.

Now consider the case of one space dimension. A staggered grid can be used. Define $x_{i+1/2} = (i+1/2)\Delta x$. Now the macroscopic density ρ will be defined at grid point x_i, while g is defined at $x_{i+1/2}$. Using upwind discretization for the space derivative, one arrives at

$$\frac{\rho_i^{n+1}-\rho_i^n}{\Delta t} + \left\langle v\frac{g_{i+1/2}^{n+1}-g_{i-1/2}^{n+1}}{\Delta x}\right\rangle = 0\,, \tag{5.36}$$

$$\begin{aligned}&\frac{g_{i+1/2}^{n+1}-g_{i+1/2}^n}{\Delta x} + \frac{1}{\varepsilon\Delta x}(I-\Pi)\left(v^+(g_{i+1/2}^n - g_{i-1/2}^n)\right.\\ &\qquad \left.+v^-(g_{i+3/2}^n - g_{i+1/2}^n)\right)\\ &= \frac{1}{\varepsilon^2}\mathcal{L}g_{i+1/2}^{n+1} - \frac{1}{\varepsilon^2}vM\frac{\rho_{i+1}^n-\rho_i^n}{\Delta x}\,,\end{aligned} \tag{5.37}$$

where $v^\pm = (v\pm|v|)/2$.

As $\varepsilon\to 0$, (5.37) gives

$$g_{i+1/2}^{n+1} = \mathcal{L}^{-1}(vM)\frac{\rho_{i+1}^n-\rho_i^n}{\Delta x}$$

which when applied to (5.36) gives the following scheme

$$\frac{\rho^{n+1}-\rho^n}{\Delta t} + D\frac{\rho_{i+1}^n - 2\rho_i^n + \rho_{i-1}^n}{(\Delta x)^2} = 0\,.$$

This is the classical three point explicit discretization of the diffusion equation (2.42) and (2.43).

The uniform stability condition ($\Delta t \le C(\Delta x)^2$, uniformly in ε) of this method was proved in (Liu and Mieussens 2010).

Among all the above approaches, in the limit $\varepsilon\to 0$, the discrete time discretization is explicit for the limiting diffusion equation. This imposes the numerical stability condition like $\Delta t = O((\Delta x)^2)$. Consider the case of $\mathcal{L} = r-\rho$, hence $\lambda = 1$, in the parity formulation (5.19) and (5.20). In (Boscarino, Pareschi and Russo 2013), the authors proposed to reformulate

the system into

$$\partial_t r = \underbrace{-v\partial_x\left(j + \frac{\nu(\varepsilon)v\partial_x r}{\sigma}\right)}_{\text{explicit}} \underbrace{-\frac{\sigma}{\varepsilon^2}(r-\rho) + \nu(\varepsilon)v^2\frac{\partial_{xx} r}{\sigma}}_{\text{implicit}}, \quad (5.38)$$

$$\partial_t j = \underbrace{-\frac{1}{\varepsilon^2}\left(j + \frac{v\partial_x r}{\sigma}\right)}_{\text{implicit}}, \quad (5.39)$$

where $\mu(\varepsilon) \in [0,1]$ is a free parameter such that $\mu(0) = 1$. $\mu = 1$ guarantees the largest stability region. When $\varepsilon \to 0$, one gets an *implicit* discretization of the diffusion equation, enabling a stability condition like $\Delta t = O(\Delta x)$.

5.5. Stochastic AP schemes for linear transport equation with uncertainties

Kinetic models usually have *uncertainties* that can arise in collision kernels, scattering coefficients, initial or boundary data, geometry, source or forcing terms (Bird 1994)(Berman, Haverkort and Woerdman 1986)(Koura and Matsumoto 1991). Understanding the impact of, quantify and even control these uncertainties, in the sense of uncertainty quantification (UQ), is crucial to the simulations of the complex kinetic systems in order to verify, validate and improve these models, and to conduct risk management.

The uncertainty is usually modelled by a random vector $z \in \mathbb{R}^n$ in a properly defined probability space $(\Sigma, \mathcal{A}, \mathbb{P})$, whose event space is Σ and equipped with σ-algebra $\mathcal{A}$ and probability measure $\mathbb{P}$. We also assume the components of z are mutually independent random variables with known probability $\omega(z) : I_z \longrightarrow \mathbb{R}^+$, obtained already through some dimension reduction technique, e.g., Karhunen-Loève (KL) expansion (Loève 1977).

The linear transport equation with isotropic scattering

Consider the linear transport equation in one dimensional slab geometry with random input:

$$\varepsilon\delta_t f + v\delta_x f = \frac{\sigma}{\varepsilon}\mathcal{L}f, \quad t > 0,\ x \in [0,1],\ v \in [-1,1],\ z \in I_z, \quad (5.40)$$

$$\mathcal{L}f(t,x,v,z) = \frac{1}{2}\int_{-1}^{1} f(t,x,v',z)dv' - f(t,x,v,z)\,, \quad (5.41)$$

with the initial condition

$$f(0,x,v,z) = f^0(x,v,z). \quad (5.42)$$

This equation arises in neutron transport, radiative transfer, etc. and describes particles (for example neutrons) transport in a background media (for example nuclei). $v = \Omega \cdot e_x = \cos\theta$ where θ is the angle between the

moving direction and x-axis. Assume

$$\sigma(x,z) \geq \sigma_{\min} > 0. \tag{5.43}$$

Denote

$$\langle \phi \rangle = \frac{1}{2}\int_{-1}^{1} \phi(v)dv \tag{5.44}$$

as the average of a velocity dependent function ϕ.

Let $\rho = \langle f \rangle$. For each fixed z, as $\varepsilon \to 0$, ρ solves the following diffusion equation:

$$\partial_t \rho = \partial_x \left(\frac{1}{3}\sigma(x,z)^{-1}\partial_x \rho \right). \tag{5.45}$$

In order to understand the property of numerical methods for uncertain kinetic equations, it is importnt to study the regularity and long-time behavior in the random space of the linear transport equation (5.40)-(5.42). Consider the Hilbert space of the random variable

$$H(I_z;\, \omega dz) = \Big\{ f \mid I_z \to \mathbb{R}^+,\, \int_{I_z} f^2(z)\omega(z)dz < +\infty \Big\}, \tag{5.46}$$

equipped with the inner product and norm defined as

$$\langle f, g \rangle_\omega = \int_{I_z} f g\, \omega(z)dz, \quad \|f\|_\omega^2 = \langle f, f \rangle_\omega . \tag{5.47}$$

Define the kth order differential operator with respect to z as

$$D^k f(t,x,v,z) := \partial_z^k f(t,x,v,z), \tag{5.48}$$

and the Sobolev norm in z as

$$\|f(t,x,v,\cdot)\|_{H^k}^2 := \sum_{\alpha \leq k} \|D^\alpha f(t,x,v,\cdot)\|_\omega^2. \tag{5.49}$$

Finally, introduce norms in space and velocity as follows,

$$\|f(t,\cdot,\cdot,\cdot)\|_\Gamma^2 := \int_Q \|f(t,x,v,\cdot)\|_\omega^2\, dx\, dv, \qquad t \geq 0, \tag{5.50}$$

$$\tag{5.51}$$

where $Q = [0,1] \times [-1,1]$ denotes the domain in the phase space. The following results were established in (Jin, Liu and Ma 2017*a*).

Theorem 5.4. (Uniform regularity) If for some integer $m \geq 0$,

$$\|D^k \sigma(z)\|_{L^\infty} \leq C_\sigma, \qquad \|D^k f_0\|_\Gamma \leq C_0, \qquad k = 0, \ldots, m, \tag{5.52}$$

then the solution f to the linear transport equation (5.40)–(5.42), with periodic boundary condition in x, satisfies,

$$\|D^k f(t,\cdot,\cdot,\cdot)\|_\Gamma \leq C, \qquad k = 0, \cdots, m, \qquad \forall t > 0, \tag{5.53}$$

where C_σ, C_0 and C are constants independent of ε.

The above theorem shows that, under some smoothness assumption on σ, the regularity of the initial data is preserved in time and the Sobolev norm of the solution is bounded uniformly in ε.

Stochastic Galerkin approximation

An interesting and important scenario is when the uncertainty and small scaling are both present in the equation. Among various UQ methods (Xiu 2010)(Gunzburger, Webster and Zhang 2014), we consider the stochastic Galerkin (SG) method, which is suitable for our AP analysis thanks to its Galerkin formulation.

Assume the complete orthogonal polynomial basis in the Hilbert space $H(I_z;\omega(z)dz)$ corresponding to the weight $\omega(z)$ is $\{\phi_i(z), i = 0, 1, \cdots,\}$, where $\phi_i(z)$ is a polynomial of degree i and satisfies the orthonormal condition:

$$\langle \phi_i, \phi_j \rangle_\omega = \int \phi_i(z)\phi_j(z)\omega(z)dz = \delta_{ij}.$$

Here $\phi_0(z) = 1$, and δ_{ij} is the Kronecker delta function. Since the solution $f(t,\cdot,\cdot,\cdot)$ is defined in $L^2\big([0,1]\times[-1,1]\times\mathbb{I}_z;d\mu\big)$, one has the generalized polynomial chaos expansion (Xiu and Karniadakis 2002)

$$f(t,x,v,z) = \sum_{i=0}^{\infty} f_i(t,x,v)\,\phi_i(z), \quad \hat{f} = \big(\,f_i\,\big)_{i=0}^{\infty} := \big(\bar{f}, \hat{f}_1\big).$$

The mean and variance of f can be obtained from the expansion coefficients as

$$\bar{f} = E(f) = \int_{I_z} f\omega(z)\,dz = f_0, \quad \text{var}\,(f) = |\hat{f}_1|^2\,.$$

Denote the SG solution by

$$f^K = \sum_{i=0}^{K} f_i\,\phi_i, \quad \hat{f}^K = \big(\,f_i\,\big)_{i=0}^{K} := \big(\bar{f}, \hat{f}_1^K\big), \tag{5.54}$$

from which one can extract the mean and variance of f^K from the expansion coefficients as

$$E(f^K) = \bar{f}, \quad \text{var}\,(f^K) = |\hat{f}_1^K|^2\,.$$

Furthermore, define

$$\begin{aligned} &\sigma_{ij} = \big\langle \phi_i,\, \sigma\phi_j \big\rangle_\omega, \quad \Sigma = \big(\,\sigma_{ij}\,\big)_{M+1,M+1};\\ &\sigma_{ij}^a = \big\langle \phi_i,\, \sigma^a\phi_j \big\rangle_\omega, \quad \Sigma^a = \big(\,\sigma_{ij}^a\,\big)_{M+1,M+1}, \end{aligned} \tag{5.55}$$

for $0 \le i,j \le M$. Let I be the $(K+1)\times(K+1)$ identity matrix. Σ, Σ^a

are symmetric positive-definite matrices satisfying

$$\Sigma \geq \sigma_{\min} \, \mathrm{I} \, .$$

If one applies the polynomial chaos ansatz (5.54) into the transport equation (5.40), and conduct the Galerkin projection, one obtains

$$\varepsilon \partial_t \hat{f} + v \partial_x \hat{f} = -\frac{1}{\varepsilon}(I - [\cdot])\Sigma \hat{f}. \tag{5.56}$$

Note the SG method makes the random transport equations into deterministic systems (5.56) which are vector analogue of the original scalar deterministic transport equations. Therefore one can naturally utilize the deterministic AP machinery to solve the SG system to achieve the desired AP goals, hence minimize "intrusion" to the legacy deterministic codes. To this aim, the notion of *stochastic asymptotic preserving (sAP)* was introduced in (Jin, Xiu and Zhu 2015). A scheme is sAP if an SG method for the random kinetic equation becomes an SG approximation for the limiting macroscopic, random (hydrodynamic or diffusion) equation as $\varepsilon \to 0$, with K, mesh size and time step all held fixed. Such schemes guarantee that for $\varepsilon \to 0$, *all* numerical parameters, including K, can be chosen only for accuracy requirement, but *independent* of ε.

We now use the micro-macro decomposition:

$$\hat{f}(t, x, v, z) = \hat{\rho}(t, x, z) + \varepsilon \hat{g}(t, x, v, z), \tag{5.57}$$

where $\hat{\rho} = [\hat{f}]$ and $[\hat{g}] = 0$, in (5.56) to get

$$\partial_t \hat{\rho} + \partial_x \langle v \hat{g} \rangle = -\Sigma^a \hat{\rho} + \hat{S}, \tag{5.58a}$$

$$\partial_t \hat{g} + \frac{1}{\varepsilon}(I - \langle . \rangle)(v \partial_x \hat{g}) = -\frac{1}{\varepsilon^2}\Sigma \hat{g} - \Sigma^a \hat{g} - \frac{1}{\varepsilon^2} v \partial_x \hat{\rho}, \tag{5.58b}$$

with initial data

$$\hat{\rho}(0, x, z) = \hat{\rho}_0(x, z), \quad \hat{g}(0, x, v, z) = \hat{g}_0(x, v, z) \, .$$

As $\varepsilon \to 0$, system (5.58) formally approaches the diffusion limit

$$\partial_t \hat{\rho} = \partial_x \left(\frac{1}{3} \Sigma^{-1} \partial_x \hat{\rho} \right) \, . \tag{5.59}$$

This is the SG approximation to the random diffusion equation (5.45). Thus the SG approximation is sAP in the sense of (Jin et al. 2015).

The following result was proved in (Jin et al. 2017*a*).

Theorem 5.5. If for some integer $m \geq 0$,

$$\|\sigma(z)\|_{H^k} \leq C_\sigma, \quad \|D^k f_0\|_\Gamma \leq C_0, \quad \|D^k(\partial_x f_0)\|_\Gamma \leq C_x, \quad k = 0, \ldots, m, \tag{5.60}$$

then for $t \leq T$, the error of the sG method is

$$\|f - f^K\|_\Gamma \leq \frac{C(T)}{K^k}, \tag{5.61}$$

where $C(T)$ is a constant independent of ε.

Theorem 5.5 gives a uniform in ε spectral convergence rate, thus one can choose K independent of ε, a very strong sAP property. Such a result is also obtained with the anisotropic scattering case, for the linear semiconductor Boltzmann equation (Jin and Liu 2017).

A full discretization

Here, we adopt the micro-macro decomposition based fully discrete scheme for the SG system (5.58).

Corresponding to (5.36) and (5.37), one has

$$\frac{\hat\rho_i^{n+1} - \hat\rho_i^n}{\Delta t} + \langle v \frac{\hat g_{i+1/2}^{n+1} - \hat g_{i-1/2}^{n+1}}{\Delta x} \rangle = 0, \tag{5.62a}$$

$$\frac{\hat g_{i+1/2}^{n+1} - \hat g_{i+1/2}^n}{\Delta t} + \frac{1}{\varepsilon \Delta x}(I - \langle \Pi \rangle)\left(v^+(\hat g_{i+1/2}^n - \hat g_{i-1/2}^n) + v^-(\hat g_{i+3/2}^n - \hat g_{i+1/2}^n)\right) \tag{5.62b}$$

$$= -\frac{1}{\varepsilon^2}\Sigma_i \hat g_{i+1/2}^{n+1} - \frac{1}{\varepsilon^2} v \frac{\hat\rho_{i+1}^n - \hat\rho_i^n}{\Delta x}.$$

Its formal limit, when $\varepsilon \to 0$, is given by

$$\frac{\hat\rho_i^{n+1} - \hat\rho_i^n}{\partial_t} - \frac{1}{3}\Sigma^{-1} \frac{\hat\rho_{i+1}^n - 2\hat\rho_i^n + \hat\rho_{i-1}^n}{\Delta x^2} = 0. \tag{5.63}$$

This is the fully discrete sG scheme for (5.59). Thus the fully discrete scheme is sAP.

One important property for an AP scheme is to have a stability condition independent of ε, so one can take $\Delta t \gg O(\varepsilon)$. The next theorem from (Jin et al. 2017*a*) confirms this.

Theorem 5.6. If Δt satisfies the following CFL condition

$$\Delta t \leq \frac{\sigma_{\min}}{3}(\Delta x)^2 + \frac{2\varepsilon}{3}\Delta x, \tag{5.64}$$

then the solution obtained by scheme (5.62) satisfies the energy estimate

$$\sum_{i=0}^{N-1}\left(\left(\hat\rho^{n+}\right)^2 + \frac{\varepsilon^2}{2}\int_{-1}^1 \left(\hat g_{i+1/2}^n\right)^2 dv \right) \leq \sum_{i=0}^{N-1}\left(\left(\hat\rho_i^0\right)^2 + \frac{\varepsilon^2}{2}\int_{-1}^1 \left(\hat g_{i+\frac12}^0\right)^2 dv \right)$$

for every n, and hence the scheme (5.62) is stable.

Since the right hand side of (5.64) has a lower bound, which is essentially a stability condition of the discrete diffusion equation (5.63)), when $\varepsilon \to 0$, the scheme is asymptotically stable and Δt remains finite even if $\varepsilon \to 0$.

Next we consider a numerical example from (Jin et al. 2017*a*). Consider a random coefficient with one dimensional random parameter:

$$\sigma(z) = 2 + z, \quad z \text{ is uniformly distributed in } (-1, 1).$$

The limiting random diffusion equation is

$$\partial_t \rho = \frac{1}{3\sigma(z)} \partial_{xx} \rho \,, \tag{5.65}$$

with initial condition and boundary conditions:

$$\rho(t, 0, z) = 1, \quad \rho(t, 1, z) = 0, \quad \rho(0, x, z) = 0.$$

The analytical solution for (5.65) with the given initial and boundary conditions is

$$\rho(t, x, z) = 1 - \text{ erf } \left(\frac{x}{\sqrt{\frac{4}{3\sigma(z)} t}} \right). \tag{5.66}$$

When ε is small, this can be used as the reference solution. For large ε or in the case one can not get an analytic solution, we will use the collocation method (see (Gunzburger et al. 2014)) with the same time and spatial discretization to the micro-macro system (5.62) as a comparison in the following examples. In addition, the standard 30-points Gauss-Legendre quadrature set is used for the velocity space to compute ρ.

To examine the accuracy, two error norms are used: the differences in the mean solutions and in the corresponding standard deviation, with ℓ^2 norm in x:

$$e_{mean}(t) = \left\| \mathbb{E}[u^h] - \mathbb{E}[u] \right\|_{\ell^2},$$

$$e_{std}(t) = \left\| \sigma[u^h] - \sigma[u] \right\|_{\ell^2},$$

where u^h, u are the numerical solutions and the reference solutions, respectively.

In Figure 5.9, the errors in mean and standard deviation of the SG solutions at $t = 0.01$ with different K are plotted. Three sets of results are included: solutions with $\Delta x = 0.04$ (squares), $\Delta x = 0.02$ (circles), $\Delta x = 0.01$ (stars), with $\Delta t = 0.0002/3$ always used. One observes that the errors become smaller with finer mesh, and the solutions decay rapidly in K and then saturate where spatial discretization error dominates.

In Figure 5.10, we examine the difference between the solution $t = 0.01$

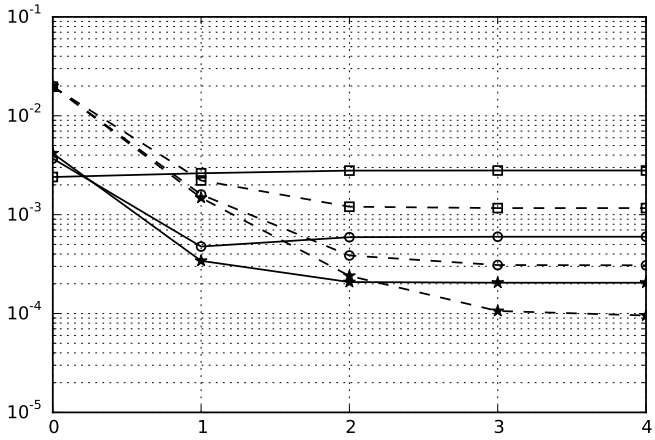

Figure 5.9. Example 1. Errors of the mean (solid line) and standard deviation (dash line) of ρ with respect to the polynomial chaos order K at $\varepsilon = 10^{-8}$: $\Delta x = 0.04$ (squares), $\Delta x = 0.02$ (circles), $\Delta x = 0.01$ (stars).

obtained by SG with $K = 4$, $\Delta x = 0.01$, $\Delta t = \Delta x^2/12$ and the limiting analytical solution (5.66). One can observe the differences become smaller as ε is smaller in a quadratic fashion, before the numerical errors become dominant. Therefore the method works for all range of ε.

A discontinuous Galerkin method based sAP scheme for the same problem was developed in (Chen, Liu and Mu 2017), where uniform stability and rigorous sAP property were also proven.

5.6. Stochastic Galerkin methods for general nonlinear kinetic equations with uncertainties

Consider a general nonlinear kinetic equation with multi-dimensional uncertainties:

$$\begin{cases} \varepsilon^\alpha \partial_t f + v \cdot \nabla_x f - \nabla_{\mathbf{x}} \phi \cdot \nabla_v f = \dfrac{1}{\varepsilon} \mathcal{Q}(f), \quad t > 0,\ x \in \Omega,\ v \in \mathbb{R}^d,\ z \in \mathbb{R}^n, \\ f(0, x, v) = f^0(x, v). \end{cases} \tag{5.67}$$

Here $\alpha = 0$ or 1 corresponds to the Euler (acoustic) or incompressible Navier-Stokes scaling respectively (Bardos, Golse and Levermore 1991).

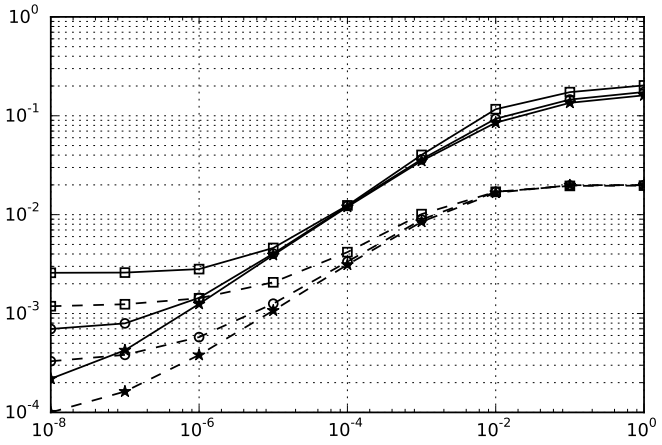

Figure 5.10. Example 1. Differences in the mean (solid line) and standard deviation (dash line) of ρ with respect to ε^2, between the limiting analytical solution (5.66) and the SG solution with $K = 4$, $\Delta x = 0.04$ (squares), $\Delta x = 0.02$ (circles) and $\Delta x = 0.01$ (stars).

We again use the generalized polynomial chaos approximation

$$f(t,x,v,z) \approx \sum_{|k|=0}^{K} f_k(t,x,v)\Phi_k(z) := f^K(t,x,v,z), \tag{5.68}$$

where $k = (k_1, \ldots, k_n)$ is a multi-index with $|k| = k_1 + \cdots + k_n$. $\{\Phi_k(z)\}$ are orthornomal polynomials from $\mathbb{P}_K^n$, the set of all n-variate polynomials of degree up to M and satisfy

$$\langle \Phi_k, \Phi_j \rangle_\omega = \int_{I_z} \Phi_k(z)\Phi_j(z)\omega(z)\,\mathrm{d}z = \delta_{kj}, \quad 0 \le |k|, |j| \le K.$$

Here δ_{kj} is the Kronecker delta function.

Now inserting (5.68) into (5.67). Upon a standard Galerkin projection, one obtains, for each $0 \le k \le M$,

$$\begin{cases} \varepsilon^\alpha \partial_t f_k + v \cdot \nabla_x f_k - \displaystyle\sum_{|j|=0}^{K} \nabla_x \phi_{kj} \cdot \nabla_v f_j = \frac{1}{\varepsilon} \mathcal{Q}_k(f^K), \\ f_k(0,x,v) = f_k^0(x,v), \end{cases} \tag{5.69}$$

with

$$\mathcal{Q}_k(f^K) := \int_{I_z} \mathcal{Q}(f^K)(t,x,v,z)\Phi_k(z)\omega(z)\,dz,$$
$$\phi_{kj} := \int_{I_z} \phi(t,x,z)\Phi_k(z)\Phi_j(z)\omega(z)\,dz,$$
$$f_k^0 := \int_{I_z} f^0(x,v,z)\Phi_k(z)\omega(z)\,dz.$$

We also assume that the potential $\phi(t,x,z)$ is given a priori for simplicity (the case that it is coupled to a Poisson equation can be treated similarly (Zhu and Jin 2017)).

Hypocoercivity estimate of the SG system

The hypocoercivity theory (Villani 2009) can be used to study the properties of the SG methods. For general linear transport with uncertainty see (Li and Wang 2017). For nonlinear problems one needs to consider the perturbative form (Jin and Zhu 2018)(Liu and Jin 2018)

$$f_k = \mathcal{M} + \varepsilon\, M h_k\,, \tag{5.70}$$

where h_k is the coefficient of the following gPC expansion

$$h(t,x,v,z) \approx \sum_{|k|=0}^{M} h_k(t,x,v)\Phi_k(z) := h^K(t,x,v,z)\,. \tag{5.71}$$

Inserting ansatz (5.70) and (5.71) into (5.69) and conducting a standard Galerkin projection, one obtains the SG system for h_k (consider the case of $\phi = 0$) (Hu and Jin 2016):

$$\begin{cases} \partial_t h_k + \dfrac{1}{\varepsilon^\alpha} v\cdot\nabla_x h_k = \dfrac{1}{\varepsilon^{1+\alpha}}\mathcal{L}_k(h^K) + \dfrac{1}{\varepsilon^\alpha}\mathcal{F}_k(h^K,h^K), \\ h_k(0,x,v) = h_k^0(x,v), \qquad x\in\Omega\subset\mathbb{T}^d,\ v\in\mathbb{R}^d, \end{cases} \tag{5.72}$$

for each $1 \le |k| \le K$, with initial data given by

$$h_k^0 := \int_{I_z} h^0(x,v,z)\psi_k(z)\,\pi(z)dz.$$

For the Boltzmann equation, the collision parts are given by

$$\mathcal{L}_k(h^K) = \mathcal{L}_k^+(h^K) = \sum_{|i|=1}^K \int_{\mathbb{R}^d\times\mathbb{S}^{d-1}} \widetilde{S}_{ki}\,\phi(|v-v_*|)\,(h_i(v')M(v'_*) \\ +h_i(v'_*)M(v'))\,M(v_*)\,dv_*d\sigma \\ -M(v)\sum_{|i|=1}^K \int_{\mathbb{R}^d\times\mathbb{S}^{d-1}} \widetilde{S}_{ki}\,\phi(|v-v_*|)\,h_i(v_*)M(v_*)\,dv_*d\sigma - \sum_{|i|=1}^K \nu_{ki}h_i\,,$$

$$\mathcal{F}_k(h^K,h^K)(t,x,v) = \sum_{|i|,|j|=1}^K \int_{\mathbb{R}^d\times\mathbb{S}^{d-1}} S_{kij}\,\phi(|v-v_*|)\,M(v_*) \\ \cdot(h_i(v')h_j(v'_*) - h_i(v)h_j(v_*))\,dv_*d\sigma,$$

with

$$\widetilde{S}_{ki} := \int_{I_z} b(\cos\theta,z)\,\psi_k(z)\psi_i(z)\,\pi(z)dz,$$
$$\widetilde{\nu}_{ki} := \int_{\mathbb{R}^d\times\mathbb{S}^{d-1}} \widetilde{S}_{ki}\,\phi(|v-v_*|)\,\mathcal{M}(v_*)\,dv_*d\sigma,$$
$$\text{and} \qquad S_{kij} := \int_{I_z} b(\cos\theta,z)\,\psi_k(z)\psi_i(z)\psi_j(z)\,\pi(z)dz.$$

For technical reasons, we assume $z \in I_z$ is one dimensional and I_z has finite support $|z| \le C_z$ (which is the case, for example, for the uniform and Beta distribution). Define

$$\|h\|^2_{H^s_{x,v}} = \sum_{|j|+|l|\le s} \|\partial_l^j h\|^2_{L^2_{x,v}}\,, \quad \|h\|^2_{H^s_z} = \int_{I_z} \|h\|^2_{H^s_{x,v}}\pi(z)dz\,.$$

In (Liu and Jin 2018)(Daus, Jin and Liu 2019) the following results are given, under some suitable assumption on b:

Theorem 5.7. Assume the collision kernel B is given by

$$B(|v-v_*|),\cos\theta,z) = \phi(|v-v_*|)b(\cos\theta,z), \quad \phi(\xi) = C_\phi\xi^\gamma \quad \text{with}\gamma\in[0,1], C_\phi > 0$$

$$\forall\eta\in[-1,1]. \qquad |\partial_\eta b(\eta,z)| \le C_b, \quad |\partial_z^k b(\eta,z)| \le C_b^*, \quad \forall\, 0\le k\le r,$$

where b is linear in z, given in the form

$$b(\cos\theta,z) = b_0(\cos\theta) + b_1(\cos\theta)z\,. \tag{5.73}$$

Assume some upper and positive lower boundedness on b and its derivatives. In addition, assume (Jin and Shu 2017)

$$||\psi_k||_{L^\infty} \le Ck^p, \qquad \forall\, k, \tag{5.74}$$

with a parameter $p > 0$. Let $q > p + 2$, define the energy E^K by

$$E^K(t) = E^K_{s,q}(t) = \sum_{k=1}^{K} ||k^q h_k||^2_{H^s_{x,v}}, \tag{5.75}$$

with the initial data satisfying $E^K(0) \leq \eta$. Then for all $s \geq s_0$, $0 \leq \varepsilon_d \leq 1$, such that for $0 \leq \varepsilon \leq \varepsilon_d$, if h^K is an SG solution (5.72) in $H^s_{x,v}$, then:
(i) Under the incompressible Navier-Stokes scaling ($\alpha = 1$),

$$E^K(t) \leq \eta\, e^{-\tau t}\,.$$

(ii) Under the acoustic scaling ($\alpha = 0$),

$$E^K(t) \leq \eta\, e^{-\varepsilon\tau t}\,,$$

where η, τ are all positive constants that only depend on s and q, independent of K and z.

From here, one also concludes that, $||h^K||_{H^s_{x,v}L^\infty_z}$ decays exponentially in time, with the same rate as $E^K(t)$, namely

$$||h^K||_{H^s_{x,v}L^\infty_z} \leq \eta\, e^{-\tau t} \tag{5.76}$$

in the incompressible Navier-Stokes scaling, and

$$||h^K||_{H^s_{x,v}L^\infty_z} \leq \eta\, e^{-\varepsilon\,\tau t}$$

in the acoustic scaling.

(Liu and Jin 2018) also gives the following error estimates on the SG method.

Theorem 5.8. Suppose the assumptions on the collision kernel and basis functions in Theorem 5.7 are satisfied, and the initial data are the same as those in Theorem 5.7, then
(i) Under the incompressible Navier-Stokes scaling,

$$||h - h^K||_{H^s_z} \leq C_e\, \frac{e^{-\lambda t}}{K^r}, \tag{5.77}$$

(ii) Under the acoustic scaling,

$$||h - h^K||_{H^s_z} \leq C_e\, \frac{e^{-\varepsilon\lambda t}}{K^r}\,, \tag{5.78}$$

with the constants C_e, $\lambda > 0$ independent of K and ε.

The above results show that the regularity of the SG solutions is the same as the initial data. Furthermore, the numerical fluctuation h^K converges to h with spectral accuracy, and the numerical error will decay exponentially in time in the random space.

5.7. Asymptotic-preserving neural network approximation

Kinetic equations have curse-of-dimensionality since it solves equations in the phase space. While this survey mainly concentrates on dealing with multiscale issues, it will be interesting to also dealt with the issue of high dimensionality together with multiple scales. To this aim the deep neural network (DNN) offers a possible direction, since there have been examples in which DNNs offer some advantages for high dimensional PDEs (E and Yu 2018)(Raissi, Perdikaris and Karniadakis 2019)(Lu, Jin, Pang, Zhang and Karniadakis 2021*a*)(Li, Kovachki, Azizzadenesheli, Liu, Bhattacharya, Stuart and Anandkumar 2020*c*).

Unlike classical numerical schemes, a neural network uses a non-polynomial approximation to approximate the training data through an optimization of an empirical loss/risk. For multiscale kinetic equations it is essential to construct a neural network that is AP (Li and Yang 2021) (referred to APNNs).

We first introduce conventional notations for deep neural networks (DNNs). An L-layer feed forward neural network is defined recursively as,

$$\begin{aligned} &f_\theta^{[0]}(x) = x, \\ &f_\theta^{[l]}(x) = \sigma \circ (W^{[l-1]} f_\theta^{[l-1]}(x) + b^{[l-1]}),\ 1 \le l \le L-1, \\ &f_\theta(x) = f_\theta^{[L]}(x) = W^{[L-1]} f_\theta^{[L-1]}(x) + b^{[L-1]}, \end{aligned} \tag{5.79}$$

where $W^{[l]} \in \mathbb{R}^{m_{l+1}\times m_l}, b^l \in \mathbb{R}^{m_{l+1}}, m_0 = d_{in} = d$ is the input dimension, $m_L = d_0$ is the output dimension, σ is a scalar function and " $\circ$ " means entry-wise operation. We denote the set of parameters by θ. The layers are denoted by a list, i.e., $[m_0, \cdots, m_L]$.

Consider the linear transport equation with initial and boundary conditions over a bounded domain $\mathcal{T} \times \mathcal{D} \times \Omega$:

$$\begin{cases} \varepsilon \partial_t f + v \cdot \nabla_x f = \frac{1}{\varepsilon} \mathcal{L} f, & (t,x,v) \in \mathcal{T} \times \mathcal{D} \times \Omega, \\ \mathcal{B} f = F_{\mathrm{B}}, & (t,x,v) \in \mathcal{T} \times \partial\mathcal{D} \times \Omega, \\ \mathcal{I} f = f_0, & (t,x,v) \in \{t=0\} \times \mathcal{D} \times \Omega, \end{cases} \tag{5.80}$$

where F_{B}, f_0 are given functions; $\partial\mathcal{D}$ is the boundary of $\mathcal{D}$, and $\mathcal{B}, \mathcal{I}$ are initial and boundary operators, respectively. $\mathcal{L} = \sigma(\rho - f)$.

The failure of PINNs to resolve small scales

PINNs is a standard neural network to solve PDEs. There the density function $f(t,x,v)$ is approximated by a neural network

$$\mathrm{NN}_\theta(t,x,v) \approx f(t,x,v). \tag{5.81}$$

The inputs of DNN are (t,x,v), i.e., $m_0 = 3, 5$ for 1-d and 2-d respectively. The output is a scalar which represents the value of f at (t,x,v). Since f is always non-negative, we put an exponential function at the last output

layer of the DNN:

$$f_\theta^{\mathrm{NN}}(t,x,v) := \exp\left(-\tilde{f}_\theta^{\mathrm{NN}}(t,x,v)\right) \approx f(t,x,v) \tag{5.82}$$

to represent the numerical solution of f. Then the least square of the residual of the original transport equation (5.80) is used as the target loss function, together with boundary and initial conditions as penalty terms,

$$\begin{aligned}\mathcal{R}^{\varepsilon}_{\mathrm{PINN}} =& \frac{1}{|\mathcal{T}\times\mathcal{D}\times\Omega|}\int_{\mathcal{T}}\int_{\mathcal{D}}\int_{\Omega}\left|\varepsilon^2\partial_t f_\theta^{\mathrm{NN}} + \varepsilon v\cdot\nabla_x f_\theta^{\mathrm{NN}} - \mathcal{L}f_\theta^{\mathrm{NN}}\right|^2 dvdx\,dt \\ &+ \frac{\lambda_1}{|\mathcal{T}\times\partial\mathcal{D}\times\Omega|}\int_{\mathcal{T}}\int_{\partial\mathcal{D}}\int_{\Omega}|\mathcal{B}f_\theta^{\mathrm{NN}} - F_{\mathrm{B}}|^2 dv\,dx\,dt \\ &+ \frac{\lambda_2}{|\mathcal{D}\times\Omega|}\int_{\mathcal{D}}\int_{\Omega}|\mathcal{I}f_\theta^{\mathrm{NN}} - f_0|^2 dv\,dx,\end{aligned} \tag{5.83}$$

where λ_1 and λ_2 are the penalty weights to be tuned. Then a standard stochastic gradient method (SGD) or Adam optimizer is used to find the global minimum of this loss.

Now let us check whether this PINN method is AP. One only needs to focus on the first term of (5.83)

$$\mathcal{R}^{\varepsilon}_{\mathrm{PINN,\ residual}} := \frac{1}{|\mathcal{T}\times\mathcal{D}\times\Omega|}\int_{\mathcal{T}}\int_{\mathcal{D}}\int_{\Omega}\left|\varepsilon^2\partial_t f_\theta^{\mathrm{NN}} + \varepsilon v\cdot\nabla_x f_\theta^{\mathrm{NN}} - \mathcal{L}f_\theta^{\mathrm{NN}}\right|^2 dv\,dx\,dt. \tag{5.84}$$

Taking $\varepsilon\to 0$, formally this will lead to

$$\mathcal{R}_{\mathrm{PINN,\ residual}} := \frac{1}{|\mathcal{T}\times\mathcal{D}\times\Omega|}\int_{\mathcal{T}}\int_{\mathcal{D}}\int_{\Omega}\left|-\mathcal{L}f_\theta^{\mathrm{NN}}\right|^2 dv\,dx\,dt, \tag{5.85}$$

which can be viewed as the PINN loss of the equilibrium equation

$$\mathcal{L}f = 0. \tag{5.86}$$

This shows that when ε is very small, to the leading order we are solving equation $\mathcal{L}f = 0$ which gives $f = \rho$. This does not give the desired diffusion equation (2.42). This explains why PINN will fail when ε is small.

The APNN, introduced in (Jin, Ma and Wu 2021*b*), puts the micro-macro system (5.32) or (5.33) into the loss, instead of the original equation (5.80).

First the DNN needs to parametrize two functions $\rho(x,v)$ and $g(t,x,v)$. So here two networks are used. First

$$\rho_\theta^{\mathrm{NN}}(t,x) := \exp\left(-\tilde{\rho}_\theta^{\mathrm{NN}}(t,x)\right) \approx \rho(t,x). \tag{5.87}$$

Notice here ρ is non-negative. Second,

$$g_\theta^{\mathrm{NN}}(t,x,v) := \tilde{g}_\theta^{\mathrm{NN}}(t,x,v) - \langle\tilde{g}_\theta^{\mathrm{NN}}\rangle(t,x) \approx g(t,x,v). \tag{5.88}$$

Here $\tilde{\rho}$ and $\tilde{g}$ are both fully-connected neural networks. Notice that by

choosing $g_\theta^{\mathrm{NN}}(t,x,v)$ as in (5.88) it will automatically satisfy the constraint

$$\langle g\rangle = 0\,, \tag{5.89}$$

because

$$\langle g_\theta^{\mathrm{NN}}\rangle = \langle \tilde{g}_\theta^{\mathrm{NN}}\rangle - \langle \tilde{g}_\theta^{\mathrm{NN}}\rangle = 0, \quad \forall\, t,x. \tag{5.90}$$

Then the APNN loss is defined as

$$\begin{aligned}\mathcal{R}^{\varepsilon}_{\mathrm{APNN}} =& \frac{1}{|\mathcal{T}\times\mathcal{D}|}\int_{\mathcal{T}}\int_{\mathcal{D}} |\partial_t \rho_\theta^{\mathrm{NN}} + \nabla_x\cdot\langle v g_\theta^{\mathrm{NN}}\rangle|^2 dx\,dt\\ &+\frac{1}{|\mathcal{T}\times\mathcal{D}\times\Omega|}\int_{\mathcal{T}}\int_{\mathcal{D}}\int_{\Omega} |\varepsilon^2\partial_t g_\theta^{\mathrm{NN}} + \varepsilon(I-\Pi)(v\cdot\nabla_x g_\theta^{\mathrm{NN}})\\ &\quad + v\cdot\nabla_x\rho_\theta^{\mathrm{NN}} - \mathcal{L} g_\theta^{\mathrm{NN}}|^2 dv\,dx\,dt\\ &+\frac{\lambda_1}{|\mathcal{T}\times\partial\mathcal{D}\times\Omega|}\int_{\mathcal{T}}\int_{\partial\mathcal{D}}\int_{\Omega} |\mathcal{B}(\rho_\theta^{\mathrm{NN}}+\varepsilon g_\theta^{\mathrm{NN}}) - F_{\mathrm{B}}|^2 dv\,dx\,dt\\ &+\frac{\lambda_2}{|\mathcal{D}\times\Omega|}\int_{\mathcal{D}}\int_{\Omega} |\mathcal{I}(\rho_\theta^{\mathrm{NN}}+\varepsilon g_\theta^{\mathrm{NN}}) - f_0|^2 dv\,dx.\end{aligned} \tag{5.91}$$

A schematic plot of the method is given in Figure 5.11.

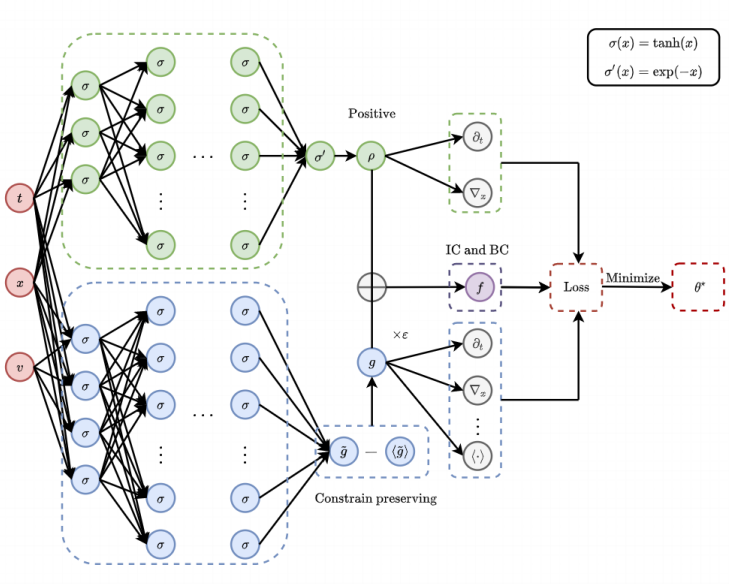

Figure 5.11. Schematic of APNNs for solving the linear transport equation with initial and boundary conditons.

To show formally the AP property of this loss, one only needs to focus on

the first two terms of (5.91)

$$\begin{aligned}\mathcal{R}^{\varepsilon}_{\text{APNN, residual}} =& \frac{1}{|\mathcal{T}\times\mathcal{D}|}\int_{\mathcal{T}}\int_{\mathcal{D}} |\partial_t \rho_\theta^{\text{NN}} + \nabla_x\cdot\langle v g_\theta^{\text{NN}}\rangle - Q|^2 dx\,dt \\ &+ \frac{1}{|\mathcal{T}\times\mathcal{D}\times\Omega|}\int_{\mathcal{T}}\int_{\mathcal{D}}\int_{\Omega}\Big|\varepsilon^2\partial_t g_\theta^{\text{NN}} + \varepsilon(I-\Pi)(v\cdot\nabla_x g_\theta^{\text{NN}}) \\ &\quad + v\cdot\nabla_x\rho_\theta^{\text{NN}} - \mathcal{L}g_\theta^{\text{NN}} - (I-\Pi)\varepsilon Q\Big|^2 dv\,dx\,dt\,.\end{aligned} \tag{5.92}$$

Taking $\varepsilon\to 0$, formally this will lead to

$$\begin{aligned}\mathcal{R}_{\text{APNN, residual}} =& \frac{1}{|\mathcal{T}\times\mathcal{D}|}\int_{\mathcal{T}}\int_{\mathcal{D}} |\partial_t \rho_\theta^{\text{NN}} + \nabla_x\cdot\langle v g_\theta^{\text{NN}}\rangle - Q|^2 dx\,dt \\ &+ \frac{1}{|\mathcal{T}\times\mathcal{D}\times\Omega|}\int_{\mathcal{T}}\int_{\mathcal{D}}\int_{\Omega}\Big|v\cdot\nabla_x\rho_\theta^{\text{NN}} - \mathcal{L}g_\theta^{\text{NN}}\Big|^2 dv\,dx\,dt,\end{aligned} \tag{5.93}$$

which is the least square loss of equations

$$\begin{cases}\partial_t\rho + \nabla_x\cdot\langle vg\rangle = Q,\\ v\cdot\nabla_x\rho = \mathcal{L}g.\end{cases} \tag{5.94}$$

The second equation above yields $g = \mathcal{L}^{-1}(v\cdot\nabla_x\rho)$, which, when plugging into the first equation and integrating over v, gives the diffusion equation (2.42). Hence this proposed method is an APNN method.

Example 5.9. We present a numerical example from (Jin et al. 2021*b*). Let $\sigma = 1$. Consider the initial data as follows

$$f_0(x,v) = \frac{\rho(x)}{\sqrt{2\pi}}e^{-\frac{v^2}{2}}, \tag{5.95}$$

where

$$\rho(x) = 1 + \cos(4\pi x), \tag{5.96}$$

and the isotropic in-flow boundary conditions:

$$F_L(v) = 1, \quad F_R(-v) = 0, \quad \text{for } v > 0. \tag{5.97}$$

The results are shown in Figure 5.12. Clearly PINN fails to conserve the mass, and for small ε does not give accurate results, while APNN gives quite accurate results even when ε is very small.

Remark 5.10. Not all AP schemes yield an APNN method when put into the loss. For example it was shown in (Jin et al. 2021*b*) the parity formulation (5.19)-(5.20) does not give an APNN network.

A similar loss function also based on micro-macro decomposition, but with

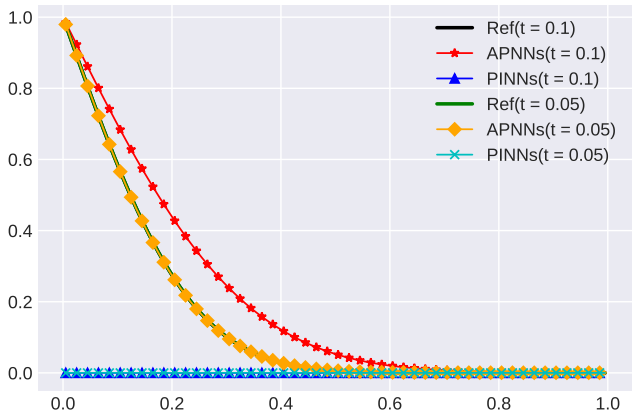

Figure 5.12. Example 5.9. $\varepsilon = 10^{-8}$. Plots of density ρ at $t = 0.05, 0.1$ by PINN, APNN and Reference solutions. The neural networks are $[2, 128, 128, 128, 128, 1]$ for ρ and $[3, 256, 256, 256, 256, 1]$ for g, f. Batch size is 1000 in domain, 400×2 with penalty $\lambda_1 = 10$ for boundary condition and 1000 with penalty $\lambda_2 = 10$ for initial condition, the number of quadrature points is 30. Relative ℓ^2 errors of PINNs and APNNs are $9.40 \times 10^{-1}, 2.76 \times 10^{-3}$ respectively.

a constraint (5.89) as a penalty, was proposed in (Lu, Wang and Xu 2021*b*) for stationary problem.

6. Other related multiscale problems

6.1. Nonlinear hyperbolic systems with stiff source terms

Numerical methods for nonlinear hyperbolic systems with stiff relaxation terms were among the earliest AP schemes for time-dependent problems. A prototype equation is given by:

$$\begin{cases} \partial_t u + \partial_x g(u, v) = 0, \\ \partial_t v + \partial_x h(u, v) = \dfrac{1}{\varepsilon} R(u, v), \end{cases} \tag{6.1}$$

where the term R is dissipative: $\partial_v R \leq 0$ and possesses a unique local equilibrium: $R(u, v) = 0$, which implies $v = f(u)$. Then when $\varepsilon \to 0$, one has the macroscopic limit

$$\partial_t u + \partial_x g(u, f(u)) = 0.$$

This is an analogy of the Euler limit of the Boltzmann equation. If one uses the Chapman-Enskog expansion to $O(\varepsilon)$ term, then (6.1) can be approxi-

mated by a parabolic equation

$$\partial_t u + \partial_x g(u, f(u)) = \varepsilon \partial_x [h(u) \partial_x u] \,. \tag{6.2}$$

Here one needs $h(u) > 0$, which requires the characteristic speeds of the original system (6.1) interwine with that of the limiting equation (6.1). This condition is called the *subcharacteristic condition* (Chen, Levermore and Liu 1994). (6.2) is an analogy of the Navier-Stokes approximation to the Boltzmann equation.

Numerical study of system of the type (6.1) began in the works (Jin and Levermore 1996) (Jin 1995)(Caflisch, Jin and Russo 1997), where the AP principle was applied to design numerical schemes to handle the stiff relaxation term. High order IMEX type schemes were developed in (Pareschi and Russo 2005)(Dumbser, Enaux and Toro 2008). Combining AP and positivity preserving property was done in (Hu and Shu 2019). The relation between AP and well-balanced scheme is revealed in (Gosse and Toscani 2002). For AP schemes for gas dynamics with external force and frictions see (Bouchut, Ounaissa and Perthame 2007)(Chalons, Coquel, Godlewski, Raviart and Seguin 2010). A rigorous uniform accuracy proof of AP schemes for linear problems was recently made in (Hu and Shu 2021).

6.2. Quasi-neutral limit in plasma

In many plasma applications, one can disregard charge separations, and then the quasi-neutral approximation can be used. However, near the plasma boundary, electrostatic sheathes may appear, then one needs to consider more complex models (Degond and Deluzet 2017*a*).

Consider the one-species recaled Euler-Poisson (EP) equations for charged particles:

$$\partial_t n + \nabla \cdot q = 0 \,, \tag{6.3}$$

$$\partial_t q + \nabla \cdot \left(\frac{q \otimes q}{n} \right) + \nabla p(n) = n \nabla \phi \,, \tag{6.4}$$

$$\varepsilon^2 \Delta \phi = n - 1 \,, \tag{6.5}$$

where $n = n(x,t)$ is the particle number density, $q = q(x,t) = nu$ is the momentum (u is the average velocity), $p(n) = n^\gamma$ is the pressure law with $\gamma \geq 1$, and $\phi = \phi(x,t)$ is the electric potential. Here the negatively charged electrons with scaled charge equal to -1 is considered, with a uniform ion background density equal to 1. The dimensionless parameter $\varepsilon = \lambda_D / L$ is the scaled Debye length, i.e., the ratio of the actual Debye length λ_D to the macroscopic length scale L. In the quasineutral regime, $\varepsilon \ll 1$. Letting $\varepsilon \to 0$ in (6.5), one has $n = 1$, and the following limiting equations arise

(Brenier 2000):

$$\nabla \cdot q = 0\,, \tag{6.6}$$

$$\partial_t q + \nabla \cdot (q \otimes q) = \nabla \phi\,. \tag{6.7}$$

This is the incompressible Euler equations.

A typical stable time discretization of the Euler-Poisson system requires $\Delta t \leq \varepsilon$, which is quite restrictive.

The main difficulty here is that when $\varepsilon \to 0$, the Poisson equation (6.5) becomes degenerate, hence a naive discretization would lead to poor numerical performance for small ε. A key idea introduced by Degond etc. in (Crispel, Degond and Vignal 2005) is to reformulate the system to a new one that remains *uniformly elliptic*. Taking ∂_t on (6.3), $\nabla\cdot$ on (6.4) and ∂_{tt} on (6.5) give

$$\partial_{tt} n + \nabla \cdot \partial_t q = 0\,, \tag{6.8}$$

$$\nabla \cdot \partial_t q + \nabla^2 : \left(\frac{q \otimes q}{n} + p(n)\mathrm{I} \right) = \nabla \cdot (n \nabla \phi)\,, \tag{6.9}$$

$$\varepsilon^2 \Delta \partial_{tt} \phi = \partial_{tt} n\,. \tag{6.10}$$

Eliminating $\nabla \cdot \partial_t q$ by combining (6.8) and (6.9) and using (6.10), one gets

$$-\nabla \cdot [(n + \varepsilon^2 \partial_{tt}) \nabla \phi] + \nabla^2 : \left[\frac{q \otimes q}{n} + p(n)\mathrm{I} \right] = 0\,. \tag{6.11}$$

Although this system is equivalent to the original Euler-Poisson system, Equation (6.11) now is *uniformly elliptic* in ε, discretizing it suitably in time will guarantee the asymptotic stability with respect to ε.

This framework is quite general, and has been generalized to two-fluid model (Crispel, Degond and Vignal 2007), Particle-in-Cell method for Vlasov-Poisson system (Degond, Deluzet, Navoret, Sun and Vignal 2010*c*), Euler-Maxwell system (Degond, Deluzet and Savelief 2012*a*), and Vlasov-Maxwell system (Degond, Deluzet and Doyen 2017), among other plasma models. See a recent comprehensive review (Degond and Deluzet 2017*b*).

6.3. High-field limits

In kinetic equations, often there is a strong external field, such as the electric or magnetic field, that balances the collision term, leading to the so-called high field limit (Cercignani, Gamba and Levermore 1997).

High electric field

Consider for example the interaction between the electrons and a surrounding bath through Coulomb force in electrostatic plasma, where the electron density distribution $f(t, x, v)$ is governed by the Vlasov-Poisson-Fokker-

Planck system:

$$\partial_t f + v \cdot \nabla_x f - \frac{1}{\varepsilon}\nabla_x \phi \cdot \nabla_v f = \frac{1}{\varepsilon}\nabla_v \cdot (vf + \nabla_v f), \tag{6.12}$$

$$-\Delta \phi = \rho - h, \tag{6.13}$$

where $\varepsilon = \left(\frac{l_e}{\Lambda}\right)^2$ is the ratio between the mean free path and the Debye length. Let $\varepsilon \to 0$ in (6.16), one obtains the high-field limit (Nieto, Poupaud and Soler 2001)(Goudon, Nieto, Poupaud and Soler 2005):

$$\partial_t \rho - \nabla_x \cdot (\rho \nabla_x \phi) = 0, \tag{6.14}$$

$$-\Delta \phi = \rho - h(x). \tag{6.15}$$

One can combine the force term with the Fokker-Planck term as

$$\partial_t f + v \cdot \nabla_x f = \frac{1}{\varepsilon}\nabla_v \cdot [M \nabla_v (Mf)] \tag{6.16}$$

where $M = e^{-|v+\nabla_x \phi|^2/2}$. This form is convenient for designing AP schemes (Jin and Wang 2011)(Crouseilles and Lemou 2011), based on which one can easily use other well-developed AP frameworks. For more general collision operator, for example the semiconductor Boltzmann collision operator, this trick does not apply and one needs other ideas, for example the BGK penalization (Jin and Wang 2013). A variational approach was recently proposed in (Carrillo, Wang, Xu and Yan 2021), using the Wasserstein gradient structure, to get positivity and AP easily.

High magnetic field

Magnetized plasmas are encountered in a wide variety of astrophysical situations, but also in magnetic fusion devices such as Tokamaks, where a large external magnetic field needs to be applied in order to keep the particles on the desired tracks. The Vlasov equation for such problems takes the following form:

$$\varepsilon \partial_t f + v \cdot \nabla_x f \; + \; \left(E(t,x) \; + \; \frac{1}{\varepsilon} v \wedge B_{\text{ext}}(t,x) \right) \cdot \nabla_v f \; = \; 0.$$

Here, for simplicity we set all physical constants to one and consider that $\varepsilon > 0$ is a small parameter related to the ratio between the reciprocal Larmor frequency and the advection time scale. We consider a constant magnetic field acting in the vertical z-direction, hence it yields the two-dimensional Vlasov-Poisson system with an external strong force:

$$\begin{cases} \varepsilon \partial_t f + v \cdot \nabla_x f \; + \; \left(E(t,x) \; - \; \dfrac{b\, v^\perp}{\varepsilon} \right) \cdot \nabla_v f \; = \; 0, \\ \\ E = -\nabla_x \phi, \quad -\Delta_x \phi = \rho^\varepsilon, \quad \rho = \displaystyle\int_{\mathbb{R}^2} f dv, \end{cases}$$

where we use notation $v^\perp = (-v_y, v_x)$.

Most of the numerical schemes for the Vlasov-Poisson system are based on particle methods, which consist of approximating the distribution function by a finite number of macro-particles. The trajectories of these particles are determined from the characteristic curves corresponding to the Vlasov equation

$$\begin{cases} \varepsilon \dfrac{\mathrm{d}X^\varepsilon}{\mathrm{d}t} = V^\varepsilon, \\ \varepsilon \dfrac{\mathrm{d}V^\varepsilon}{\mathrm{d}t} = -\dfrac{b\, V^{\varepsilon\perp}}{\varepsilon} + E^\varepsilon(t, X^\varepsilon), \end{cases} \tag{6.17}$$

where we use the conservation of f along the characteristic curves

$$f(t, X^\varepsilon(t), V^\varepsilon(t)) = f(t^0, X^0, V^0).$$

In the limit $\varepsilon \to 0$ one expects oscillations occurring on typical time scales $O(1/\varepsilon^2)$ to coexist with a slow dynamics evolving on a time scale $O(1)$. We sketch now how to identify a closed system describing in the leading order the slow evolution. To begin with, note that from the second line of system (6.17) it does follow that V^ε oscillates at order $1/\varepsilon^2$ thus remains bounded and converges weakly[2] to zero. As we detail below, one may also combine both lines of the system to obtain

$$\frac{\mathrm{d}}{\mathrm{d}t}\left(X^\varepsilon - \varepsilon\, \frac{V^{\varepsilon\perp}}{b}\right) = -\frac{1}{b}\, E^\perp(t, X^\varepsilon).$$

This shows that X^ε evolves slowly but, as such, does not provide a closed asymptotic evolution in the limit $\varepsilon \to 0$ and the corresponding asymptotic model is an equation for the density ρ

$$\begin{cases} \partial_t \rho - b\, E^\perp \cdot \nabla_x \rho = 0, \\ E = -\nabla_x \phi, \quad -\Delta_x \phi = \rho. \end{cases}$$

When b is not constant, one also needs to know what happens to expressions that are quadratic in V^ε and this does not follow readily from the weak convergence of V^ε (Filbet and Rodrigues 2017).

One of the oldest of these strategies (Frénod, Salvarani and Sonnendrücker 2009) is directly inspired by theoretical results on two-scale convergence and relies on the fact that at the limit $\varepsilon \to 0$ the τ-dependence ($\tau = t/\varepsilon$) may be explicitly filtered out. Its main drawback is probably that it computes only

[2] Though we do not want to be too precise here, let us mention that in the present discussion *weakly* and *strongly* refer to the weak-* and strong topologies of L^∞ and that the weak convergences that we encounter actually correspond to strong convergence in $W^{-1,\infty}$.

the leading order term in the limit $\varepsilon \to 0$. In particular it is only available when ε is very small.

This may be fixed by keeping besides the stiff term to which a two-scale treatment is applied a non-stiff part that is smaller in the limit $\varepsilon \to 0$ but becomes important when ε is not small. Such a decomposition may be obtained by using a micro-macro approach as in (Crouseilles, Frénod, Hirstoaga and Mouton 2013*a*) and some references therein. This does allow to switch from one regime to another without any treatment of the transition between those but results in relatively heavy schemes,.

Another approach with similar advantages, developed in (Crouseilles, Lemou and Méhats 2013*b*) and (Frénod, Hirstoaga, Lutz and Sonnendrücker 2015), consists in explicitly doubling time variables and seeking higher-dimensional partial differential equations and boundary conditions in variables (t, τ, x, v) that contains the original system at the ε-diagonal $(t, \tau) = (t, t/\varepsilon)$. While the corresponding methods are extremely good at capturing oscillations their design requires a deep *a priori* understanding of the detailed structure of oscillations. Also a class of semi-implicit schemes have been proposed (Filbet and Rodrigues 2016, Filbet and Rodrigues 2017)(Hairer, Lubich and Wang 2020)(Ricketson and Chacón 2020) to capture accurately the non stiff part of the evolution while allowing for coarse discretization parameters. It allows to capture the asymptotic limit of the two dimensional Vlasov-Poisson system with a *uniform* magnetic field (Filbet and Rodrigues 2016)(Filbet, Rodrigues and Zakerzadeh 2021). In many respects those schemes are remarkably natural and simple and can be adapted to totroidal geometry as in (Filbet and Rodrigues 2020).

6.4. Highly anisotropic diffusion

In magnetized plasma simulations, magnetic field confines the particles around the field lines, which leads to highly anisotropic problems. The model problem writes

$$\begin{aligned} -\nabla \cdot (A \nabla u) &= f, && \text{on } \Omega, \\ \mathbf{n} \cdot A \nabla u &= 0, && \text{on } \Gamma_N, \\ u &= g, && \text{on } \Gamma_D, \end{aligned} \tag{6.18}$$

where $\Omega \subset \mathbb{R}^2$ or $\Omega \subset \mathbb{R}^3$ is a bounded domain with boundary $\partial\Omega = \Gamma_D \cup \Gamma_N$ and outward normal $\mathbf{n}$. The direction of the anisotropy is given by a unit vector field $\mathbf{b}$ and the anisotropic diffusion matrix is then given by

$$A = \frac{1}{\varepsilon} A_{||} \mathbf{b} \otimes \mathbf{b} + (Id - \mathbf{b} \otimes \mathbf{b}) A_{\perp} (Id - \mathbf{b} \otimes \mathbf{b}) \tag{6.19}$$

$A_{||} > 0$ is a scalar and $A_{\perp}$ is a symmetric positive definite matrix field, both of them are of order one. The problem becomes highly anisotropic when $\epsilon \ll 1$. Let (ξ, η) be the aligned coordinate system, the formal limit of $\epsilon \to 0$

leads to

$$\begin{aligned} -\partial_\xi(A_{||}\partial_\xi u) &= f, && \text{on } \Omega,\\ \partial_\xi u &= 0, && \text{on } \Gamma_N,\\ u &= g, && \text{on } \Gamma_D. \end{aligned}$$

Any function that remains constant along the $\mathbf{b}$ field solves the above limit equation, which indicates that the limit model is not well-posed. Due to the existence of infinitely many solutions when $\epsilon \to 0$, standard numerical discretizations suffer from large condition numbers when ϵ is small and usually lose convergence when $\varepsilon \ll h$ (h is the mesh size).

To avoid the aforementioned problem, the common approach is to use magnetic field aligned coordinates, which may run into problems when there are magnetic re-connections or highly fluctuating field directions. The other approach is to design methods whose condition numbers do not scale with the anisotropy strength and the convergence orders are uniform with respect to ε. The main idea is to construct new systems that keep well-posed when $\varepsilon \to 0$. In a series of papers by Degond, Narski, Negulescu, *et. al.* (Degond, Deluzet and Negulescu 2010*a*) (Degond, Lozinski, Narski and Negulescu 2012*b*)(Degond, Deluzet, Lozinski, Narski and Negulescu 2010*b*)(Narski and Ottaviani 2014), various reformulations and discretization strategies based on macro-micro decomposition are proposed. Another idea is based on field line integration. By substituting (6.19) into (6.18), one gets

$$\begin{aligned} &-\partial_\xi\big(\frac{1}{\epsilon}A_{||}\partial_\xi u\big) - \nabla\cdot\Big((Id-\mathbf{b}\otimes\mathbf{b})A_\perp(Id-\mathbf{b}\otimes\mathbf{b})\nabla u\Big) = f, && \text{on } \Omega,\\ &\frac{1}{\epsilon}A_{||}\partial_\xi u + \mathbf{n}\cdot(Id-\mathbf{b}\otimes\mathbf{b})A_\perp(Id-\mathbf{b}\otimes\mathbf{b})\nabla u = 0, && \text{on } \Gamma_N,\\ &u = g, && \text{on } \Gamma_D, \end{aligned} \tag{6.20}$$

Taking the integration of the first equation in Eq. (6.20) along a field line and using the second equation of the Neumann boundary condition, one can get

$$\begin{aligned} &\int_0^L \Big(\nabla\cdot\Big((Id-\mathbf{b}\otimes\mathbf{b})A_\perp(Id-\mathbf{b}\otimes\mathbf{b})\nabla u\Big) + f\Big)\mathrm{d}\xi\\ =&\Big(\mathbf{n}\cdot(Id-\mathbf{b}\otimes\mathbf{b})A_\perp(Id-\mathbf{b}\otimes\mathbf{b})\nabla u\Big)\Big|_0^L, \end{aligned} \tag{6.21}$$

where 0 and L are the two end points of a field line. (6.21) is an equation independent of ϵ and provides the information of how to determine the limit solution. Similar idea can be extended to more complex models like the closed field line (Wang, Ying and Tang 2018)(Narski and Ottaviani 2014) and high order differential operators arising in plasma physics (Yang, Deluzet and Narski 2019).

6.5. Low Mach number limit of compressible flows

Recently there has been increasing research activities in developing Mach number uniform fluid solvers. Consider the case of isentropic Navier-Stokes equations:

$$\partial_t \rho + \nabla_x \cdot (\rho u) = 0\,, \tag{6.22}$$

$$\partial_t (\rho u) + \nabla_x \cdot (\rho u \otimes u) + \frac{1}{\varepsilon^2}\nabla_x p = \frac{1}{\mathrm{Re}}\Delta u\,. \tag{6.23}$$

Here ρ is density, u velocity, $p = \rho^\gamma$ pressue, ε being the Mach number and Re the Reynolds number. When $\varepsilon \ll 1$, one seeks the asymptotic expansions: $\rho = \rho^{(0)} + \varepsilon^2\rho^{(2)} + \cdots$ and $p = p^{(0)} + \varepsilon^2 p^{(2)} + \cdots$ which then yieds (Klainerman and Majda 1981):

$$\nabla \cdot u^{(0)} = 0\,, \tag{6.24}$$

$$\partial_t u^{(0)} + \left(u^{(0)} \cdot \nabla\right) u^{(0)} + \frac{1}{\rho^{(0)}}\nabla p^{(2)} = \frac{1}{\mathrm{Re}}\Delta u^{(0)}\,. \tag{6.25}$$

The characteristic speeds of system (6.22) are of $O(1/\varepsilon)$, corresponding to fast acoustic waves. One would think the low Mach number problem is mainly a numerically stiff problem hence a small time step of $O(\varepsilon)$ is needed if an explicit method is used. In fact, the constraints are more severe. For shock capturing methods, the numerical viscosity, a necessary ingredient to suppress artificial oscillations, is inversely proportional to the speed of sound hence $\Delta x = \mathcal{O}(\varepsilon)$ is needed to reduce numerical dissipation (Guillard and Viozat 1999)(Dellacherie 2010). One then needs $\Delta t = \mathcal{O}(\varepsilon\Delta x)$ for numerical stability in an explicit scheme.

In developing a numerical scheme that is efficient for all Mach numbers, ideally one hopes to use mesh size and time step *independent* of ε, namely the scheme is AP. This is usually achieved by splitting the flux into the fast moving (corresponding to the acoustic waves) one and the slowly moving one. An earlier attempt in this direction is a splitting by Klein (Klein 1995), which was further improved in (Noelle, Bispen, Arun, Lukacova-Medvidova and Munz 2014). Here we mention an approach introduced in (Haack, Jin and Liu 2012) (see a related approach in (Degond and Tang 2011)(Cordier, Degond and Kumbaro 2012)) which takes the following splitting:

$$\begin{cases} \partial_t \rho + \alpha\nabla\cdot(\rho u) + (1-\alpha)\nabla\cdot(\rho u) = 0 \\ \partial_t(\rho u) + \nabla\cdot(\rho u\otimes u) + \nabla\left(\frac{p(\rho)-a(t)\rho}{\varepsilon^2}\right) + \frac{a(t)}{\varepsilon^2}\nabla\rho = \frac{1}{\mathrm{Re}}\Delta u \end{cases}, \tag{6.26}$$

where α and $a(t)$ are artificial parameters. By choosing $a(t)$ well approximating $p'(\rho)$, the third term in the second equation is non-stiff, thus will be treated explicitly. An implicit treatment on term $\nabla\rho$ is necessary, but thanks to its linearity this can be done easily, since only Poisson solvers are needed. The scheme is shock-capturing in the high Mach number regime,

and reduces to a projection method–a popular method for incompressible Navier-Stokes equations (Temam 1969) (Chorin 1968) when $\varepsilon \to 0$, hence the AP property for $\varepsilon \to 0$ is justified.

This direction is still rapidly evolving. One can find other techniques such as a Langrange-Projection scheme (Chalons, Girardin and Kokh 2016)(Zakerzadeh 2017), a modification of the Roe solver (Miczek, Röpke and Edelmann 2015)(Barsukow, Edelmann, Klingenberg, Miczek and Röpke 2017) with applications to astrophysics problems, careful choice of numerical viscosity (Dimarco, Loubère and Vignal 2017), and error estimates on AP schemes for low-Mach number flows (Feireisl, Lukacova-Medvidova, Necasova, Novotny and She 2018).

Acknowledgements

Many of the presented works were partially supported by NSF Divison of Mathematical Sciences Focused Research Group: "Collaborative Research on Kinetic Description of Multiscale Phenomena: Modeling, Theory and Computation" (2008-2011), and NSF Division of Mathematical Sciences Research Network "KI-Net: Kinetic description of emerging challenges in multiscale problems of natural sciences" (2012-2019). The author thanks Eitan Tadmor for his tireless effort in making these projects successful, and for his long-time support.

The author also thanks Francis Filbet for contributing to subsection 6.3, and Min Tang for contributing subsection 6.4.

REFERENCES

A. Abdulle, E. Weinan, B. Engquist and E. Vanden-Eijnden (2012), 'The heterogeneous multiscale method', *Acta Numerica* **21**, 1–87.

R. Agarwal, K.-Y. Yun and R. Balakrishnan (1999), Beyond navier stokes-burnett equations for flow simulations in continuum-transition regime, in *30th fluid dynamics conference*, p. 3580.

G. Albi and L. Pareschi (2013), 'Binary interaction algorithms for the simulation of flocking and swarming dynamics', *Multiscale Modeling & Simulation* **11**(1), 1–29.

G. Albi, N. Bellomo, L. Fermo, S.-Y. Ha, J. Kim, L. Pareschi, D. Poyato and J. Soler (2019), 'Vehicular traffic, crowds, and swarms: from kinetic theory and multiscale methods to applications and research perspectives', *Math. Models Methods Appl. Sci.* **29**(10), 1901–2005.

W. Bao and J. Shen (2005), 'A fourth-order time-splitting Laguerre-Hermite pseudospectral method for Bose-Einstein condensates', *SIAM J. Sci. Comput.* **26**(6), 2010–2028 (electronic).

W. Bao, S. Jin and P. A. Markowich (2002), 'On time-splitting spectral approximations for the Schrödinger equation in the semiclassical regime', *J. Comput. Phys.* **175**(2), 487–524.

W. Bao, S. Jin and P. A. Markowich (2003), 'Numerical study of time-splitting spectral discretizations of nonlinear Schrödinger equations in the semiclassical regimes', *SIAM J. Sci. Comput.* **25**(1), 27–64 (electronic).

C. Bardos, F. Golse and D. Levermore (1991), 'Fluid dynamic limits of kinetic equations. I. Formal derivations', *J. Statist. Phys.* **63**(1-2), 323–344.

C. Bardos, R. Santos and R. Sentis (1984), 'Diffusion approximation and computation of the critical size', *Trans. Amer. Math. Soc.* **284**(2), 617–649.

J. Barnes and P. Hut (1986), 'A hierarchical O(NlogN) force-calculation algorithm', *Nature* **324**, 446–449.

W. Barsukow, P. V. Edelmann, C. Klingenberg, F. Miczek and F. K. Röpke (2017), 'A numerical scheme for the compressible low-mach number regime of ideal fluid dynamics', *Journal of Scientific Computing* **72**(2), 623–646.

M. Bennoune, M. Lemou and L. Mieussens (2008), 'Uniformly stable numerical schemes for the boltzmann equation preserving the compressible navier–stokes asymptotics', *Journal of Computational Physics* **227**(8), 3781–3803.

P. R. Berman, J. E. M. Haverkort and J. P. Woerdman (1986), 'Collision kernels and transport coefficients', *Phys. Rev. A* **34**, 4647–4656.

G. A. Bird (1994), *Molecular Gas Dynamics and the Direct Simulation of Gas Flows*, Clarendon Press, Oxford.

R. H. Bisseling, R. Kosloff, R. B. Gerber, M. A. Ratner, L. Gibson and C. Cerjan (1987), 'Exact time-dependent quantum mechanical dissociation dynamics of I2He: Comparison of exact time-dependent quantum calculation with the quantum time-dependent self-consistent field (TDSCF) approximation', *J. Chem. Phys.* **87**(5), 2760–2765.

S. Boscarino, L. Pareschi and G. Russo (2013), 'Implicit-explicit runge–kutta schemes for hyperbolic systems and kinetic equations in the diffusion limit', *SIAM Journal on Scientific Computing* **35**(1), A22–A51.

F. Bouchut, F. Golse and M. Pulvirenti (2000*a*), *Kinetic equations and asymptotic theory*, Elsevier.

F. Bouchut, F. Golse and M. Pulvirenti (2000*b*), *Kinetic equations and asymptotic theory*, Vol. 4 of *Series in Applied Mathematics (Paris)*, Gauthier-Villars, Éditions Scientifiques et Médicales Elsevier, Paris. Edited and with a foreword by Benoît Perthame and Laurent Desvillettes.

F. Bouchut, H. Ounaissa and B. Perthame (2007), 'Upwinding of the source term at interfaces for euler equations with high friction', *Computers & mathematics with applications* **53**(3-4), 361–375.

J. Bourgat, P. Le Tallec, B. Perthame and Y. Qiu (1994), 'Coupling boltzmann and euler equations without overlapping', *Contemporary Mathematics* **157**, 377–377.

Y. Brenier (2000), 'Convergence of the vlasov-poisson system to the incompressible euler equations', *Communications in Partial Differential Equations* **25**(3-4), 737–754.

R. E. Caflisch, S. Jin and G. Russo (1997), 'Uniformly accurate schemes for hyperbolic systems with relaxation', *SIAM Journal on Numerical Analysis* **34**(1), 246–281.

J. A. Carrillo, L. Pareschi and M. Zanella (2019), 'Particle based gPC methods for

mean-field models of swarming with uncertainty', *Communications in Computational Physics*.

J. A. Carrillo, L. Wang, W. Xu and M. Yan (2021), 'Variational asymptotic preserving scheme for the vlasov–poisson–fokker–planck system', *Multiscale Modeling & Simulation* **19**(1), 478–505.

C. Cercignani (1988), *The Boltzmann equation and its applications*, Vol. 67 of *Applied Mathematical Sciences*, Springer-Verlag, New York.

C. Cercignani, I. Gamba and C. Levermore (1997), 'High field approximations to a boltzmann-poisson system and boundary conditions in a semiconductor', *Applied Mathematics Letters* **10**(4), 111–117.

C. Chalons, F. Coquel, E. Godlewski, P.-A. Raviart and N. Seguin (2010), 'Godunov-type schemes for hyperbolic systems with parameter-dependent source: the case of euler system with friction', *Mathematical Models and Methods in Applied Sciences* **20**(11), 2109–2166.

C. Chalons, M. Girardin and S. Kokh (2016), 'An all-regime lagrange-projection like scheme for the gas dynamics equations on unstructured meshes', *Communications in Computational Physics* **20**(1), 188–233.

G.-Q. Chen, C. D. Levermore and T.-P. Liu (1994), 'Hyperbolic conservation laws with stiff relaxation terms and entropy', *Communications on Pure and Applied Mathematics* **47**(6), 787–830.

H. Chen, S. Chen and W. H. Matthaeus (1992), 'Recovery of the navier-stokes equations using a lattice-gas boltzmann method', *Physical review A* **45**(8), R5339.

S. Chen and G. D. Doolen (1998), 'Lattice boltzmann method for fluid flows', *Annual review of fluid mechanics* **30**(1), 329–364.

Z. Chen, L. Liu and L. Mu (2017), 'Dg-imex stochastic galerkin schemes for linear transport equation with random inputs and diffusive scalings', *Journal of Scientific Computing* **73**(2), 566–592.

A. J. Chorin (1968), 'Numerical solution of the navier-stokes equations', *Mathematics of computation* **22**(104), 745–762.

G. Ciccotti, D. Frenkel and I. R. McDonald (1987), *Simulation of liquids and solids: Molecular Dynamics and Monte Carlo Methods in Statistical Mechanics*, North-Holland, Amsterdam.

F. Cordier, P. Degond and A. Kumbaro (2012), 'An asymptotic-preserving all-speed scheme for the euler and navier–stokes equations', *Journal of Computational Physics* **231**(17), 5685–5704.

F. Coron and B. Perthame (1991), 'Numerical passage from kinetic to fluid equations', *SIAM Journal on Numerical Analysis* **28**(1), 26–42.

L. Corry (2004), *David Hilbert and the axiomatization of physics (1898–1918): From Grundlagen der Geometrie to Grundlagen der Physik*, Vol. 10, Springer Science & Business Media.

M. G. Crandall and P.-L. Lions (1983), 'Viscosity solutions of Hamilton-Jacobi equations', *Trans. Amer. Math. Soc.* **277**(1), 1–42.

P. Crispel, P. Degond and M.-H. Vignal (2005), 'An asymptotically stable discretization for the euler–poisson system in the quasi-neutral limit', *Comptes Rendus Mathematique* **341**(5), 323–328.

P. Crispel, P. Degond and M.-H. Vignal (2007), 'An asymptotic preserving scheme

for the two-fluid euler–poisson model in the quasineutral limit', *Journal of Computational Physics* **223**(1), 208–234.

N. Crouseilles and M. Lemou (2011), 'An asymptotic preserving scheme based on a micro-macro decomposition for collisional vlasov equations: diffusion and high-field scaling limits', *Kinetic & Related Models* **4**(2), 441.

N. Crouseilles, E. Frénod, S. A. Hirstoaga and A. Mouton (2013*a*), 'Two-scale macro-micro decomposition of the Vlasov equation with a strong magnetic field', *Math. Models Methods Appl. Sci.* **23**(8), 1527–1559.

N. Crouseilles, M. Lemou and F. Méhats (2013*b*), 'Asymptotic preserving schemes for highly oscillatory Vlasov–Poisson equations', *J. Comput. Phys.* **248**, 287–308.

F. Cucker and S. Smale (2007), 'Emergent behavior in flocks', *IEEE Transactions on automatic control* **52**(5), 852–862.

E. S. Daus, S. Jin and L. Liu (2019), 'Spectral convergence of the stochastic Galerkin approximation to the Boltzmann equation with multiple scales and large random perturbation in the collision kernel', *Kinet. Relat. Models* **12**(4), 909–922.

P. Degond and F. Deluzet (2017*a*), 'Asymptotic-preserving methods and multiscale models for plasma physics', *Journal of Computational Physics* **336**, 429–457.

P. Degond and F. Deluzet (2017*b*), 'Asymptotic-preserving methods and multiscale models for plasma physics', *Journal of Computational Physics* **336**, 429–457.

P. Degond and M. Tang (2011), 'All speed scheme for the low mach number limit of the isentropic euler equations', *Communications in Computational Physics* **10**(1), 1–31.

P. Degond, F. Deluzet and D. Doyen (2017), 'Asymptotic-preserving particle-in-cell methods for the vlasov–maxwell system in the quasi-neutral limit', *Journal of Computational Physics* **330**, 467–492.

P. Degond, F. Deluzet and C. Negulescu (2010*a*), 'An asymptotic preserving scheme for strongly anisotropic elliptic problems', *Multiscale Modeling & Simulation* **8**(2), 645–666.

P. Degond, F. Deluzet and D. Savelief (2012*a*), 'Numerical approximation of the euler–maxwell model in the quasineutral limit', *Journal of computational physics* **231**(4), 1917–1946.

P. Degond, F. Deluzet, A. Lozinski, J. Narski and C. Negulescu (2010*b*), 'Duality-based asymptotic-preserving method for highly anisotropic diffusion equations', *arXiv preprint arXiv:1008.3405*.

P. Degond, F. Deluzet, L. Navoret, A.-B. Sun and M.-H. Vignal (2010*c*), 'Asymptotic-preserving particle-in-cell method for the vlasov–poisson system near quasineutrality', *Journal of Computational Physics* **229**(16), 5630–5652.

P. Degond, S. Jin and L. Mieussens (2005), 'A smooth transition model between kinetic and hydrodynamic equations', *Journal of Computational Physics* **209**(2), 665–694.

P. Degond, A. Lozinski, J. Narski and C. Negulescu (2012*b*), 'An asymptotic-preserving method for highly anisotropic elliptic equations based on a micro–macro decomposition', *Journal of Computational Physics* **231**(7), 2724–2740.

S. Dellacherie (2010), 'Analysis of godunov type schemes applied to the compressible euler system at low mach number', *Journal of Computational Physics* **229**(4), 978–1016.

J. Deng (2012), 'Asymptotic preserving schemes for semiconductor boltzmann equation in the diffusive regime', *Numerical Mathematics: Theory, Methods and Applications* **5**(2), 278–296.

M. Deserno and C. Holm (1998), 'How to mesh up Ewald sums. II. An accurate error estimate for the particle-particle particle-mesh algorithm', *The Journal of Chemical Physics* **109**(18), 7694–7701.

S. Deshpande (1986), Kinetic theory based new upwind methods for inviscid compressible flows, in *24th Aerospace Sciences Meeting*, p. 275.

G. Dimarco and L. Pareschi (2011), 'Exponential runge–kutta methods for stiff kinetic equations', *SIAM Journal on Numerical Analysis* **49**(5), 2057–2077.

G. Dimarco and L. Pareschi (2014), 'Numerical methods for kinetic equations', *Acta Numerica* **23**, 369–520.

G. Dimarco, R. Loubère and M.-H. Vignal (2017), 'Study of a new asymptotic preserving scheme for the euler system in the low mach number limit', *SIAM journal on Scientific Computing* **39**(5), A2099–A2128.

K. Drukker (1999), 'Basics of surface hopping in mixed quantum/classical simulations', *J. Comp.. Phys.* **153**, 225–272.

Z. H. Duan and R. Krasny (2000), 'An Ewald summation based multipole method', *J. Chem. Phys.* **113**, 3492–3495.

M. Dumbser, C. Enaux and E. F. Toro (2008), 'Finite volume schemes of very high order of accuracy for stiff hyperbolic balance laws', *Journal of Computational Physics* **227**(8), 3971–4001.

R. Durstenfeld (1964), 'Algorithm 235: random permutation', *Communications of the ACM* **7**(7), 420.

W. E and B. Engquist (2003), 'The heterogeneous multiscale methods', *Commun. Math. Sci.* **1**(1), 87–132.

W. E and B. Yu (2018), 'The deep ritz method: A deep learning-based numerical algorithm for solving variational problems', *Communications in Mathematics and Statistics* **6**(1), 1–12.

D. Fang, S. Jin and C. Sparber (2018), 'An efficient time-splitting method for the Ehrenfest dynamics', *Multiscale Model. Simul.* **16**(2), 900–921.

E. Feireisl, M. Lukacova-Medvidova, S. Necasova, A. Novotny and B. She (2018), 'Asymptotic preserving error estimates for numerical solutions of compressible navier–stokes equations in the low mach number regime', *Multiscale Modeling & Simulation* **16**(1), 150–183.

F. Filbet and S. Jin (2010), 'A class of asymptotic-preserving schemes for kinetic equations and related problems with stiff sources', *Journal of Computational Physics* **229**(20), 7625–7648.

F. Filbet and L. M. Rodrigues (2016), 'Asymptotically stable particle-in-cell methods for the Vlasov–Poisson system with a strong external magnetic field', *SIAM J. Numer. Anal.* **54**(2), 1120–1146.

F. Filbet and L. M. Rodrigues (2017), 'Asymptotically preserving particle-in-cell methods for inhomogeneous strongly magnetized plasmas', *SIAM J. Numer. Anal.* **55**(5), 2416–2443.

F. Filbet and L. M. Rodrigues (2020), 'Asymptotics of the three-dimensional Vlasov equation in the large magnetic field limit', *J. Éc. polytech. Math.* **7**, 1009–1067.

F. Filbet, J. Hu and S. Jin (2012), 'A numerical scheme for the quantum boltzmann equation with stiff collision terms', *ESAIM: Mathematical Modelling and Numerical Analysis* **46**(2), 443–463.

F. Filbet, L. M. Rodrigues and H. Zakerzadeh (2021), 'Convergence analysis of asymptotic preserving schemes for strongly magnetized plasmas', *Numer. Math.* **149**(3), 549–593.

J. Foch (1973), On higher order hydrodynamic theories of shock structure, in *The Boltzmann Equation*, Springer, pp. 123–140.

B. Fornberg (1996), *A practical guide to pseudospectral methods*, Vol. 1 of *Cambridge Monographs on Applied and Computational Mathematics*, Cambridge University Press, Cambridge.

D. Frenkel and B. Smit (2001), *Understanding molecular simulation: from algorithms to applications*, Vol. 1, Elsevier.

E. Frénod, S. A. Hirstoaga, M. Lutz and E. Sonnendrücker (2015), 'Long time behaviour of an exponential integrator for a vlasov-poisson system with strong magnetic field', *Communications in Computational Physics* **18**(2), 263–296.

E. Frénod, F. Salvarani and E. Sonnendrücker (2009), 'Long time simulation of a beam in a periodic focusing channel via a two-scale PIC-method', *Math. Models Methods Appl. Sci.* **19**(2), 175–197.

I. Gallagher, L. Saint-Raymond and B. Texier (2013), *From Newton to Boltzmann: hard spheres and short-range potentials*, Zurich Lectures in Advanced Mathematics, European Mathematical Society (EMS), Zürich.

I. M. Gamba, S. Jin and L. Liu (2019), 'Micro-macro decomposition based asymptotic-preserving numerical schemes and numerical moments conservation for collisional nonlinear kinetic equations', *Journal of Computational Physics* **382**, 264–290.

A. Georges, G. Kotliar, W. Krauth and M. J. Rozenberg (1996), 'Dynamical mean-field theory of strongly correlated fermion systems and the limit of infinite dimensions', *Reviews of Modern Physics* **68**(1), 13.

P. Gérard, P. A. Markowich, N. J. Mauser and F. Poupaud (1997), 'Homogenization limits and Wigner transforms', *Comm. Pure Appl. Math.* **50**(4), 323–379.

F. Golse (2003), 'The mean-field limit for the dynamics of large particle systems', *Journées équations aux dérivées partielles* **9**, 1–47.

F. Golse and T. Paul (2017), 'The Schrödinger equation in the mean-field and semiclassical regime', *Arch. Ration. Mech. Anal.* **223**(1), 57–94.

F. Golse, S. Jin and C. D. Levermore (1999), 'The convergence of numerical transfer schemes in diffusive regimes i: Discrete-ordinate method', *SIAM journal on numerical analysis* **36**(5), 1333–1369.

F. Golse, S. Jin and T. Paul (2021), 'On the convergence of time splitting methods for quantum dynamics in the semiclassical regime', *Found. Comput. Math.* **21**(3), 613–647.

L. Gosse and G. Toscani (2002), 'An asymptotic-preserving well-balanced scheme for the hyperbolic heat equations', *Comptes Rendus Mathematique* **334**(4), 337–342.

T. Goudon, J. Nieto, F. Poupaud and J. Soler (2005), 'Multidimensional high-field limit of the electrostatic vlasov–poisson–fokker–planck system', *Journal of Differential Equations* **213**(2), 418–442.

L. Greengard and V. Rokhlin (1987), 'A fast algorithm for particle simulations', *J. Comput. Phys.* **73**, 325–348.

H. Guillard and C. Viozat (1999), 'On the behaviour of upwind schemes in the low mach number limit', *Computers & fluids* **28**(1), 63–86.

M. D. Gunzburger, C. G. Webster and G. Zhang (2014), 'Stochastic finite element methods for partial differential equations with random input data', *Acta Numerica* **23**, 521–650.

J. Haack, S. Jin and J.-G. Liu (2012), 'An all-speed asymptotic-preserving method for the isentropic euler and navier-stokes equations', *Communications in Computational Physics* **12**(4), 955–980.

E. Hairer, C. Lubich and B. Wang (2020), 'A filtered Boris algorithm for charged-particle dynamics in a strong magnetic field', *Numer. Math.* **144**(4), 787–809.

X. He and L.-S. Luo (1997), 'Theory of the lattice boltzmann method: From the boltzmann equation to the lattice boltzmann equation', *Physical review E* **56**(6), 6811.

E. J. Heller (2006), 'Guided gaussian wave packets', *Accounts of Chemical Research* **39**(2), 127–134.

B. Hetenyi, K. Bernacki and B. J. Berne (2002), 'Multiple "time step" Monte Carlo', *J. Chem. Phys.* **117**(18), 8203–8207.

N. Hill (1990), 'Gaussian beam migration', *Geophysics* **55**(11), 1416–1428.

J. Hu and S. Jin (2016), 'A stochastic galerkin method for the boltzmann equation with uncertainty', *Journal of Computational Physics* **315**, 150–168.

J. Hu and R. Shu (2019), 'A second-order asymptotic-preserving and positivity-preserving exponential runge–kutta method for a class of stiff kinetic equations', *Multiscale Modeling & Simulation* **17**(4), 1123–1146.

J. Hu and R. Shu (2021), 'On the uniform accuracy of implicit-explicit backward differentiation formulas (imex-bdf) for stiff hyperbolic relaxation systems and kinetic equations', *Mathematics of Computation* **90**(328), 641–670.

J. Hu, S. Jin and Q. Li (2017), Asymptotic-preserving schemes for multiscale hyperbolic and kinetic equations, in *Handbook of Numerical Analysis*, Vol. 18, Elsevier, pp. 103–129.

J. Hu, S. Jin and B. Yan (2012), 'A numerical scheme for the quantum fokker-planck-landau equation efficient in the fluid regime', *Communications in Computational Physics* **12**(5), 1541–1561.

P.-E. Jabin and Z. Wang (2017), Mean field limit for stochastic particle systems, in *Active Particles, Volume 1*, Springer, pp. 379–402.

S. Jin (1995), 'Runge-kutta methods for hyperbolic conservation laws with stiff relaxation terms', *Journal of Computational Physics* **122**(1), 51–67.

S. Jin (1999), 'Efficient asymptotic-preserving (ap) schemes for some multiscale kinetic equations', *SIAM Journal on Scientific Computing* **21**(2), 441–454.

S. Jin (2010), 'Asymptotic preserving (ap) schemes for multiscale kinetic and hyperbolic equations: a review', *Lecture notes for summer school on methods and models of kinetic theory (M&MKT), Porto Ercole (Grosseto, Italy)* pp. 177–216.

S. Jin and C. D. Levermore (1996), 'Numerical schemes for hyperbolic conservation laws with stiff relaxation terms', *Journal of computational physics* **126**(2), 449–467.

S. Jin and L. Li (2021*a*), 'On the mean field limit of the random batch method for interacting particle systems', *Science China Mathematics* pp. 1–34.

S. Jin and L. Li (2021*b*), 'Random batch methods for classical and quantum interacting particle systems and statistical samplings', *arXiv preprint arXiv:2104.04337*.

S. Jin and Q. Li (2013), 'A bgk-penalization-based asymptotic-preserving scheme for the multispecies boltzmann equation', *Numerical Methods for Partial Differential Equations* **29**(3), 1056–1080.

S. Jin and X. Li (2020), 'Random batch algorithms for quantum Monte Carlo simulations', *Commun. Comput. Phys.* **28**(5), 1907–1936.

S. Jin and L. Liu (2017), 'An asymptotic-preserving stochastic galerkin method for the semiconductor boltzmann equation with random inputs and diffusive scalings', *Multiscale Modeling & Simulation* **15**(1), 157–183.

S. Jin and L. Pareschi (2001), Asymptotic-preserving (ap) schemes for multiscale kinetic equations: a unified approach, in *Hyperbolic problems: theory, numerics, applications*, Springer, pp. 573–582.

S. Jin and R. Shu (2017), 'A stochastic asymptotic-preserving scheme for a kinetic-fluid model for disperse two-phase flows with uncertainty', *J. Comput. Phys.* **335**, 905–924.

S. Jin and L. Wang (2011), 'An asymptotic preserving scheme for the vlasov-poisson-fokker-planck system in the high field regime', *Acta Mathematica Scientia* **31**(6), 2219–2232.

S. Jin and L. Wang (2013), 'Asymptotic-preserving numerical schemes for the semiconductor boltzmann equation efficient in the high field regime', *SIAM Journal on Scientific Computing* **35**(3), B799–B819.

S. Jin and Z. Xin (1995), 'The relaxation schemes for systems of conservation laws in arbitrary space dimensions', *Communications on pure and applied mathematics* **48**(3), 235–276.

S. Jin and B. Yan (2011), 'A class of asymptotic-preserving schemes for the fokker–planck–landau equation', *Journal of Computational Physics* **230**(17), 6420–6437.

S. Jin and Z. Zhou (2013), 'A semi-lagrangian time splitting method for the schrödinger equation with vector potentials', *Communications in Information and Systems* **13**(3), 247–289.

S. Jin and Y. Zhu (2018), 'Hypocoercivity and uniform regularity for the vlasov–poisson–fokker–planck system with uncertainty and multiple scales', *SIAM Journal on Mathematical Analysis* **50**(2), 1790–1816.

S. Jin, C. D. Levermore and D. W. McLaughlin (1999), 'The semiclassical limit of the defocusing NLS hierarchy', *Comm. Pure Appl. Math.* **52**(5), 613–654.

S. Jin, L. Li and J.-G. Liu (2020*a*), 'Random batch methods (rbm) for interacting particle systems', *Journal of Computational Physics* **400**, 108877.

S. Jin, L. Li and Y. Sun (2020*b*), 'On the Random Batch Method for second order interacting particle systems', *arXiv preprint arXiv:2011.10778*.

S. Jin, L. Li, Z. Xu and Y. Zhao (2021*a*), 'A Random Batch Ewald Method for Particle Systems with Coulomb Interactions', *SIAM J. Sci. Comput.* **43**(4), B937–B960.

S. Jin, J.-G. Liu and Z. Ma (2017*a*), 'Uniform spectral convergence of the stochastic galerkin method for the linear transport equations with random inputs in diffusive regime and a micro–macro decomposition-based asymptotic-preserving method', *Research in the Mathematical Sciences* **4**(1), 1–25.

S. Jin, Z. Ma and K. Wu (2021*b*), 'Asymptotic-preserving neural networks for multiscale time-dependent linear transport equations', *arXiv preprint arXiv:2111.02541*.

S. Jin, P. Markowich and C. Sparber (2011), 'Mathematical and computational methods for semiclassical Schrödinger equations', *Acta Numer.* **20**, 121–209.

S. Jin, L. Pareschi and G. Toscani (2000), 'Uniformly accurate diffusive relaxation schemes for multiscale transport equations', *SIAM Journal on Numerical Analysis* **38**(3), 913–936.

S. Jin, C. Sparber and Z. Zhou (2017*b*), 'On the classical limit of a time-dependent self-consistent field system: analysis and computation', *Kinet. Relat. Models* **10**(1), 263–298.

S. Jin, H. Wu and X. Yang (2008), 'Gaussian beam methods for the Schrödinger equation in the semi-classical regime: Lagrangian and Eulerian formulations', *Commun. Math. Sci.* **6**(4), 995–1020.

S. Jin, D. Xiu and X. Zhu (2015), 'Asymptotic-preserving methods for hyperbolic and transport equations with random inputs and diffusive scalings', *Journal of Computational Physics* **289**, 35–52.

I. G. Kevrekidis, C. W. Gear and G. Hummer (2004), 'Equation-free: The computer-aided analysis of complex multiscale systems', *AIChE Journal* **50**(7), 1346–1355.

S. Klainerman and A. Majda (1981), 'Singular limits of quasilinear hyperbolic systems with large parameters and the incompressible limit of compressible fluids', *Communications on pure and applied Mathematics* **34**(4), 481–524.

A. Klar (1998), 'An asymptotic-induced scheme for nonstationary transport equations in the diffusive limit', *SIAM journal on numerical analysis* **35**(3), 1073–1094.

A. Klar and C. Schmeiser (2001), 'Numerical passage from radiative heat transfer to nonlinear diffusion models', *Mathematical Models and Methods in Applied Sciences* **11**(05), 749–767.

A. Klar, H. Neunzert and J. Struckmeier (2000), 'Transition from kinetic theory to macroscopic fluid equations: a problem for domain decomposition and a source for new algorithms', *Transport Theory and Statistical Physics* **29**(1-2), 93–106.

R. Klein (1995), 'Semi-implicit extension of a godunov-type scheme based on low mach number asymptotics i: One-dimensional flow', *Journal of Computational Physics* **121**(2), 213–237.

K. Koura and H. Matsumoto (1991), 'Variable soft sphere molecular model for inverse-power-law or Lennard-Jones potential', *Phys. Fluids A* **3**, 2459–2465.

K. Kupper, M. Frank and S. Jin (2016), 'An asymptotic preserving two-dimensional

staggered grid method for multiscale transport equations', *SIAM Journal on Numerical Analysis* **54**(1), 440–461.

O. E. Lanford, III (1975), Time evolution of large classical systems, in *Dynamical systems, theory and applications (Rencontres, Battelle Res. Inst., Seattle, Wash., 1974)*, pp. 1–111. Lecture Notes in Phys., Vol. 38.

E. W. Larsen and J. E. Morel (1989), 'Asymptotic solutions of numerical transport problems in optically thick, diffusive regimes ii'.

E. W. Larsen, J. E. Morel and W. F. Miller Jr (1987), 'Asymptotic solutions of numerical transport problems in optically thick, diffusive regimes', *Journal of Computational Physics* **69**(2), 283–324.

C. Lasser and C. Lubich (2020), 'Computing quantum dynamics in the semiclassical regime', *Acta Numer.* **29**, 229–401.

P. D. Lax and D. Levermore (1983), 'The small dispersion limit of the korteweg-de vries equation. i', *Communications on Pure and Applied Mathematics* **36**(3), 253–290.

T. Lelievre and G. Stoltz (2016), 'Partial differential equations and stochastic methods in molecular dynamics', *Acta Numerica* **25**, 681–880.

M. Lemou and L. Mieussens (2008), 'A new asymptotic preserving scheme based on micro-macro formulation for linear kinetic equations in the diffusion limit', *SIAM Journal on Scientific Computing* **31**(1), 334–368.

S. Leung and J. Qian (2009), 'Eulerian gaussian beams for schrödinger equations in the semi-classical regime', *J. Comput. Phys.* **228**(8), 2951–2977.

E. E. Lewis and W. F. Miller (1984), 'Computational methods of neutron transport'.

L. Li and C. Yang (2021), 'Asymptotic preserving scheme for anisotropic elliptic equations with deep neural network', *arXiv preprint arXiv:2104.05337*.

L. Li, Y. Li, J.-G. Liu, Z. Liu and J. Lu (2020*a*), 'A stochastic version of stein variational gradient descent for efficient sampling', *Communications in Applied Mathematics and Computational Science* **15**(1), 37–63.

L. Li, Z. Xu and Y. Zhao (2020*b*), 'A random-batch Monte Carlo method for many-body systems with singular kernels', *SIAM Journal on Scientific Computing* **42**(3), A1486–A1509.

Q. Li and L. Pareschi (2014), 'Exponential runge–kutta for the inhomogeneous boltzmann equations with high order of accuracy', *Journal of Computational Physics* **259**, 402–420.

Q. Li and L. Wang (2017), 'Uniform regularity for linear kinetic equations with random input based on hypocoercivity', *SIAM/ASA Journal on Uncertainty Quantification* **5**(1), 1193–1219.

Z. Li, N. Kovachki, K. Azizzadenesheli, B. Liu, K. Bhattacharya, A. Stuart and A. Anandkumar (2020*c*), 'Fourier neural operator for parametric partial differential equations', *arXiv preprint arXiv:2010.08895*.

J. Liang, P. Tan, Y. Zhao, H. Liu, L. Li, S. Jin, L. Hong and Z. Xu (In preparation), 'Linear scalable algorithm to calculate coulomb interaction', *preprint*.

P.-L. Lions and T. Paul (1993), 'Sur les mesures de Wigner', *Rev. Mat. Iberoamericana* **9**(3), 553–618.

C. Liu, K. Xu, Q. Sun and Q. Cai (2016), 'A unified gas-kinetic scheme for continuum and rarefied flows iv: Full boltzmann and model equations', *Journal of Computational Physics* **314**, 305–340.

J.-G. Liu and L. Mieussens (2010), 'Analysis of an asymptotic preserving scheme for linear kinetic equations in the diffusion limit', *SIAM Journal on Numerical Analysis* **48**(4), 1474–1491.

L. Liu and S. Jin (2018), 'Hypocoercivity based sensitivity analysis and spectral convergence of the stochastic galerkin approximation to collisional kinetic equations with multiple scales and random inputs', *Multiscale Modeling & Simulation* **16**(3), 1085–1114.

T.-P. Liu and S.-H. Yu (2004), 'Boltzmann equation: micro-macro decompositions and positivity of shock profiles', *Communications in mathematical physics* **246**(1), 133–179.

M. Loève (1977), *Probability Theory*, fourth edn, Springer-Verlag, New York.

L. Lu, P. Jin, G. Pang, Z. Zhang and G. E. Karniadakis (2021*a*), 'Learning nonlinear operators via deeponet based on the universal approximation theorem of operators', *Nature Machine Intelligence* **3**(3), 218–229.

Y. Lu, L. Wang and W. Xu (2021*b*), 'Solving multiscale steady radiative transfer equation using neural networks with uniform stability', *arXiv preprint arXiv:2110.07037*.

B. A. Luty, M. E. Davis, I. G. Tironi and W. F. Van Gunsteren (1994), 'A comparison of particle-particle, particle-mesh and Ewald methods for calculating electrostatic interactions in periodic molecular systems', *Mol. Simul.* **14**, 11–20.

N. Makri and W. H. Miller (1987), 'Time-dependent self-consistent field (TDSCF) approximation for a reaction coordinate coupled to a harmonic bath: Single and multiple configuration treatments', *J. Chem. Phys.* **87**(10), 5781–5787.

P. A. Markowich, P. Pietra and C. Pohl (1999), 'Numerical approximation of quadratic observables of Schrödinger-type equations in the semi-classical limit', *Numer. Math.* **81**(4), 595–630.

P. A. Markowich, C. A. Ringhofer and C. Schmeiser (1990), *Semiconductor equations*, Springer-Verlag, Vienna.

M. G. Martin, B. Chen and J. I. Siepmann (1998), 'A novel Monte Carlo algorithm for polarizable force fields: application to a fluctuating charge model for water', *The Journal of chemical physics* **108**(9), 3383–3385.

D. Marx and J. Hutter (2009), *Ab Initio Molecular Dynamics: Basic Theory and Advanced Methods*, Cambridge University Press.

H. P. McKean (1967), 'Propagation of chaos for a class of non-linear parabolic equations', *Stochastic Differential Equations (Lecture Series in Differential Equations, Session 7, Catholic Univ., 1967)* pp. 41–57.

F. Miczek, F. K. Röpke and P. V. Edelmann (2015), 'New numerical solver for flows at various mach numbers', *Astronomy & Astrophysics* **576**, A50.

S. Motsch and E. Tadmor (2014), 'Heterophilious dynamics enhances consensus', *SIAM Review* **56**(4), 577–621.

J. Narski and M. Ottaviani (2014), 'Asymptotic preserving scheme for strongly anisotropic parabolic equations for arbitrary anisotropy direction', *Computer Physics Communications* **185**(12), 3189–3203.

J. Nieto, F. Poupaud and J. Soler (2001), 'High-field limit for the vlasov-poisson-fokker-planck system', *Archive for rational mechanics and analysis* **158**(1), 29–59.

S. Noelle, G. Bispen, K. R. Arun, M. Lukacova-Medvidova and C.-D. Munz (2014), 'A weakly asymptotic preserving low mach number scheme for the euler equations of gas dynamics', *SIAM Journal on Scientific Computing* **36**(6), B989–B1024.

L. Pareschi and G. Russo (2005), 'Implicit–explicit runge–kutta schemes and applications to hyperbolic systems with relaxation', *Journal of Scientific computing* **25**(1), 129–155.

B. Perthame (1990), 'Boltzmann type schemes for gas dynamics and the entropy property', *SIAM Journal on Numerical Analysis* **27**(6), 1405–1421.

K. H. Prendergast and K. Xu (1993), 'Numerical hydrodynamics from gas-kinetic theory', *Journal of Computational Physics* **109**(1), 53–66.

Y.-H. Qian, D. d'Humières and P. Lallemand (1992), 'Lattice bgk models for navier-stokes equation', *EPL (Europhysics Letters)* **17**(6), 479.

M. Raissi, P. Perdikaris and G. E. Karniadakis (2019), 'Physics-informed neural networks: A deep learning framework for solving forward and inverse problems involving nonlinear partial differential equations', *Journal of Computational Physics* **378**, 686–707.

L. F. Ricketson and L. Chacón (2020), 'An energy-conserving and asymptotic-preserving charged-particle orbit implicit time integrator for arbitrary electromagnetic fields', *Journal of Computational Physics* **418**, 109639.

T. Rivell (2006), 'Notes on earth atmospheric entry for mars sample return missions', *NASA Ames Research Center, Moffett Field, California, Tech. Rep. TP-2006-213486*.

V. Rokhlin (1985), 'Rapid solution of integral equations of classical potential theory', *Journal of computational physics* **60**(2), 187–207.

G. Russo and P. Smereka (2013), 'The Gaussian wave packet transform: efficient computation of the semi-classical limit of the Schrödinger equation. Part 1—Formulation and the one dimensional case', *J. Comput. Phys.* **233**, 192–209.

C. Schütte and F. A. Bornemann (1999), 'On the singular limit of the quantum-classical molecular dynamics model', *SIAM J. Appl. Math.* **59**(4), 1208–1224.

C. Sparber, P. Markowich and N. Mauser (2003), 'Wigner functions versus WKB-methods in multivalued geometrical optics', *Asymptot. Anal.* **33**(2), 153–187.

H. E. Stanley (1971), *Phase transitions and critical phenomena*, Clarendon Press, Oxford.

W. Sun, S. Jiang and K. Xu (2015), 'An asymptotic preserving unified gas kinetic scheme for gray radiative transfer equations', *Journal of Computational Physics* **285**, 265–279.

A. Szepessy (2011), 'Langevin molecular dynamics derived from Ehrenfest dynamics', *Math. Models Methods Appl. Sci.* **21**(5), 2289–2334.

D. C. Tan, T. Zhang, T. Chang and Y. Zheng (1994), 'Delta-shock waves as limits of vanishing viscosity for hyperbolic systems of conservation laws', *Journal of Differential Equations* **112**(1), 1–32.

R. Temam (1969), 'Sur l'approximation de la solution des équations de navier-stokes par la méthode des pas fractionnaires (ii)', *Archive for rational mechanics and analysis* **33**(5), 377–385.

J. C. Tully (1998), 'Mixed quantum–classical dynamics', *Faraday Discussions* **110**, 407–419.

T. Vicsek, A. Czirók, E. Ben-Jacob, I. Cohen and O. Shochet (1995), 'Novel type of phase transition in a system of self-driven particles', *Physical review letters* **75**(6), 1226.

C. Villani (2009), 'Hypocoercivity'.

Y. Wang, W. Ying and M. Tang (2018), 'Uniformly convergent scheme for strongly anisotropic diffusion equations with closed field lines', *SIAM Journal on Scientific Computing* **40**(5), B1253–B1276.

E. P. Wigner (1932), 'On the quantum correction for thermodynamic equilibrium', *Phys. Rev.* **40**, 749–759.

D. Xiu (2010), *Numerical methods for stochastic computations*, Princeton university press.

D. Xiu and G. E. Karniadakis (2002), 'The wiener–askey polynomial chaos for stochastic differential equations', *SIAM journal on scientific computing* **24**(2), 619–644.

B. Yan and S. Jin (2013), 'A successive penalty-based asymptotic-preserving scheme for kinetic equations', *SIAM Journal on Scientific Computing* **35**(1), A150–A172.

C. Yang, F. Deluzet and J. Narski (2019), 'On the numerical resolution of anisotropic equations with high order differential operators arising in plasma physics', *Journal of Computational Physics* **386**, 502–523.

L. Ying, G. Biros and D. Zorin (2004), 'A kernel-independent adaptive fast multipole algorithm in two and three dimensions', *J. Comput. Phys.* **196**, 591–626.

H. Zakerzadeh (2017), 'On the mach-uniformity of the lagrange-projection scheme', *ESAIM: Mathematical Modelling and Numerical Analysis* **51**(4), 1343–1366.

Y. Zhu and S. Jin (2017), 'The vlasov–poisson–fokker–planck system with uncertainty and a one-dimensional asymptotic preserving method', *Multiscale Modeling & Simulation* **15**(4), 1502–1529.